Giovanni Boschian
Department of Biology, University of Pisa, via Derna 1, I-56100 Pisa, Italy
giovanni.boschian@unipi.it (Corresponding Author)

Katarina Gerometta
Department of Humanities, Juraj Dobrila University of Pula, Ivana Matetića Ronjgova 1, HR-52100 Pula, Croatia

Brooks B. Ellwood
Department of Geology and Geophysics, Louisiana State University, E235 Howe Russell Kniffen, Baton Rouge, LA 70803, USA

Ivor Karavanić
Department of Archaeology, University of Zagreb, Ivana Lučića 3, HR-10000 Zagreb, Croatia
Department of Anthropology, University of Wyoming, Laramie, WY 82071, USA

Late Neandertals in Dalmatia: site formation processes, chronology, climate change and human activity at Mujina Pećina, Croatia

Abstract
Geoarchaeological studies based on standard sedimentological and soil micromorphological analyses were carried out at Mujina Pećina, a cave site with Mousterian lithic industries situated in Dalmatia, a region of Croatia facing the present-day Adriatic Sea coast. These studies were integrated with a large set of datings and magnetic susceptibility data. Part of the resulting radiocarbon dates were biased by erratic behaviour of the applied pre-treatment methods; however, pedostratigraphic and magnetic susceptibility data allowed for a better assessment of the chronology of the sequence, which is dated to a period between ~49 and ~39 cal ka BP. Neandertals frequented Mujina Pećina more intensively during the deposition of the first part of the sequence, partly corresponding to Heinrich event H5, whereas their presence was episodic in later phases, when the cave was shared with carnivores.

Keywords: Mousterian; Geoarchaeology; Magnetic susceptibility; Radiocarbon dating; Croatia

1. Introduction

Times and modes of the substitution of Neandertals by Ancient Modern Humans have been a key issue in European prehistory for the last decade.
Recent work by Higham et al. (2014) shed new light on the timing of the Middle to Upper Palaeolithic transition (MUPT), *i.e.* the shift from Mousterian to Aurignacian industries, respectively, ascribed to Neandertals and Anatomically Modern Humans (AMH); in particular, the disappearance of Neandertals from the western and central European scene is dated to 41,030–39,260 calibrated years BP (at 95.4% probability), with a significant overlap of 2,600–5,400 years (at 95.4%probability) with AMH.
The combined data suggest that the Mousterian ended at a very similar time, across sites ranging from the Black Sea and the Near East, to the Atlantic coast (Higham et al., 2014:pag. 307), even if relevant differences exist at regional or local scales (Longo et al., 2012; Mallol et al., 2012).
Even if Mousterian industries are reasonably widespread along the eastern coast of the Adriatic

Sea, the Middle to Upper Palaeolithic Transition is not documented in any site, neither transitional industries are documented in any site (Karavanić 2009). The relationships between Neandertals and AMHs, if any, and their timing are therefore still largely unknown in this area, also because of a generalised lack of geochronometric information.
The framework is further complicated by the revision (Higham et al., 2006) of previously dated (Smith et al., 1999) Neandertal specimens from the Vindija sequence in north-western Croatia, indicating that Neandertals would still have been present in the area at around 33-32 uncalibrated ka^{14}C BP (37.5-36.5 to 36.0-35.5 ka cal BP). However, this age is recent if compared to the new data (but see Smith et al., 2016). Re-dating of the same specimens from Vindija level G1 may clear this issue.
Within this framework, Middle Palaeolithic sites of the eastern Adriatic with Mousterian industries, commonly considered as produced by Neandertals (Peresani, 2012; Higham et al., 2014), are relevant to infer the adaptations and the timing of the presence of these humans in the Mediterranean part of Europe. All lithic finds from Middle Palaeolithic sites of the eastern Adriatic can be ascribed to the Mousterian industry, but no human skeletal remains were recovered associated with these industries (Malez 1979; Karavanić et al. 2008). Although results of geochronometric dating place the sequences of these sites alongside the presence of the Neandertals and the earliest known modern humans in Europe, no early Upper Palaeolithic finds were recovered from any of these sites (Karavanić 2009). Although several sites of this cultural context are known in the Dalmatian part of the Adriatic, research on this topic was relatively scanty here until recent times. Mousterian artefacts were mainly found on the surface in open-air sites, and were determined mainly upon typology (Batović, 1965; Vujević, 2007). Mujina Pećina is the only site in this area with a clear and relatively long stratigraphic sequence, and where the Mousterian was systematically excavated and chronometrically dated.
Archaeological excavations carried out in the 1970s by M. Malez (1979) and N. Petrić (1979) yielded some Mousterian artefacts. Excavations were resumed in 1995 by I. Karavanić (Karavanić and Bilich-Kamenjarin, 1997) and lasted until 2003. These new excavations identified a sequence of at least eight levels including a rich Mousterian industry. The upper part of this sequence was ^{14}C dated to an age of 39'222±2956 uncal BP, averaged over five dates from levels D2, D1, C and B (Rink et al., 2002:949); however, these figures were somewhat uncertain because dates on bone did not fit perfectly with charcoal ages, even if almost all of these fell largely within the range for the ESR ages of level E1, *i.e.* 39±5-49±9 (LU) or 46±8-32±4 (EU) ka (Rink et al., 2002).
Considering the extremely scanty evidence of Aurignacian presence in this area, the simplest approach to solving the problem of the peopling of the area at the Middle to Upper Palaeolithic Transition, is to systematically date the most recent evidence of Neandertal presence in all stratigraphically reliable Mousterian sites. Secondarily, climate change versus human adaptations should be explored in order to infer possible correlations between climatic events and Neandertal demise.
The main goals of this paper are the following.
1) Reconstruct climate change and Neandertal behaviour in the Dalmatia area during MIS3 by using geoarchaeological data, in order to correlate modes and peculiarities of the human presence in Mujina Pećina with climatic constraints that may have resulted in Neandertal adaptation and possibly demise. This goal can be achieved through a detailed sedimentological and soil micromorphological analysis of the sequence.
2) Improve the chronology of the sequence by new datings on previously undated contexts, and by re-dating the ones that yielded contrasting results.
3) Discuss previous radiometric datings carried out on the Mujina Pećina sequence in the light of the climate data obtained by the geoarchaeological study, with the help of bayesian modelling of

the dates.

2. Site presentation

Mujina Pećina is situated on the right side of a deep karstic gorge crossing the Labinštica Hills, north of the city of Trogir, and facing on Kaštela Bay. It lies about 60 m above the present-day bottom of the gorge, and a few tens of metres below the top of the overlying plateau (Fig. 1). The area is tectonically complex, with stratified limestones and massive and stratified limestones overthrust onto foraminiferal limestones. The close surroundings of the cave are characterised by outcrops of deeply karstified limestone and moderately high cliffs deeply fractured by a minor fault that can be followed for several tens of metres on the gorge side; coarse scree and rock-fall/debris-fall deposits (*sensu* Blikra and Nemec, 1998) are active within the steep and often narrow spaces among the rocky outcrops, and are also widely developed all over the gorge side. The cave opens at the base of a 10-12 m-high, vertical and smooth cliff that is the hanging wall of the fault. A small debris-fall cone flowing out from a narrow couloir partly enters the cave from the southern side of its entrance (Fig. 2). The cave comprises an inner, elliptically shaped chamber 6x8 m wide, connected with the exterior by a short but wide corridor (Fig. 3). Walls and ceiling are rather smooth, but strong fracturing is evident within the overlying rock mass.

3. Cultural background and lithic industry

Excavations carried between 1995 and 2000 (Rink et al., 2002) put into light a sequence about 180 cm thick, including archaeological stratigraphic units A, B, C, D1, D2, E1-E2, E3 (from top to bottom). Further fieldwork carried out until 2003 deepened the excavation to the cave bedrock, at about 220 cm, and a more articulated set of stratigraphic units E2A, E2B (subdivisions of E2) and E3A, E3B and E3C (subdivisions and extensions of E3) was put into light. Correspondence between these archaeological stratigraphic units and the lithologic units defined in this paper (Fig. 4) is given in Table 1.

All lithic finds excavated from the stratigraphic units of the site can be ascribed to the Mousterian industry (Petrić, 1979; Malez, 1979; Karavanić et al., 2008). Levallois débitage, without Levallois cores, was detected in levels D1 and D2 (about 20%), whereas the frequency of such finds in level B is questionable. In levels B and C flakes are the dominant technological product, and up to 1/3 of the lithic assemblage is comprised of tools. The most frequent tool types are denticulates and notched pieces; these are mostly small (around 3 cm in length) and strongly resemble the so-called Micromousterian. Of the total lithic material from levels D1 and D2, only about 1/5 are definite tools, the most frequent types being simply retouched flakes. These tools were made from local chert pebbles and nodules, which are often small. It seems more likely that the expedient use of small pebbles available near the cave, as well as the poor technological properties of larger pieces of some local chert, limited the tool size in the Mousterian of Dalmatia, rather than the intentional choice of small pebbles for the production of small tools (Karavanić et al., 2008).

Pollen of deciduous and coniferous taxa was found in levels E3, E2 and E1, i.e. hornbeam (*Carpinus betulus*) and alder (*Alnus* sp.), and pine (*Pinus* sp.) and spruce (*Picea* sp.), together with pollen of grass (Gramineae). In the charcoal assemblage, pine was common, as well as a number of deciduous species, such as blackthorn (*Prunis spinosa*), rowan (*Sorbus* sp.), and hawthorn (*Crataegus* sp.). Small fragments of the heliophilic sea-buckthorn (*Hippophae rhamnoides*) are also present. Charcoal fragments from unit D are mostly juniper (46 pieces), with some linden (only 2 pieces) and indicate a colder climatic oscillation; only pine pollen was found in unit C, whereas charcoal and pollen of pine, spruce and birch were found in unit B, as well as grassland vegetation

pollen and the heliophilic shrub joint–pine (M. Culiberg personal communication; Karavanić et al. 2008).
Faunal remains were identified and studied only for the uppermost levels (B-D) of the sequence (Miracle, 2005), whereas the study of the lower part of the sequence is still in progress. The faunal composition shifts from a codominance of red deer and chamois-ibex in Layer D1-D2, to a clear dominance of wild caprids followed by large bovids and equids in Layer B-C (Miracle, 2005:84). These faunal remains also show clear differences in species frequency between D1 and D2 (Miracle, 2005). There is strong evidence that people used the cave in autumn throughout the sequence (at least in some of the analysed layers), as well as for spring visits in level B (Miracle, 2005). Conversely, there is no evidence for human activity in Mujina in summer and winter, whereas bears occupied the cave in winter during the deposition of level B. Two localized areas of burning, probably representing open, unstructured and unpaved, Mousterian hearths, were found in occupation level D2; anthracotomical analyses show that *Juniperus sp*. was used for fuel in both hearths (M. Culiberg personal communication; Karavanić et al., 2008). The oldest levels (E3, E2, E1) of the Mujina Pećina sequence are the richest in finds, indicating much more intensive human activity than in the more recent levels. Although no human skeletal remains were recovered, given the nature of the lithic assemblage and the radiometric dates, it can be assumed that Neandertals were responsible for the evidence of human occupation at the site. The analysis of lithics and animal remains from the lower levels is still in progress.

4. Materials and methods

4.1. Geoarchaeology

The geoarchaeological study of Mujina Pećina was carried out on the sequence uncovered during the I. Karavanić excavations of 1995-2003. Study of the sequence and sampling of the lithologic units were carried out *a posteriori* on the excavation profiles, well after the end of the excavation; consequently, little information about the 3D geometry of the boundaries was available in the field. However, the good quality of the documentation, as well as productive interaction with the excavation team, proved vital in the interpretation of the field evidence.
The deposit was divided into lithologic units largely corresponding to the stratigraphic units observed during the excavation; only in a few cases were these split into more lithologic units; the description follows the guidelines of Catt (1991). The architecture of the units and their stratigraphic relationships were interpreted based on the geomorphologic characteristics of the cave and of its outside catchment. Each lithologic unit was sampled for grain-size analyses, the size of the bulk samples depending on the grading of the unit, generally 15 to 20 kg because of the large number of stones. The coarse (>2 mm) component was measured on the whole sample at 1Φ precision by dry sieving and direct weighing in the field. Note that the clasts were sieved based on their minimum diameter, consequently, elements significantly longer than the mesh size may fall within each class. Two-dimensional estimates of clast shapes were carried out by image analysis techniques on photographs of the whole 16-32 mm grain-size fraction, which is the most abundant in almost all units. Aliquots of 50-100 g of the fine (<2 mm) sediment were graded at 0.5Φ by wet sieving for the 2-0.063 mm fraction, and by Bouyoucos aerometer for the < 0.063 mm fraction; grain-size analyses of the fine (<2 mm) fraction were also conducted on HCl 1N decalcified samples.
Undisturbed sediment monoliths for thin-section preparation were also collected. Not all the lithologic units were sampled: in large part of the sequence, the fine fraction is few if compared to the whole sediment volume, and is situated in small spaces among large limestone clast. Consequently, there were technical difficulties in sample collecting that were not justified by the expected results, i.e. sample size versus sample area useful for soil micromorphology. Six samples

for micromorphological analysis (units B, D-4, D-5, two samples from E2A-8, and E3C-12) were collected from the southern profile, located between squares D 7-8 and E 7-8. The monoliths were air-dried at 30°C in a ventilated oven for 7 days, and then impregnated by low-viscosity acetone-diluted polyester resin under moderate suction; polymerisation was carried out under atmospheric pressure for about 90 days.
The thin sections were cut using a diamond disk and ground to 30 μm by corundum abrasive powders, using petroleum for cooling, and covered by a standard optic glass slide. Depending on the monolith size, 90x60 mm or 60x45 mm thin-sections were prepared. The thin-sections were observed under a Leica DM/LP standard petrographic microscope equipped with reflected light and UV/blue epifluorescence kits. The descriptions follow the standard formalised by Bullock et al. (1985) and Stoops (2003) for soil thin-sections.

4.2. Magnetic susceptibility (χ): general aspects
For many years the magnetic susceptibility (χ) of micro-stratigraphic, essentially continuous samples has been measured for sediments recovered from well-documented Pleistocene and Holocene archaeological sites in Europe (*e.g.*, Harrold et al., 2004). Changes in χ are based on the fact that pedogenesis produces magnetic grains, primarily magnetite and maghemite, and that regional, long-term climate cycles (hundreds to thousands of years) control pedogenic variations and therefore the amount of magnetic material created. This material is then eroded from outside of caves and deposited in caves, with the resulting stratigraphy providing samples for χ measurement. It is clear that caves and deep rock shelters are ideal for χ studies of palaeoclimate, because, due to their isolation within caves, deposited sediments are not strongly modified by pedogenic effects after deposition. Therefore, cave sediments often provide a good record of climate change as a result of variable rates/intensities of soil formation outside of caves, primarily as a result of variations in pedogenesis versus eolian influxes (Harrold et al., 2004).
It has been possible to evaluate empirically the χ method for sediments deposited over the last 46 ka, because there are a number of cave successions that have been dated using ^{14}C methods. These data were used to build a composite reference section (CRS) for southern Europe using χ data and available uncalibrated ^{14}C dates in combination with climatic indicators from many successions sampled. These data were then correlated using the graphic correlation method (Shaw, 1964). Harrold et al. (2004) demonstrated that the CRS developed using this approach correlates well with independent climate indicators. It was argued that χ can be used to correlate among widely separated caves throughout Europe because the regional climate signature resulting from pedogenesis outside caves is recorded in caves by the slow, systematic influx of eroded surface material into caves, producing the time-depth-climate pattern observed. These trends may be modified locally, but in general the variations in χ produced by changing climate provide stratigraphic sequences that can be correlated between excavation units that overlap in age.
In developing an effective relative dating technique, there must be some age constraints before relative ages can be useful, but once such constraints are applied in developing an effective CRS, they can often provide very precise estimates of age in the stratigraphic section to which the CRS is being compared. Here, this CRS is applied to three measured sections from Mujina Pećina; MPA and MPC (to the East side of the cave, one sampled in 2003 and a second sampled in 2004), and MPB (to the West side, one section), where 19 ^{14}C dates are available.
Three continuous sample profiles, each sample covering approximately 2-3 cm of the vertical section, were collected from excavated profiles in Mujina Pećina (Fig. 3). Thirty one samples were collected for χ measurement from the western MPB succession, and sixty one samples from the

eastern MPA succession in 2003, and sixty five samples were collected in 2004 from the eastern MPC succession for measurement. Each sample was then sieved and carefully weighed, and the <1 mm sediment fraction was measured 3 times using the susceptibility bridge in the Rock Magnetism Laboratory at Louisiana State University. Measured χ was then calculated and interpreted. The <1 mm fraction was used in this measurement to remove non-detrital sediment material from samples, such as bone and large carbonate fragments, that are not climate controlled constituents and because of their large mass might otherwise dominate the mass-dependent χ.

5. Results

5.1. Architecture of the stratigraphic units

The layering of the cave infill is largely comprised of units shaped as more or less continuous layers, or as lenses thinning down towards the inside of the cave (Fig. 5). When observed along the longitudinal axis, all these units dip more or less gently towards the outside; their slope is largely controlled by the dip of the limestone bedrock, which is inclined towards the outside with an angle of about 15°. The dip of the stratigraphic units decreases from the bottom upwards, the lowermost ones being roughly parallel to the cave bottom, whereas the uppermost ones are approximately horizontal. Along the transversal profiles, the situation is not always fully clear, mostly in the entrance area, which is key to understanding the infilling process. A large part of the excavation area is situated in the wider catchment inside the cave, whereas only a narrow trench could be excavated along the northern wall of the entrance. Here, the units are approximately horizontal along the transversal profile of the cave, or dip gently towards the North, or are concave upwards, climbing slightly against the northern wall. The boundaries of units are somewhat complicated by undulations and probably also by erosional features, particularly in the lower part of the sequence. Unfortunately, the coarse texture of the units complicates the real shape of the boundaries of the units and hinders a fully reliable interpretation of their geometry. The top of unit E1-6 is marked by a discontinuity: it is concave-upwards, mostly along the transversal profile of the cave and to the inside, and dips gently outwards in the entrance area; its shape is also clearly defined by the vertical distribution of flint artefacts and of bones (Nizek and Karavanić, 2012). It divides the sequence into two distinct parts: the units overlying it are mostly rather thick and well-developed tabular layers with linear limits, covering the whole cave area. Conversely, the units from E1-6 downwards are mainly lenses tiled one upon the other towards the inside of the cave, the upper ones being more extended inwards. Within the lower part of the sequence, represented by the bottom limit of unit E2B-9, is apparently an erosional feature. This is observed along the longitudinal axis of the cave and is characterised by some major undulations, whereas it is clearly concave-upwards along the transversal direction in the entrance area. Here, it dips towards the centre of the cave, unlike the underlying layers that dip in the opposite direction. Consequently, unit E3A-10 is somewhat eroded and occurs only in the outermost part of the cave. One other minor erosional feature can be observed at the top of unit D in the inner part of the cave; this is filled by unit C, which consequently occurs only in a limited area.

5.2. Sediment texture

The whole Mujina Pećina sequence is largely dominated by stony sediments (Fig. 4), with stones mostly included within the fine- to medium-size gravel classes, and without major differences between units. Conversely, matrix quantity, though always less than 20%, varies significantly throughout the sequence, and in some cases also within the same unit. Figures 6 and 7 represent grain-size profiles in two areas of the cave, the former from a sequence (Tab. 1) close to the

entrance and the latter (Tab. 2) from well within the cave (Fig. 3). This matrix is more abundant in the lower part of the sequence, underneath the erosional surface situated at the top of unit E1-6; here, it ranges between 7 and 17%, with two peaks corresponding to the dark units E3C-12 and E3A-10. It then decreases slowly from E3A-10 upwards, and peaks again in the reddish horizon that marks the top of E1-6. There is very little matrix material in the upper units, with a minimum of 3% in all of Level D and a secondary peak of 6-7% in B-3. It is noteworthy that D is much richer in matrix (up to almost 20%) in the inner part of the cave.
The grain-size of the fine (<2 mm) fraction includes an almost constant silicate sand component (Fig. 6 and 7, decalcified sample diagrams) that can be identified as quartz in thin section. In the undecalcified samples, the sandy fraction is much more abundant, including limestone elements and $CaCO_3$-cemented aggregates of finer particles. The clay-size fraction is generally more abundant in the decalcified samples (Tab. 3), showing that there is a component of fine carbonates, probably deriving from secondary crystallisation, apart from units E3C-12, E3A-10. The distribution of the fine-grained component is always poorly sorted, with a principal maximum in the <2 μm class and a secondary one usually in the 31-23 μm range; a secondary maximum in the 11-7 μm class characterises the units where clay is >50%, *i.e.*, unit D in its bottom part, in the facies found in the cave interior, and E1-6. In all the other cases the clay component is around 20% of the fine-grained component. Clay is at a minimum in unit E2B-9 (about 20%), where the graphic mean is 14.6 μm, significantly higher than in the other units, where it is bracketed between 9 and 12 μm. All the lowermost units, up to E1-7 (Fig. 8, panel C), are rather silty, with clay between 20 and 40% and roughly increasing upwards. Conversely, units E1-5 and B are dominated by clay that ranges between 50 and 70% (Fig. 8, panel B). The uppermost units are again more-silty, with clay around 25-30% (Fig. 8, panel A). Higher matrix quantity usually corresponds to a smaller grain-size of the skeleton, or to its poorer sorting.
In general, the coarse elements are not homogeneously distributed throughout each unit, but tend to be organised into secondary horizons that are characterised by elements of different size, or by somewhat better sorting. This is evident mostly in the thicker units, like D and B, where these horizons are well developed. These features are evident from the orientation of the platy and elongated clasts, which generally lie parallel or subparallel to the unit boundaries. However, a better orientation is evident in the units of the lower part of the sequence, where the elongated elements are more common; some convoluted features can be observed between units E2A-9, E2B-10, E3B-11 along the longitudinal profile. The size of the skeleton elements does not change strongly through the profiles, and is generally included largely within the grain-size classes of the 16-32 and 32-50 mm, with minor maxima of coarser elements corresponding to units E3B-11, E1-7, and to the lower part of B in the outer part of the cave. Conversely, B is somewhat finer and D is coarser toward the inside of the cave. Larger pebbles and cobbles occur sparsely within units E1-7 and E3A-10, and sometimes also elsewhere.
The coarse fraction (>2 mm) is characterised mostly by elongated and some platy elements, and these can be subdivided into two shape classes based upon their breadth versus length (B/L) ratio; those between 0.6 and 0.8 being the most frequent, whereas much more elongated elements, with 0.25<B/L<0.4 are less frequent. Linear best-fits computed for all the samples divide them into two strongly different groups (Fig. 9), indicating the statistical weight of each of the two classes within samples. The lesser is the slope of the interpolating line, the more relevant is the amount of shorter/broader elements. These are apparently dominant in units B and D, mostly in the upper part of the latter, whereas the elongated elements occur mostly in the units of the lower part of the sequence. Unit E3A-10 differs strongly from adjacent units because it includes a strong component of subequant elements; although, this estimate may be uncertain because of the small number of measured elements. The skeleton elements are generally angular of somewhat

subangular because of surface dissolution, whereas the subrounded or rounded elements never occur.
The rather battered aspect of some stone tools is not unexpected in the stony sedimentary environment of Mujina Pećina, and may derive from movements of the sediment and/or pressure exerted on flints by the clasts, due to load during compaction of the lithologic units.

5.3. Soil micromorphology

The main micromorphological characteristics of Mujina Pećina sediments are summarised in Table 4.
The fine component of the sediment does not always occupy the whole space among stones, leaving wide voids in a generally clast-supported structure. The coarse skeleton component is relatively scarce at microscopic scale, and the larger clasts are almost only limestone or cultural remains, whereas the silcate component is absent.
Microstructure is almost always granular, weakly to well developed, and more or less disturbed by channels and chambers. In some cases it is subangular and blocky with moderately to highly separated peds (unit B), or pellicular-grained (unit D-5). The granular microstructure (Fig. 10a-b) can be referred to sediments subject to frost action (Van Vliet-Lanoë, 2010, and reference therein), whereas the blocky aggregation can also be due to subsequent shrinking-and-swelling of the relatively clayey sediment under wetting/desiccation cycles. The occurrence of silt cappings on skeleton grains (Fig. 10c-d) corroborates the hypothesis of seasonal frost affecting the sediments.
The related distribution pattern is porphyric (layers E2A-8, E3C-12) to open porphyric (layers B and D-4) with the exception of layer D-5 where it is chitonic and gefuric. The b-fabric is always crystallitic in the upper units (B, D-4 and D-5), mostly due to widespread microsparite impregnating the whole micromass, while stipple-speckled fabric dominates in the lower units (E), occasionally with more complex patterns of strial (E2A-8) or parallel striated (E3C-12) b-fabric. Granostriated b-fabric occurs in units B-3, E2A-8, and E3C-12, and is more common in E3C-12, where it is also associated with porostriated b-fabric. These characteristics of the b-fabric are in accordance with the aforementioned wetting-drying cycles, indicating some reorientation of clay particles due to stress within the sediment.
In general, the aforementioned characteristics are remarkably homogeneous throughout the sequence, with minor variations between the units of the whole sequence, and some lateral change within the same unit.
The assemblage of minerals identified in thin sections is relatively homogeneous throughout the sequence, with the same minerals and rock fragments occurring in almost all layers. Quartz is the most important mineral among the silicate components. Muscovite is also very common and occurs in silt-size laminae; biotite was also sometimes observed. These minerals do not occur in the local limestone and dolomitic limestone bedrock, and are likely to derive from exotic inputs as windblown dust, because of the angular shape and small size of the particles (very fine sand- to silt-size) . Calcite occurs everywhere in the sediment, mostly as micrite aggregates or as sparite subhedral to euhedral crystals deriving from the fragmentation of speleothems, less frequently as impregnative pedofeatures.
Among the rock fragments, the coarse skeleton includes mainly limestone (biomicrite and subordinate biosparite embedding detrital carbonatic grains, foraminifera, bryozoans etc.) (Fig. 10c-d). Micritic limestone clasts are somewhat altered and can be sometimes subrounded. The limestone clasts are often platy, their shape being controlled by the layering and fracturing of the local bedrock. There is also a significant amount of chert in unit B and in the group of units E, mostly within the lowermost layer E3C-12. This component is generally not present within the

local rock, but control micromorphological samples collected from soils and colluvia in the surroundings of the site indicate that detrital chert is very common in some relatively close areas situated higher in the Labinštica Hills, and that chert may derive from colluvia. Chert clasts with special shape may also derive from human activities (Fig. 10e-f) (Angelucci, 2010), and occur mostly in unit E3C-12, which includes a larger amount of cultural remains also at eye-scale.
Among the organic components, bone is almost always present, sometimes also burnt; in units E3C and E2A bone fragments (cancellous and compact tissue) sand-size or larger and unsorted are extremely frequent and give the sediment a peculiar yellowish-brownish colour under parallel polars (Fig. 11a-c). Sand- and silt-sized amorphous organic matter aggregates, sometimes mineralised and sometimes charred, and charcoal fragments are also present, as well as organic punctuation, occasionally giving a darker colour to the matrix (Fig. 11d). No structure can be observed in small-size elements, whereas the larger ones sometimes preserve shapes that are evocative of vegetal tissues. These organics are frequent in E3C-12 and E2A-8, and occasionally also in layer B.
A large presence of phosphate aggregates is evident in units B-3, D, E2A-8. In unit B-3, these are greyish, with quartz grains inclusions, small bone fragments, teardrop vesicles, casts of hairs and hair follicles. In D-4, the most relevant of these aggregates are yellowish with greyish speckles in PPL, the speckles being more strongly fluorescent under blue epifluorescence; the background is formed by small rounded aggregates of grains/nodules. Mineral grains, vesicles and hairs are also common(Fig. 12a-d). All these can be be identified as carnivore coprolites (Kolska Horwitz and Golberg, 1979; Goldberg 1980).
Nodules of Fe and/or Mn oxides often occur in all the units; clay aggregates (pedorelics) including angular quartz skeletal grains (Fig. 13a-b) and sometimes with stipple speckled b-fabric are also present, together with reddish clay aggregates, papules *sensu* Brewer (1976) (Fig. 13c), and occasional “rolling pedofeatures” (Fig. 13d). Together with the poor sorting of particles, all these are indicators of colluvium processes (Goldberg, 1979; Coutry et al. 1989:93; Boschian, 1997). Secondary carbonates were also observed in E3C-12 and E2A-8 samples.

5.4. Chronology

The chronology of Mujina Pećina is based on ^{14}C datings that were carried out in three phases and by three different laboratories (Table 5): the upper units of the sequence and the E1/E2 interface were dated in the early 2000s, when excavations were still ongoing (Rink et al., 2002). These units include the last phase of the intense frequentation of the site by humans, and the subsequent phase that was dominated by the presence of cave bears (Miracle, 2005). The lowermost units, including the main phase of most intense human frequentation, were dated recently and are presented in this paper. All the datings were performed on bone, apart two on charcoal from unit D2.
Dating bone posed serious problems when different pre-treatment methods were applied (Fig.14). The bone samples dated during the excavation were processed at the AMS facility of Gröningen University, where the pre-treatment procedure of Longin (1970) was performed (Rink et al., 2002). The samples from the lower units, including some overlapping with the previously dated ones, were dated at the Beta Analytic AMS facility, where bone "collagen" was extracted by alkali attack and ultrafiltration. In this case, a large part of the results are much younger than expected (approximately between 33 and 24 ka uncalibrated BP), and apparently inconsistent with the stratigraphic and chrono-cultural data (Higham et al., 2014). Considering that no cultural horizons younger than the Mousterian were found in the site, and that no recent contamination was expected or detected on the samples, the dating was repeated twice on remaining aliquots of the

same samples, using again alkali attack/ultrafiltration, and also standard alkali attack pre-treatment (D. Hood, personal communication). The results of the second ultrafiltration batch are somewhat comparable with those of the previous one, even if shifted by some thousands years (approximately between 30 and 26 ka uncalibrated BP), whereas only one sample (E3B-11) falls within the expected time interval, but is older than the Beta Analytic background age (43.5 ka). Conversely, the results of the standard alkali extraction are generally consistent with the stratigraphy and – rather interestingly – with the non-ultrafiltered Gröningen results (between 48 and 44 ka uncalibrated BP, but beyond the background), with one single sample resulting too recent (E3A-10, about 31 ka uncalibrated BP).
Regarding the reliability of these results, it must be observed that:

1) Unlike what is normally expected, the results of ultrafiltration pre-treatment are in general younger than the non-ultrafiltered ones.
2) There is a common trend in the results of ultrafiltration, as datings carried out on the same sample in the first batch are systematically younger than those carried out in the second one. Moreover, the results of alkali pre-treatment on the same samples are systematically older than the ultrafiltered ones.
3) Even if the standard deviation of the results of ultrafiltration is often quite small, the results do not overlap at 2σ (and frequently even at 3σ). This aspect poses serious doubts about the reproducibility of the measures.

A single date on charcoal (OxA-8150) collected from one of two areas of burning, that probably represent Mousterian hearths (Rink et al., 2002), gave results at least 6 ka younger than the age of the bone (GrA-9639) sampled in the same unit D2, and consequently its age is inconsistent with the other dates; when repeated on another charcoal sample from the same unit, the dating (Beta-393072) gave an age that is fully consistent with the result of bone dating (GrA-9639) and with the stratigraphy.
Eventually, a third attempt to date the oldest Mujina levels was carried out. Bone samples from units E2A, E2B, E3A and E3C were processed at the University of Oxford Radiocarbon Accelerator Unit using ultrafiltration pre-treatment, following the method described by Bronk Ramsey et Al. (2004a, 2004b). Sufficient collagen was extracted only from the samples from units E2B and E3A, which yielded dates >44'300 (OxA-31938) and >44'400 y BP (OxA-32243) respectively.
Following these considerations, a limited number of apparently consistent dates were retained for further analysis and sequence chronology assessment. These include the results of standard pre-treatment obtained by Rink et al. (2002), the new date on charcoal from unit D2 (Beta-393072), and the new Oxford resultsOxA-31938 and OxA-32243. The Beta Analytic results of standard pre-treatment are in general consistent with the stratigraphy and the Gröningen results, apart E3A, even if older than the background.
These results can be considered as largely contemporaneous after simple calibration. A bayesian model was also run by OxCal 4.2 (Bronk Ramsey, 2009), mostly in order to compute the deposition rates of the sediment. The Mujina sequence was constrained at the base by the date obtained for unit E3C-12 (Beta-393076), which is older than the background, but very close to its limit; it can also be used in the model being provided with standard deviation, unlike the Oxford ones that do not come with sigma or F14C. As suggested by the field evidence, a gap was inserted between the top of the E units sequence and the base of the D-B-units. The dates for units D2 and D1 were grouped in a phase. The results (Fig. 15 and Tab. 6) appear to be consistent with the stratigraphic sequence.

5.5. Magnetic susceptibility (χ) results

Three successions were sampled for χ from Mujina Pećina (Fig. 3), and the data are reported in

Figures 16 and 17. The MPC successions also had seven apparently reliable uncalibrated ^{14}C ages (out of the whole 19 carried out) spanning most of the section. These ages, along with the χ bar-logs developed from the χ data, made it possible to directly correlate to the Southern Europe master Composite Reference (CRS) data set of Harrold et al. (2004), and demonstrated that climate zones from CRS SE 35 through SE 31 are present in the Mujina Pećina sections (Fig. 18). The ^{14}C ages from MPA and MPC are in general agreement with the ages reported by Harrold et al. (2004). Processes like bioturbation, and others, can disrupt the record, but such effects are 'averaged out' when using a robust data set of essentially continuous samples. If there were internal cave effects that dominated the magnetic susceptibility, then there would be no possible correlation to the Harrold et al. (2004) data set, nor would there be relatively uniform, cyclic behaviour in the magnetic susceptibility pattern.

Climate interpretation for the Mujina Pećina successions indicates an alternating cyclicity of warm to cold climate lasting for ~6 ka, commencing with CRS SE 35 (Harrold et al., 2004) warm event at ~46 ka BP (uncalibrated), with warm–cold alternations through to ~39 ka BP. These data are consistent with ^{14}C ages for the successions. The transition from warm climate into cold climate occurs at ~44.5 ka, and is approximately coincident with timing of the cold marine Heinrich Event H5. This event lasted for ~5 ka, the interval in the MPC sections in Mujina Pećina representing CRS SE 34 to the beginning of SE 31, as represented in the χ data when compared to Harrold et al. (2004). Examination of this interval at Mujina Pećina shows that the χ data are generally low through that interval, Units E1 to B, with a slight, low-magnitude warming that represents the CRS SE-33 warm event (Harrold et al., 2004).

6. Discussion

6.1. Site formation processes and climate change

Three basic processes controlled deposition within Mujina Pećina, (1) accumulation of rubble deriving from roof spall within the cave, and (2) external inputs connected to the activity of the outside scree, or (3) to in-wash of fine components. Considering that the rock of the ceiling and walls usually breaks apart into elongated clasts because of its tectonic fracturing, whereas the scree rubble is somewhat equant, the relevance of each sedimentary component in the formation of a unit can be estimated upon the shape/trends of its skeleton. The upper part of the sequence (units D-4 to B) can be clearly differentiated from the lower ones (units E3B-11 to D-5) using the following observation: values of the inverse of the slope of the best fit line less than 0.75 (Fig. 9) indicate dominance of elongated clasts deriving from roof spall, whereas those greater than 0.75 are connected to external inputs. However, these groups cannot be differentiated well, and the strong superimposition of the two shape groups testifies to a mix of both components; furthermore, it is also evident that equant or moderately elongated elements are always more frequent than those that are prolate, demonstrating that external inputs were always more important than was roof spall.

The composition of the sediment also depends on its position within the cave, as is clear from the differences in the sequences of samples B-2, B-2.1, B and D-4, D. These were collected in different loci, each one progressively further inside the cave, and including progressively more prolate elements, showing an increasing relevance of roof spall to a location further inside the cave. Unit E3B-11 is the richest in internal components, while E3A-10 is problematic because of the small number of measured elements. These data show that the outer scree activity increased through time, and became more important during the last phases of deposition, *i.e.*, in units D to B. This hypothesis is also corroborated by the architecture of these units, which tend to be subhorizontal or dipping slightly towards the inside and North of the cave. These units are much

thicker, indicating higher deposition rates. Units E2B-9 to E1-6 are much thinner but can also be included within this depositional scheme, even though they dip slightly towards the outside of the cave. In fact they are subhorizontal along a transversal profile at the entrance of the cave and also tend to climb against the northern wall, as may be expected if they are connected to the outer scree. At their distal ends, these units are organised into relatively small lenses, as is normal during distal debrisflow deposition.
The lowermost units, E3C-12 to E3A-10, are organised in somewhat thicker lenses that dip more steeply towards the outside of the cave, and whose skeleton, at least in E3B-11, is dominated by elements of internal origin. This suggests deposition of internal clasts even if the scree component is always clearly present. It must also be pointed out that the top of this part of the sequence is marked by a clear erosional surface, even if not well documented in the sequence. Consequently, we hypothesize that major erosional processes shaped this part of the sequence, removing part of the sediments that had been accumulating as a result of ceiling and wall dismantling. In fact, erosional phases that may have removed relevant parts of the sequence are indicated by the occurrence of extensive residual bodies of cemented rubble without matrix, adhering to the northern wall of the inner cave, well above the present-day floor. Unfortunately, these bodies cannot be stratigraphically correlated to any of the units of the excavated sequence, and they do not include cultural or faunal remains; consequently, their stratigraphic meaning is limited.
The processes inferred through the study of the coarse fraction are corroborated also by the characteristics of the fine fraction. The matrix, though always less than 20%, is by far more abundant in the lowermost units, where it peaks in E3A and decreases steadily through the overlying units, with a second maximum in E1-6. However, major differences arise at the grain-size distribution level, indicating that different processes influenced the deposition of this component through time. The lowermost and uppermost parts of the sequence are characterised by a silty-clay loam matrix, with the exceptions of E2B-9 and E2A-8, where it is respectively silty-loam and clay. Conversely, intermediate levels D-5, D and E1-6 include a clay matrix. In general, all these matrices are too rich in clay to be classified as primary loess (Ferrari and Magaldi, 1976; Cremaschi, 1990a). In fact, the silt percentage is often greater than 60% (Table 3), but this peculiarity results from the very low sand quantity, and only E2B-9 falls within the limits of the primary loess field. The texture of the Mujina samples fits the palaeosols included within the loess sequences of Susak Island that largely overlaps the cave sequence (Cremaschi, 1990b; Mikulčić Pavlaković et al., 2011; Wacha et al., 2011; Krajcarz et al., 2106), with a significantly lower sand component, which may indicate distal loess deposition and/or a loss of wind flow energy due to the relatively high location of the cave within the hills.
Samples from units D-5, D and E1-6 are by far dominated by expansible lattice clay with reddish hue derived from Fe-oxides, which indicate colluvium of medium-long evolution soils developed outside the cave, mostly Alfisols (*sensu* Soil Survey Staff, 2014) including the local *terra rossa/zemlja crvenica* soils. This process is also identified at the microscopic level with pedorelics and/or papules indicating inputs of allochtonous sediment or soil, previously deposited outside the cave and transported into it by in-wash. The hue is reddish also in E2A, where clay is significantly less evident in the grain-size curves. However, these pedorelics are common in this unit, indicating in-wash of aggregated clay.
Two similar cycles probably correspond to layer couplets E2A-8/E1-7 and E1-6/D-5, each one including a thin matrix-rich layer overlain by a thicker accumulation of rubble with low matrix. Considering that no evidence of clay accumulation after leaching through the profile is observed at the microscopic scale, these couples probably represent phases of strong soil erosion and runoff followed by the reactivation of the scree, generally indicating morphological instability under fresh and strongly variable wet/dry conditions, as testified also in other southern Mediterranean sites

during the colder and wetter periods of the stadial phases (Di Maggio et al., 1999; Cottignoli et al., 2002).
Freezing and thawing cycles are recognisable at the microscope level in layers D-4 and D-5, where silt cappings (Fig. 10c-d) on coarse skeleton elements testify to phases of deep seasonal frost subsequent to the deposition of the sediments, *i.e.*, during the deposition of D4 or later. The uppermost units of the sequence, *i.e.*, B-1.2, and B, are characterised by a loess-like percentage of silt, even if the relatively high quantity of clay suggests some alteration. C was not sampled because it was completely removed during the excavation, but can probably be considered as a subunit of B.
All these characteristics indicate a strong variability of the environmental conditions, that were generally cold or fresh, and with oscillations between a more or less aridic *régime*. This is mostly evident in the upper part of the sequence, whose units are usually somewhat thicker than the underlying ones. These data also indicate rapid deposition of scree rubble, whereas the lowermost units were deposited more slowly and under steadier conditions, generally cold/aridic favouring the sedimentation of aeolian dust, but with somewhat warmer episodes indicated by less coarse fraction in the lowermost E3C-12 and E3B-11 units. These considerations fit also the depth model deriving from the bayesian modelling (Fig. 19), which shows higher deposition rates in the upper part of the sequence; it must also be pointed out that the minimum oldest age provided by the model is a parsimonious estimate deriving from the age of the radiocarbon determination background, consequently deposition rates may be much lower than indicated by the model in the bottom part of the sequence.
These results are consistent with the χ results discussed below. In fact, it is rather unlikely that the aeolian dust found within the cave is primary, mostly because of the peculiarity of the cave environment. It is more probable that sub-primary loess, more or less altered, entered the cave because of runoff a short time after its deposition in the outside catchment.
Unfortunately, faunal data are available only for the upper part of the sequence (Miracle, 2005), *i.e.*, for units B, C and D, and we eagerly wait for new data from the lower sequence. The hypotheses concerning palaeoenvironmental change, drawn from pedostratigraphy data, apparently match the change in faunal composition, which indicates "*more temperate conditions (perhaps with more shrub/forest cover) in layer D1+D2 changing to cooler (increase in chamois/ibex), more open (increase in equids) conditions in Layer B+C*" (Miracle, 2005: p. 90), despite previous preliminary interpretations of the sedimentological characteristics (Karavanić and Bilich-Kamenjarin, 1997; Rink et al., 2002) that apparently contrasted with the faunal data. In fact, chamois/ibex and equids fit well in an open and somewhat aridic environment dominated by aeolian processes, whereas discontinuous shrub cover is more likely than forest in phases of instability, as during the deposition of unit D.
Archaeobotanical data are in reasonable accordance with this interpretation, mostly as to the upper half of the sequence, even if it must be pointed out that charcoal data may not reflect accurately the composition of the arboreal vegetation assemblage because these woods may have been selected or haphazardly collected for fuel by hominins.
All together, the vegetal remains of units D to B indicate open vegetation with rare trees or shrubs (M. Culiberg personal communication; Karavanić et al. 2008), conversely, charcoal and pollen remains from units E3, E2 and E1 (Karavanić et al. 2008) indirectly suggests warmer climatic conditions, even though no indications were provided about oscillations within this part of the sequence.
Pine and spruce, found in association with the indicators of warmer environment, may have been connected to the colder and/or aridic phases of the E3-E1 archaeological levels, including loess unit E2B-9 and stony unit E3B-11. Conversely, thermophilous deciduous species may have been

better represented in E3C-12 and E3A-10 that are characterised by higher matrix content and less coarse fraction. It is also possible that some part of the sequence, representing a colder maximum preceding the loess deposition of E2B-9, may have been removed by erosion, as indicated by the erosional boundary between E3A-10 and E2B-9.

6.2. Chronology

Not very surprisingly, the results of the ^{14}C dating of the Mujina sequence confirm that pre-treatment is crucial to the correct determination of the sample ages (Brock et al, 2013, and reference therein). However, these results are also somewhat unexpected, because ultrafiltration gave results that are much younger than those obtained by alkali attack. Moreover, results obtained with the same pre-treatment are not consistent, showing remarkable time shifts as well as non-reproducibility of the measures (Fig. 14).

The ESR dating of unit E1-7 (Rink et al., 2002) does not fully clarify the issue, even if its results are generally consistent with the ^{14}C ones (Fig. 20). The ESR ages are strongly scattered through time, and with sigma range including widely the whole set of ^{14}C dates; consequently their age must be considered as statistically contemporaneous with any of the ^{14}C ages. However, only the most recent part of the time-span covered by the ESR dates includes the calibrated ^{14}C ages of the dates that are considered as too young. Moreover, it appears that the results are rather close to the calibrated age of the charcoal from unit D2 (stratigraphically close to E1-7) if the mean ESR is computed following a LU model with 30% moisture, which is not an unlikely result for sediments with openwork structure. These data suggest that the results of standard alkali extraction pre-treatment may be reasonably reliable at Mujina Pećina. Moreover, the new ^{14}C date on charcoal from unit D2 (Beta-393072) is consistent with the previous one (GrA-9639) carried out on a bone sample from the same unit, corroborating this hypothesis. The ages of the lowermost units also fit this hypothesis and are corroborated by the new Oxford dates, even if these must be considered older than a background of about 44 ^{14}C ka.

6.3. Utility of magnetic susceptibility (χ) for time-depth-climate correlation

Climate interpretation for the Mujina Pećina successions indicates an alternating cyclicity of warm to cold climate lasting for ~6 ka, commencing with the CRS SE 35 (Harrold et al., 2004) warm event, which starts at ~46 ka BP and ends at ~44.5 ka BP (uncalibrated), and with warm–cold alternations through to ~40 ka BP, with the sequence ending up slightly above the base of SE 31 (Harrold et al., 2004).

Before new chronology data were available, the dates of D1 and D2 may have been suspect because too young and apparently inconsistent with the Harrold et al. (2004) CRS. Similar problems are common, and shown stratigraphically by Ellwood et al. (1996) to be anomalous; essentially bad dates. However, these dates fit the stratigraphic sequence, after they were confirmed by the new dating carried out on charcoal collected from the same unit.

Interestingly, it can be observed that the top of Unit E1 is a discontinuity that marks an evident change in sedimentary processes as well as in deposition rate (Fig. 18). This discontinuity testifies to a hiatus in the sequence (estimated to about 400 to 2800 a [68.2%] and 0 to 3900 a [95.4%] by bayesian modelling), even if its aspect does not suggest strong erosional processes. Conversely, the part of sequence overlying the discontinuity clearly indicates an increase in deposition rate, suggesting that a larger quantity of sediment was deposited in the unit at this time. In this case, the two peaks of χ corresponding to E3B and E1 would represent CRS SE-35 and SE-33, divided by the minimum of E2B representing the cold CRS SE-34 phase, *i.e.* the H5 Heinrich event.

This hypothesis is consistent with all the ^{14}C ages of the Mujina Pećina sequence, as well with the occurrence of loess in E2B and a relevant increase in deposition rate from the bottom of D

upwards. The peak in frost shattering in unit E3A does not fit perfectly the maximum in the χ record, but it must be pointed out that burned sediment included within this high-frequentation context may have altered the χ values.

6.4. Human behaviour and cave use

The human frequentation of the cave was more intense during the earlier warmer phases and the rather aridic event corresponding to loess deposition, and lasted through the first period of landscape instability. After that, human presence became sparse and episodic during the last events of scree deposition. Phosphate aggregates that can be identified as fragments of carnivore coprolites, possibly hyenas (Miller, Macphail, pers. comm., Kolska Horwitz and Golberg, 1979; Goldberg 1980) are a relevant component of the sediments of almost all units at the micromorphological level, and can be considered as indicators of alternating frequentation of the cave by carnivores and more or less episodic use by humans. It is noteworthy that coprolites were not observed in unit E3C-12, which includes the highest density of faunal remains and lithic artefacts (Nizek and Karavanić, 2012) and may represent a phase of more intense and continuous use of the cave by humans.

Even if the presence of humans was probably relevant during the deposition of the first part of the sequence, the Mujina Pećina sediments were largely formed by natural processes whereas the anthropogenic component in sedimentation is scarce; the human component comprises only of lithic industries and processed bone and two possible unstructured hearths in level D2. This is indicated also by the soil micromorphological analyses, which show scanty anthropic components in the sediment. Considering that no evidence of trampling was observed throughout the sequence, the main traces of human activity are the high content of organic matter and fine charcoal fragments in units E3C-12, E2A-8 and to some extent also in B-3. However, ash remains were not observed at the micromorphological level, because they are mainly made up of calcite and were leached by water percolating through the profile, and finally recrystallised as diffuse, fine micrite inclusions and impregnations.

In some units, especially in layers E2A-8 and E3C-12, small (coarse sand- to silt-size) bone fragments are very frequent, sometimes burnt or partially burnt at relatively low temperature. The unburned part of these bones may have resulted from gnawing and digestion by carnivores, but it must be observed that no carnivore coprolites were observed in layer E3C-12, where the bone fragments are most common; consequently, these can be interpreted as anthropogenic. This may indicate intense intentional bone fracturing and subsequent heating for marrow extraction, a typical Neanderthal behaviour (Rabinovich and Hovers, 2004; Roebroeks and Villa 2011) that in the case of Mujina would have been carried out in situ. This sort of "bone sand" was observed in other Mousterian and Upper Palaeolithic contexts in cold/aridic environment, like Riparo del Poggio (Boscato et al., 2009) and Riparo Mochi (Douka et al., 2012) in Italy, and may also indicate the use of bone, or more likely the fat component of bone, as fuel in environments where wood was scarce.

7. Conclusions

The bulk of the Mujina Pećina sediments were formed by joint roof spall and scree input processes, which produced a strongly homogeneous deposit mainly comprised of limestone rubble with a small percentage of matrix. Textural and soil micromorphological observations show that the fine component of the sediment is mainly made up of more or less moderately altered loess in the lower part of the sequence (units E3C-12 to E2B-9), with a peak of poorly altered loess in unit E2B-9, which may represent the cold and strongly aridic Heinrich event H5, with an age as in the

coupled GRIP, GISP2 and NGRIP records (Seierstad et al., 2014). The ^{14}C datings of these units, though below the ^{14}C measured background, are consistent with this hypothesis, with a minimum age of about 47.8 ka BP (median deriving from bayesian modelling).
The coarse fraction of the sediment originated from frost shattering on the cave walls and ceiling, whereas the matrix was probably accumulated by moderate in-wash during short wetter episodes, possibly limited to seasonal rainstorms. Subsequently, strong erosional processes destroyed pre-existing Alfisols and reactivated slope processes, producing the upper part of the sequence (Units E2A-8 to B-3). These processes correspond to a relatively cold and aridic phase with warmer oscillations, followed by a period of generic environmental instability characterised by phases of slope erosion and runoff (probably corresponding to late GI-12 and GS-12), that removed a large part of the deposits formed under the slightly warmer conditions of the early interstadial GI-12 of the INTIMATE palaeoenvironmental record NGRIP sequence (Blockley et al., 2012). This result is in agreement with the faunal and archaeobotanical data available for the upper part of the sequence (Miracle, 2005; Karavanić et al., 2008). Despite all warmer oscillations, the general aspect of the sediment generally indicates relatively fresh conditions, with colder spikes, in accordance with the climatic variability of MIS3.
Whichever the hypotheses about the reliability of the dates, the absolute time resolution is too low to be successfully integrated with the geopedological data in order to resolve the ambiguities and refine the chronology of human occupation at the site. Even if inserted into a bayesian model (Table 6), the dates do not provide good estimates for the beginning and end of the E and D-B phases. The minimum oldest age of the sequence is about 48 ka BP, as defined by the dating background; at 2-sigma precision, the time limits of the hiatus separating units E from units D-B are widely overlapping, with median ages of respectively 46.7 and 44.7 ka BP. The sequence ends at about 43 ka BP.
Assuming that the dates on bone are reliable and precise, the D-B sequence of units may be ascribed to the period immediately subsequent to Heinrich Event H5 and including several possible stadial/interstadial oscillations, namely GI-12 to GS 11 (Blockley et al., 2012). Therefore, the main phase of human use of the cave, or at least the part of it that coincides with the peak of frost shattering, can be tentatively ascribed to Heinrich Event H5, in good accordance with the geopedological data. These conclusions are supported by the magnetic susceptibility (χ) relative dates reported here, that indicate an abrupt change from warm to cold climate at about 47.5 cal ka, coincident with the onset of the H5 event. Recovery to warmer temperatures occurs at about 44 cal ka.
Chronological evidence from Mujina Pećina suggests that Neandertals, generally accepted as the makers of Mousterian industries, were still present in the Dalmatian area at least until 43-42 cal ka BP that overlap with Uluzzian and Protoaurignacian industries in Italy. If we accept the general view that the Protoaurignacian and maybe Uluzzian are associated with AMHs, the dates obtained from Mujina Pećina indicate chronological overlapping of the late Neandertal population in the eastern Adriatic with AMH populations in the Apennine peninsula. Like at other sites of the Dalmatian area, dates between 35 and 30 cal ka BP were also obtained from radiocarbon determinations on bone; however, some clues suggest that these ages should not be accepted, deriving from still unclear reasons connected to pre-treatment prior to dating. This hypothesis fits the model of Neandertal demise proposed by Higham et al. (2014).
Even if the contribution of the anthropogenic component to the accumulated cave sediment was moderate, artefact distribution and soil micromorphological data suggest that Neandertals frequented Mujina Pećina more intensively during the deposition of the first part of the sequence, whereas their presence became more and more episodic and was shared with carnivores during the later phases of sedimentation. The occurrence of very fine fragments of partially burnt bone in

the units with a major anthropic component may indicate the use of bone for fuel, as a by-product of subsistence activities, during aridic periods characterised by scarce availability of wood.
Albeit no fully reliable dates are available for the earliest phase of cave use by humans, it results from this study that at least part the most intense frequentation of the cave corresponded to a cold extreme (Heinrich event H5). Conversely, cave use became more and more sporadic during a phase that - however possibly warmer - was characterised by strong environmental instability, i.e. soil erosion and scree reactivation, probably connected to the shrinkage of the vegetal cover and generally resulting in a decrease of the subsistence resources of the area.

Acknowledgements
Seven dates published here were obtained through a project funded by Croatian Science Foundation. Thanks go to Darden Hood (Beta Analytic Inc.), who provided extensive clarifications and was open to discussing the results of the radiocarbon datings; replicated datings were carried out for free on samples that yielded debatable results. Mujina pećina excavations (1995-2003) were funded by the Ministry of Culture and Ministry of Sciences, Education and Sports of Republic of Croatia, Town of Kaštela, Split-Dalmatia County, National Geographic Society, Northern Illinois University and the University of Zagreb (Faculty of Humanities and Social Sciences).

References

Angelucci D.E. 2010. The recognition and description of knapped lithic artifacts in thin section. Geoarchaeology. An International Journal, 25 (2), 220-232.

Batović, Š., 1965. Prvi paleolitski nalazi u srednjoj Dalmaciji. Diadora, 3, 205-209.

Blikra, L. H., Nemec, W., 1998. Postglacial colluvium in Western Norway: depositional processes, facies and palaeoclimatic record. Sedimentology, 45, 909-959.

Blockley, S.P.E., Lane, C.S., Hardiman, M., Rasmussen, S.O., Seierstad, I.K., Steffensen, J.P., Svensson, A., Lotter, A.F., Turney, C.S.M., Bronk Ramsey, C., INTIMATE members, 2012. Synchronisation of palaeoenvironmental records over the last 60,000 years, and an extended INTIMATE1 event stratigraphy to 48,000 b2k. Quaternary Science Reviews, 36, 2-10.

Boscato, P., Boschian, G., Caramia, F., Gambassini, P., 2009. Il Riparo del Poggio a Marina di Camerota (Salerno): culture ed ambiente. Rivista di Scienze Preistoriche, 59, 5-40.

Boschian, G., 1997. Sedimentology and Soil Micromorphology of the Late Pleistocene and Early Holocene Deposits of Grotta dell'Edera (Trieste Karst, NE Italy). Geoarchaeology, 12 (3), 227-249.

Brewer, R., 1976. Fabric and Mineral Analysis of Soils. Krieger, Huntington.

Brock, F., Geoghegan, V., Thomas, B., Jurkschat, K., Higham, T.F.G., 2013. Analysis of bone “collagen” extraction products for radiocarbon dating. Radiocarbon, 55, 445–463.

Ramsey, C. B., Higham, T., Bowles, A., Hedges, R. 2004a. Improvements to the pretreatment of bone at Oxford. Radiocarbon, 46(1), 155-164.

Ramsey, C. B., Higham, T., Leach, P. 2004b. Towards high-precision AMS: progress and limitations. Radiocarbon, 46 (1), 17-24.

Bronk Ramsey, C., 2009. Bayesian analysis of radiocarbon dates. Radiocarbon, 51(1), 337-360.

Bullock, P., Fedoroff, N., Jongerius, A., Stoops, G., Tursina, T., Babel, U., 1985. Handbook for Soil Thin Section Description. Waine Research Publications, Wolvehampton.

Catt, J.A., Ed., (1991). Paleopedology manual. Quaternary International, 6, 1-95.

Cremaschi, M., 1990a. The loess in northern and central Italy: a loess basin between the Alps and the Mediterranean region. In: Cremaschi, M. (Ed.), The Loess in Northern and Central Italy: A Loess Basin between the Alps and the Mediterranean Region. C.N.R. Quaderni di Geodinamica Alpina e Quaternaria, Milano.

Cremaschi, M., 1990b. Stratigraphy and palaeoenvironmental significance of the loess deposits on Susak Island (Dalmatian archipelago). Quaternary International, 5, 97-106.

Cottignoli, A., Boschian, G., Di Maggio, C., Masini, F., Petruso, D., 2002. Pedostratigraphic notes on the middle-late Pleistocene of Capo San Vito Peninsula (NW Sicily). Il Quaternario, 15 (1), 89-96.

Di Maggio, C., Incandela, A., Masini, F., Petruso, D., Renda, P., Simonelli, C., Boschian, G., 1999. Oscillazioni eustatiche, biocronologia e depositi continentali quaternari e neotettonica nella Sicilia nord-ocidentale (Penisola di S. Vito lo Capo – Trapani). Il Quaternario, 12 (1), 25-49.

Douka, K., Grimaldi, S., Boschian, G., Del Lucchese, A., Higham, T.F.G., 2012. A new chronostratigraphic framework for the Upper Palaeolithic of Riparo Mochi (Italy). Journal of Human Evolution, 62, 286-299.

Ellwood, B.B., Petruso, K.M., Harrold, F.B., Korkuti, M., 1996. Paleoclimate characterization and intra-site correlation using magnetic susceptibility measurement: an example from Konispol Cave, Albania. Journal of Field Archaeology, 23, 263–271.

Ferrari, G., Magaldi, D., 1976. Il problema del loess. In: Studio interdisciplinare del rilievo isolato di Trino, Gruppo di Studio per il Quaternario Padano, 3, 34-39.

Goldberg, P., 1979. Micromorphology of Pech-de-l'Azé II Sediments. Journal of Archaeological Science, 6, 17–47.

Harrold, F., Ellwood, B., Thacker, P., Benoist, S., 2004. Magnetic susceptibility analysis of sediments at the Middle–Upper Paleolithic transition for two cave sites in northern Spain. In Zilhão, J.; D'Errico, F. (eds.) The Chronology of the Aurignacian and of the Transitional Technocomplexes. Dating, Stratigraphies, Cultural Implications, Trabalhos de Arqueologia, 33, Instituto Português de Arqueologia, Lisboa, 301–310.

Higham, T.F.G., Bronk Ramsey, Ch., Karavanić, I., Smith, F.H., Trinkaus, E., 2006. Revised direct radiocarbon dating of the Vindija G_1 Upper Paleolithic Neandertals. Proceedings of the National Academy of Sciences of the United States of America, 103 (3) 553-557.

Higham, T., Douka, K., Wood, R., Bronk Ramsey, Ch., Brock, F., Basell, L., Camps, M., Arrizabalaga, A., Baena, J., Barroso-Ruiz, C., Bergman, Ch., Boitard, C., Boscato, P., Caparros, M., Conard, N.J.., Draily, Ch., Froment, A., Galvan, B., Gambassini, P., Garcia-Moreno, A., Grimaldi, S., Haesaerts, P., Holt, B., Iriarte-Chiapusso, M.-J., Jelinek, A., Jorda Pardo, J.F.., Maillo-Fernandez, J.-M.., Marom, A., Maroto, J., Menendez, M., Metz, L., Morin, E., Moroni, A., Negrino, F., Panagopoulou, E., Peresani, M., Pirson, S., de la Rasilla, M., Riel-Salvatore, J., Ronchitelli, A., Santamaria, D., Semal, P., Slimak, L., Soler, J., Soler, N., Villaluenga, A., Pinhasi, R., Jacobi, R., 2014. The timing and spatiotemporal patterning of Neanderthal disappearance. Nature, 512, 306-309.

Goldberg, P., 1980. Micromorphology in Archaeology and Prehistory. Paléorient, 6, 159-164.

Karavanić, I., 2009. Adriatic coast of Croatia and its hinterland from 50 000 to 25 000 BP. In: M. Camps; C. Szmidt (Eds.) The Mediterranean from 50 000 to 25 000 BP: Turning Points and New Directions. Oxbow Books, Oxford, 163-178.

Karavanić, I., Bilich-Kamenjarin, I., 1997. Musterijensko nalazište Mujina pećina kod Trogira, rezultati trogodišnjih iskopavanja. Opuscula Archaeologica, 21, 195–204.

Karavanić, I., Miracle, P.T., Culiberg, M., Kurtanjek, D., Zupanič, J., Golubić, V., Paunović, M., Mauch Lenardić, J. Malez, V., Šošić, R., Janković, I. i Smith, F. H., 2008. The Middle Paleolithic from Mujina Pećina, Dalmatia, Croatia. Journal of Field Archaeology, 33, 259-277.

Kolska Horwitz, L., Goldberg, P., 1989. A Study of Pleistocene and Holocene Hyaena Coprolites. Journal of Archaeological Science, 16, 71-94.

Krajcarz, M.T., Cyrek, K., Krajcarz, M., Mroczek, P., Sudoł, M., Szymanek, M., Tomek, T., Madeyska, T., 2016. Loess in a cave: Lithostratigraphic and correlative value of loess and loess-like layers in caves from the Kraków-Częstochowa Upland (Poland). Quaternary International 399, 13-30.

Longin, R., 1970. Extraction du collagene des os fossiles pour leur datation par la méthode du carbone 14. Thèse de doctorat d'Etat, Université de Lyon.

Longo, L., Boaretto, E., Caramelli, D., Giunti, P., Lari, M., Milani, L., Mannino, M.A., Sala, B., Thun Hohenstein, U., Condemi S., 2012. Did Neandertals and anatomically modern humans coexist in northern Italy during the late MIS 3? Quaternary International 259, 102-112.

Malez, M., 1979. Nalazišta paleolitskog i mezolitskog doba u Hrvatskoj. In: Benac A. (Ed.) Praistorija jugoslavenskih zemalja, 1, Akademija nauka i umjetnosti Bosne i Hercegovine, Sarajevo, 227–276.

Mallol, C., Hernández, C.M., Machado, J., 2012. The significance of stratigraphic discontinuities in Iberian Middle-to-Upper Palaeolithic transitional sites, Quaternary International 275, 4-13.

Miracle, P.T., 2005. Late Mousterian Subsistence and Cave Use in Dalmatia: the Zooarchaeology of Mujina Pećina, Croatia. International Journal of Osteoarchaeology, 29, 84-105.

Mikulčić Pavlaković, S., Crnjaković, M., Tibljaš, D., Šoufek, M., Wacha, L., Frechen, M., Lacković, D., 2011. Mineralogical and geochemical characteristics of Quaternary sediments from the Island of Susak (Northern Adriatic, Croatia). Quaternary International, 234, 32-49

Nizek, R., Karavanić, I., 2012. Prostorna analiza nalaza musterijenskih razina D2, E1, E2 i E3 Mujine pećine-The Spatial Analysis of Finds from Mousterian Levels D2, E1, E2 and E3 at Mujina pećina. Prilozi Instituta za arheologiju u Zagrebu, 29, 25-56.

Peresani, M., 2012. Fifty thousand years of flint knapping and tool shaping across the Mousterian and Uluzzian sequence of Fumane cave. Quaternary International 247, 125-150.

Petrić, N., 1979. Mujina pećina, Trogir – paleolitičko nalazište. Arheološki pregled, 20 (1978), 9.

Reimer, P.J., Bard, E., Bayliss, A., Beck, J.W., Blackwell, P.G., Bronk Ramsey, C., Grootes, P.M., Guilderson, T.P., Haflidason, H., Hajdas, I., Hatte, C., Heaton, T.J., Hoffmann, D.L., Hogg, A.G., Hughen, K.A., Kaiser, K.F., Kromer, B., Manning, S.W., Niu, M., Reimer, R.W., Richards, D.A., Scott, E.M., Southon, J. R., Staff, R. A., Turney, C.S.M., van der Plicht, J., 2013. IntCal13 and Marine13 Radiocarbon Age Calibration Curves 0-50,000 Years cal BP. Radiocarbon, 55(4), 1869 - 1887.

Rink, W. J., Karavanić, I., Pettitt, P.B., van der Plicht, J., Smith, F.H., Bartoll, J., 2002. ESR and AMS-based 14C Dating of Mousterian Levels at Mujina Pećina, Dalmatia, Croatia. Journal of Archaeological Science, 29, 943–952.

Seierstad, I.K, Abbott, P.M,. Bigler, M., Blunier, T., Bourne, A.J., Brook, E., Buchardt, S.L., Buizert, C., Clausen, H.B., Cook, E., Dahl-Jensen, D., Davies, S.M., Guillevic, M., Johnsen, S.J., Pedersen, D.S., Popp, T.J., Rasmussen, S.O., Severinghaus, J.P., Svensson, A., Vinther, B.M., 2014. Consistently dated records from the Greenland GRIP, GISP2 and NGRIP ice cores for the past 104 ka reveal regional millennial-scale δ18O gradients with possible Heinrich event imprint. Quaternary Science Reviews, 106, 29-46.

Shaw A.B., 1964. Time in Stratigraphy. McGraw-Hill, New York.

Smith, F.H., Trinkaus, E., Pettitt, P.B., Karavanić, I., Paunović, M., 1999. Direct radiocarbon dates for Vindija G1 and Velika Pećina Late Pleistocene hominid remains. Proceedings of the National Academy of Sciences of the United States of America, 96, 12281–12286.

Smith, F.H., Ahern, J.C.M., Janković, I., Karavanić, I. 2016. The Assimilation model of modern human origins in light of current genetic and genomic knowledge. Quaternary International, in press. http://dx.doi.org/10.1016/j.quaint.2016.06.008

Soil Survey Staff, 2014. Keys to Soil Taxonomy, 12th ed. USDA-Natural Resources Conservation Service, Washington, DC.

Stoops, G., 2003, Guidelines for Analysis and Description of Soil and Regolith Thin Sections. Soil Science Society of America, Madison.

Van Vliet-Lanoë, B. 2010. Frost action. In Stoops, G., Marcelino, V., Mees, F. (Eds), Interpretation of Micromorphological Features of Soils and Regoliths. Elsevier, Amsterdam, 81-108.

Vujević, D., 2007. Srednji paleolitik na području južno od Ražanca. Unpublished Master Thesis, University of Zadar, Zadar.

Wacha, L., Mikulčić Pavlaković, S., Frechen, M., Crnjaković, M., 2011. The Loess Chronology of the Island of Susak, Croatia. Quaternary Science Journal, 60 (1), 153-169.

Wentworth, C.K. 1922. A scale of grade and class terms for clastic sediments. Journal of Geology, 30, 377-392.

Figure captions

Figure 1. Location map of Mujina Pećina, showing the main morphological characteristics of the surrounding territory. Shaded relief map from SRTM 1 Arc-Second Global data available from the U.S. Geological Survey.

Figure 2.
View of the right (SW) side of the karstic gorge crossing the Labinštica hills. Mujina Pećina (white star) is situated at the foot of a limestone cliff and close to the toe of a small scree (red fan-like symbols) that partially enters the cave. Blue line: fault line.

Figure 3.
Plan of Mujina Pećina, with 1 m square excavation grid. Stars mark the main sampling locations for sedimentology and soil micromorphology. MPA, MPB and MPC indicate sampling locations for magnetic susceptibility.

Figure 4.
Reference stratigraphic sequence along the longitudinal profile, in excavation square D6. Letters A to E3C indicate archaeological stratigraphic units; numbers 1 to 12 indicate lithologic units. The red line indicates a major hiatus situated at the boundary between excavation levels E and D.

Figure 5.
Simplified 3D view of the longitudinal (C/D 6-10 and D/E 6-10) and transversal (D-E 5/6) profiles of the cave infill; view from the inside. Bold lines: erosional boundaries; grey lines: bedrock.

Figure 6.
Grain-size profile in excavation square D6. From left to right: simplified sequence, fine/coarse ratio (<2 mm/> 2mm), grain-size of the coarse fraction, grain-size of the fine fraction (undecalcified and decalcified).

Figure 7.
Grain-size profile in excavation square F10. From left to right: simplified sequence, fine/coarse ratio (<2 mm/> 2mm), grain-size of the coarse fraction, grain-size of the fine fraction (undecalcified and decalcified).

Figure 8.
Cumulative grain-size curves for decalcified samples. Upper (A), intermediate (B) and lower (C) units of the sequence.

Figure 9.
Length (ordinate) versus breadth (abscissa) of clasts in the 16-32 mm minimum diametre grain-size class. N: number of measured elements; a: slope of the interpolating line.

Figure 10.
Microphotographs of sediment thin sections from Mujina Pećina.
a: cryogenic loose granular microstructure; uprised and partly verticalised silt cappings, completely coating skeleton grains, PPL, unit D-5.

b: as in a, XPL; some amorphous phosphate granules (ph) occur among the coated skeleton grains; note that the b-fabric is not granostriated, as usually in silt cappings.
c: silt cappings (sc) on limestone clasts, PPL, unit D-4.
d: as in a, XPL.
e: chert artefact in bone sand-dominated sediment, PPL, unit E3C-12.
f: as in c, XPL. e: pedorelic with quartz skeleton, PPL. f: as in e, XPL.

Figure 11.
Microphotographs of sediment thin sections from Mujina Pećina.
a: large brownish fragment of burned bone, in bone sand-dominated sediment; diffuse fine black opaque amorphous organic matter, PPL, unit E3C-12.
b: as in a, XPL; note the low birefringence (amorphous in some areas) of the large bone fragment, due to heating/burning; granostriated b-fabric around some skeletal grains.
c: as in a, UV-fluorescence; brightly epifluorescent phosphate nodules and/or unburned bones contrast with the non-epifluorescent burned bone.
d: loose polyhedric microstructure, micrite-coated, on bone sand-dominated sediment; abundant finely dispersed amorphous organic matter gives the sediment mass a dark colour; PPL, unit E3C-12.

Figure 12.
Microphotographs of sediment thin sections from Mujina Pećina.
a: carnivore phosphate coprolite with dusty brown micromass, teardrop void; PPL, unit B-3.
b: as in a, XPL; frequent silt-size mineral grains, mostly quartz (light grey), are dispersed within the amorphous (dark grey/black) phosphatic mass.
c, d: as in a, under UV- and blue-fluorescence; epifluorescence observations put into light details of the internal structure, mostly rectangular void casts of hairs.

Figure 13.
Microphotographs of sediment thin sections from Mujina Pećina.
a: clayey aggregate with quartz skeleton grains (pedorelic), stained by amorphous Fe-oxides. PPL, unit E3C.
b: as in a, XPL; stipple-speckled b-fabric, partly masked by amorphous Fe-oxides.
c: silt coating on limestone clast, including reddish clay pedorelics (p), few mica flakes (m), and some organic matter punctuation; PPL, unit D-5.
d: intrusive Fe-oxides and clay nodule, with amorphous core and concentrically layered outer part (rolling pedofeature); PPL, narrow field illumination with converging condenser; unit E3C.

Figure 14.
Complete set of uncalibrated ^{14}C dates for Mujina Pećina, on bone and charcoal, classified following pre-treatment method. Arrows indicate ages “older than”. Beta Analytic dates older than background are represented with error bars, because σ was provided. The grey field indicates radiocarbon background for Beta Analytic (43.5 ka).

Figure 15.
OxCal 4.2 (Bronk Ramsey, 2009) output of a bayesian model including selected Mujna Pećina dates. From bottom upwards, the model includes one P_sequence including units E3C to E1-E2, one Gap of unknown length, a second P-sequence including a Phase (unit D2) and units D1, C, B.

Intcal13 calibration curve (Reimer et al., 2013). Light grey: distribution likelihoods for calibrated dates; dark grey: posterior distributions.

Figure 16.
Magnetic susceptibility data for the western Mujina Pećina (MPB) succession. Included are the χ data, as well as χ bar-logs built from these data, plotted relative to depth in section. Excavation levels are given. The χ bar-log represent highs and lows in χ data and are equated to the Southern Europe Master Curve of Harrold et al. (2004), and the ages at χ bar-log boundaries represent uncalibrated ages for the corresponding boundaries as reported by Harrold et al. (2004). Each bar-log is numbered with the corresponding χ bar-log number as given in Harrold et al. (2004). The red line indicates a major hiatus situated at the boundary between excavation units E and D.

Figure 17.
Magnetic susceptibility data for the eastern Mujina Pećina (MPA and MPC) successions. Data set represents two sampling events in the same area, in 2003 and in 2004. Included are the χ data for each sampling, as well as bar-logs built from the 2004 data, plotted relative to depth in section. Excavation levels are given for each sampling and correlated using dotted lines. The bar-log data are equated to the Southern Europe Master Curve of Harrold et al. (2004), and the ages at bar-log boundaries represent ages for the corresponding boundaries as reported by Harrold et al. (2004). Each bar-log is numbered with the corresponding bar-log number as given in Harrold et al. (2004). Uncalibrated ^{14}C ages for the eastern succession are given associated with the 2004 sampling. The red line indicates a major hiatus situated at the boundary between excavation levels E and D.

Figure 18.
Comparison of the Mujina Pećina χ bar-log data sets with the Southern Europe Cave Master Curve of Harrold et al. (2004). Given in the figure are levels identified for MPA and MPB data sets, with uncalibrated ^{14}C ages from Harrold et al. (2004). Black: temperate/warmer/wetter phases; white: cooler/dryer phases.

Figure 19.
OxCal 4.2 (Bronk Ramsey, 2009) output depth plot for the Mujina Pećina bayesian model of fig. 15, including estimates for deposition rates and sedimentary hiatus length. The deposition rate for the E units is a maximum estimate, based on the 1-sigma calibrated age of the last E unit, and on the age of the radiocarbon background, attributed to the lowermost E unit of the sequence. Intcal13 calibration curve (Reimer et al., 2013).

Figure 20.
Synchronisation of the INTIMATE palaeoenvironmental record (Blockley et al., 2012) with the Mujina Pećina available datings. From left to right: GICC05 NGRIP δ ^{18}O record; mean ESR ages for early (EU) and late (LU) uptake models, at 10% and 30% moisture; 1-sigma and 2-sigma calibrated (OxCal 4.2; Bronk Ramsey, 2009) dates; 2-sigma posterior calibrations for the limits of the main sequence units (*v.* Table 6 for precise figures). H3, H4, H5: Heinrich events. All ages in years b2k (before AD 2000).


43° 40' 0.0000" N
10 km
Mujina Pećina
Kaštela Bay
TROGIR
SPLIT
43° 30' 0.0000" N
16° 10' 0.0000" E
16° 30' 0.0000" E
ADRIATIC SEA
CROATIA

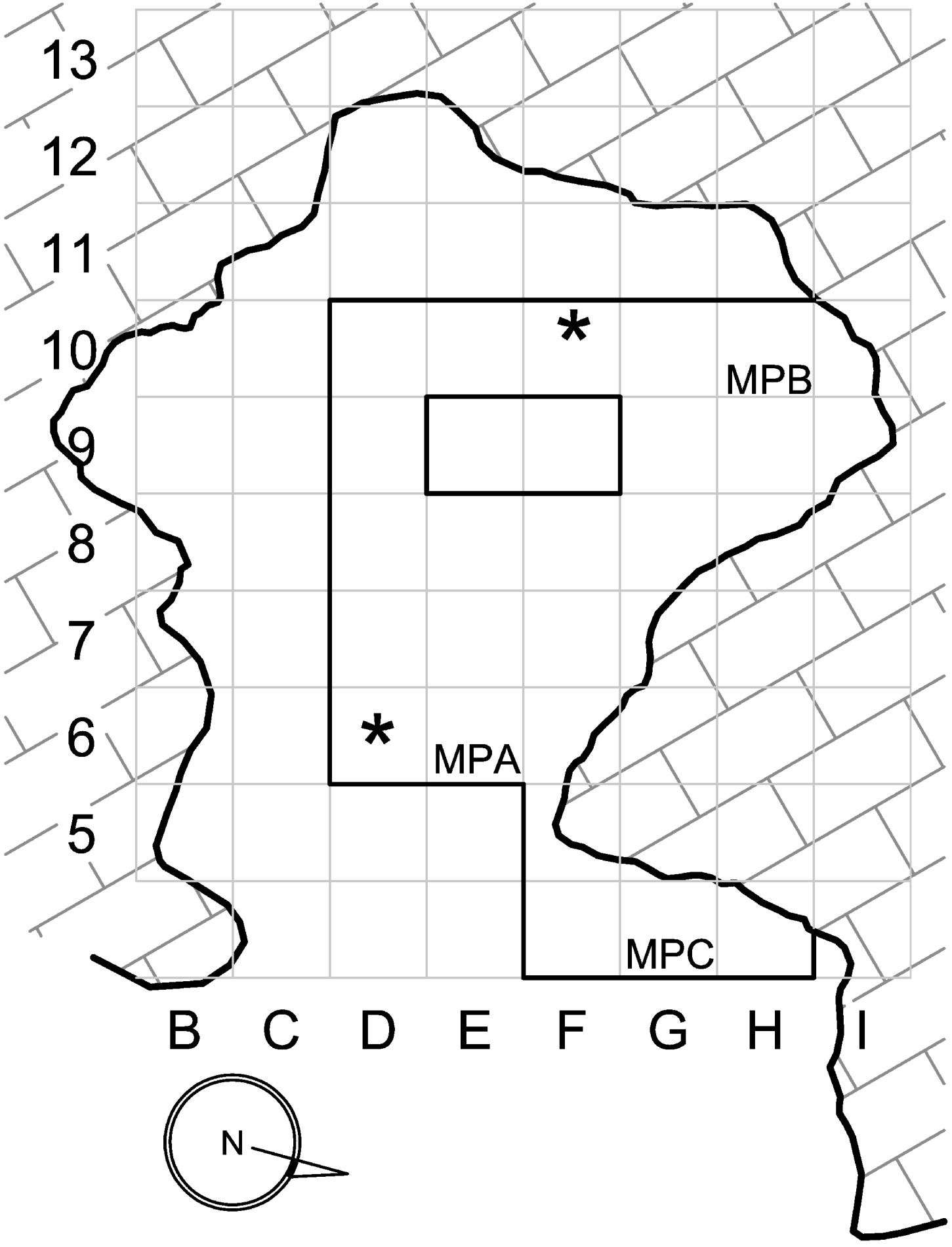
13
12
11
10
9
8
7
6
5
MPB
MPA
MPC
B
C
D
E
F
G
H
I
N

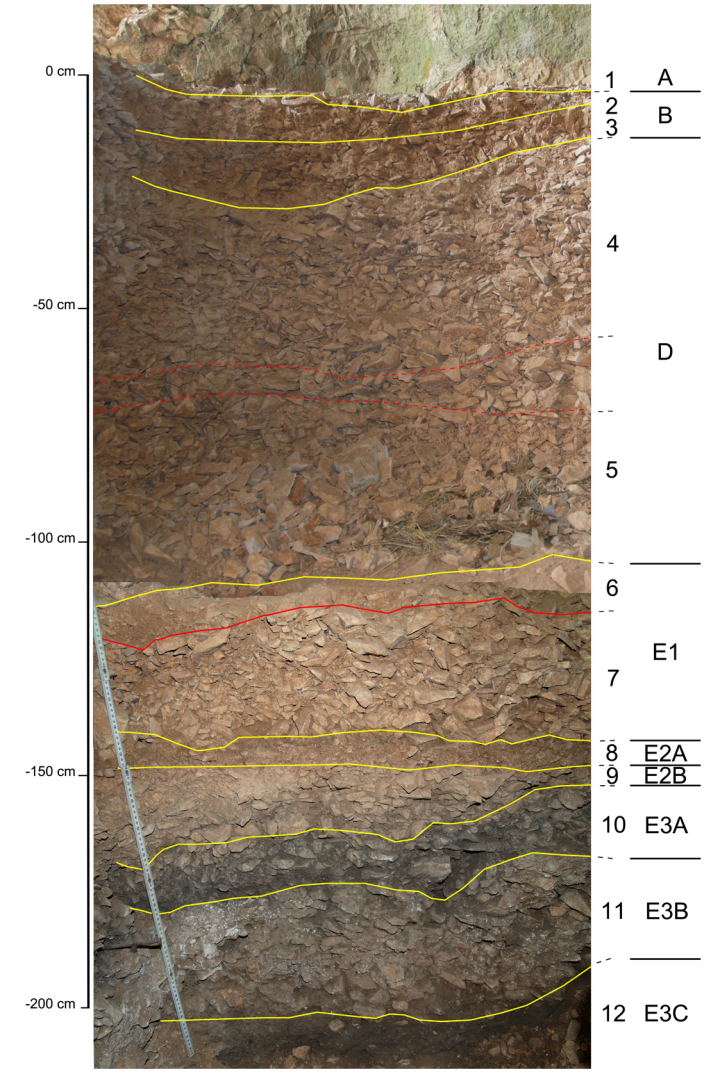
0 cm
-50 cm
-100 cm
-150 cm
-200 cm
1
A
2
B
3
4
D
5
6
E1
7
8
E2A
9
E2B
10
E3A
11
E3B
12
E3C

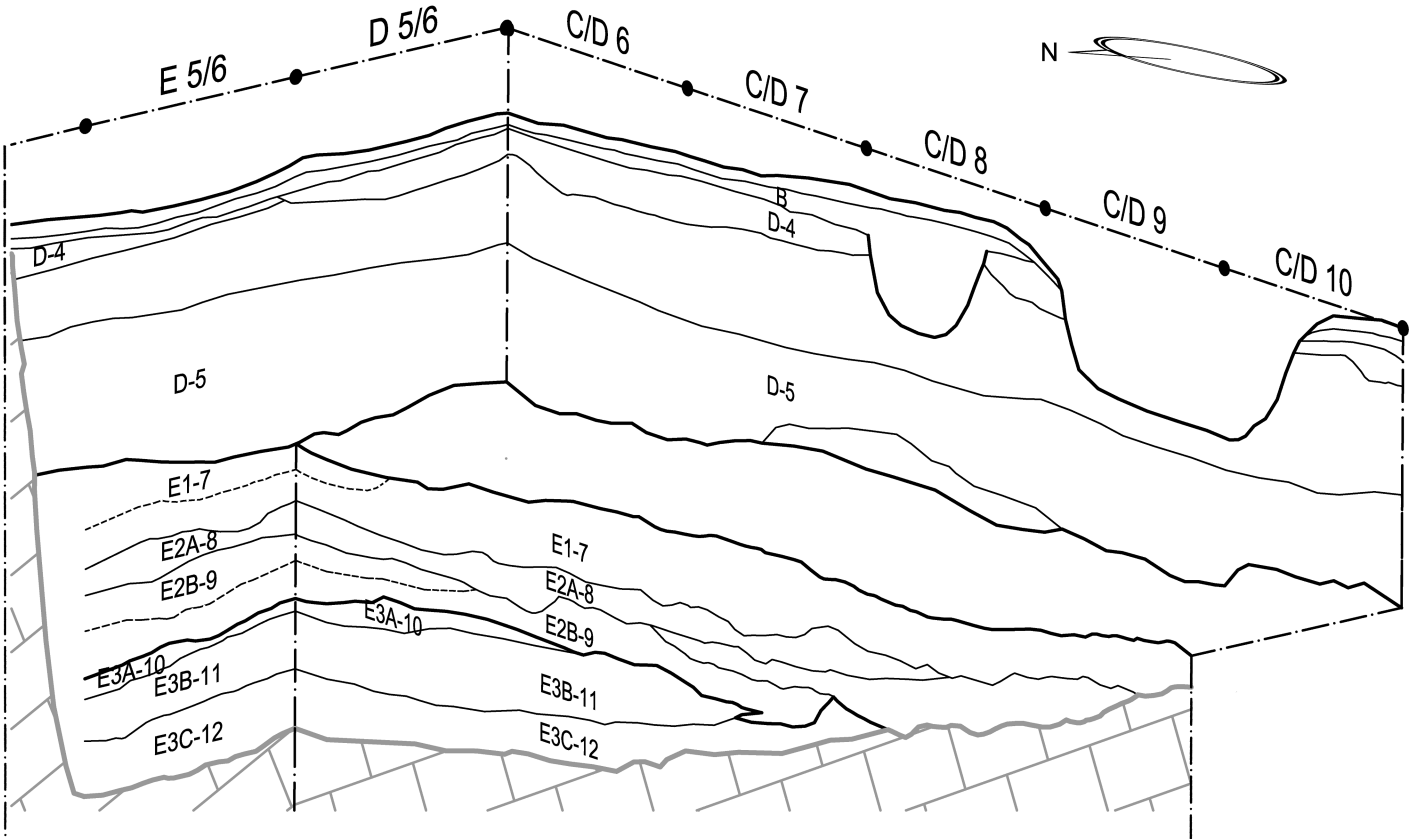
E 5/6
D 5/6
C/D 6
C/D 7
C/D 8
C/D 9
C/D 10
N
D-4
D-5
E1-7
E2A-8
E2B-9
E3A-10
E3B-11
E3C-12

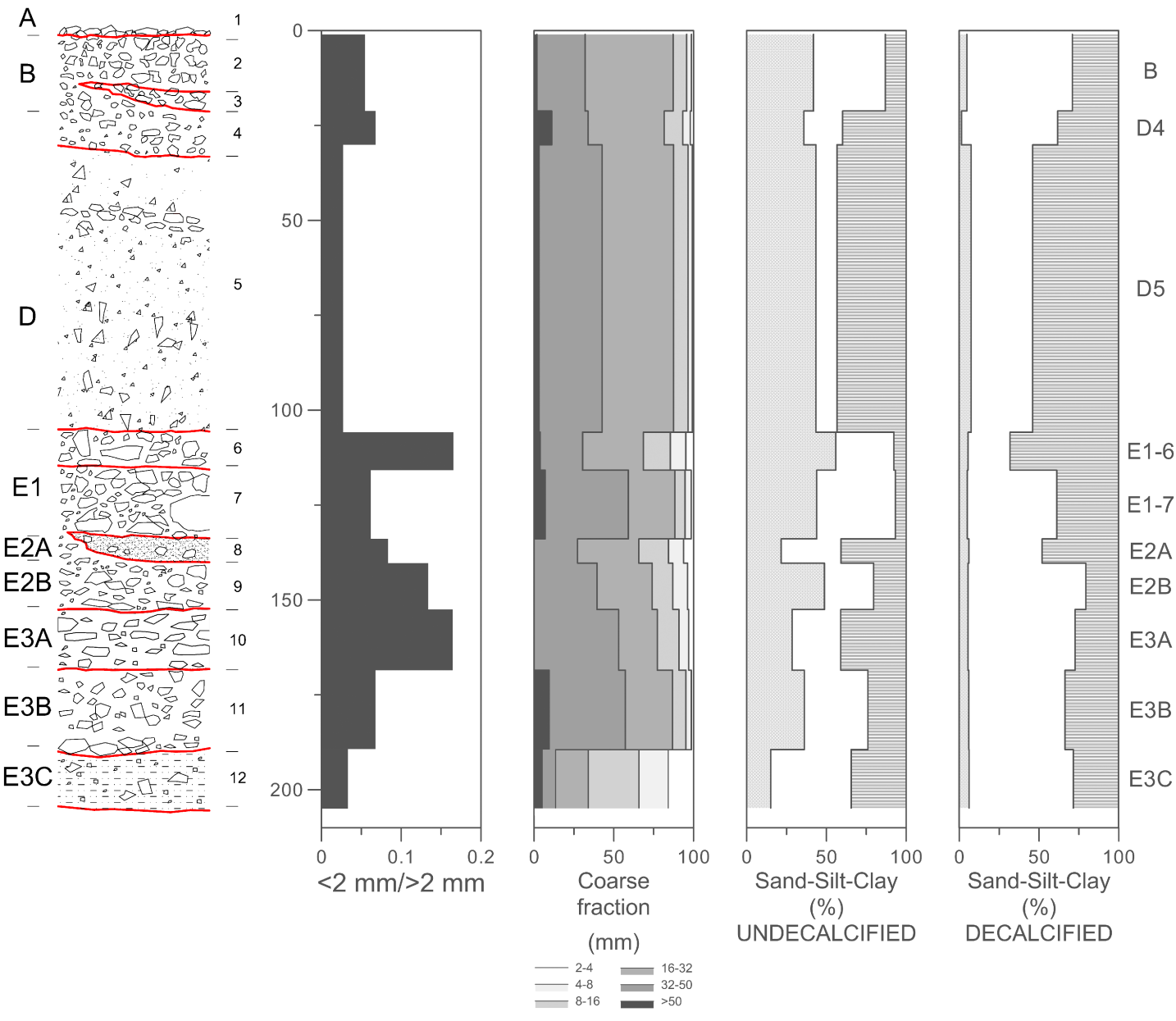
A
B
D
E1
E2A
E2B
E3A
E3B
E3C
1
2
3
4
5
6
7
8
9
10
11
12
0
50
100
150
200
0
0.1
0.2
<2 mm/>2 mm
0
50
100
Coarse fraction (mm)
2-4
4-8
8-16
16-32
32-50
>50
0
50
100
Sand-Silt-Clay (%) UNDECALCIFIED
0
50
100
Sand-Silt-Clay (%) DECALCIFIED
B
D4
D5
E1-6
E1-7
E2A
E2B
E3A
E3B
E3C

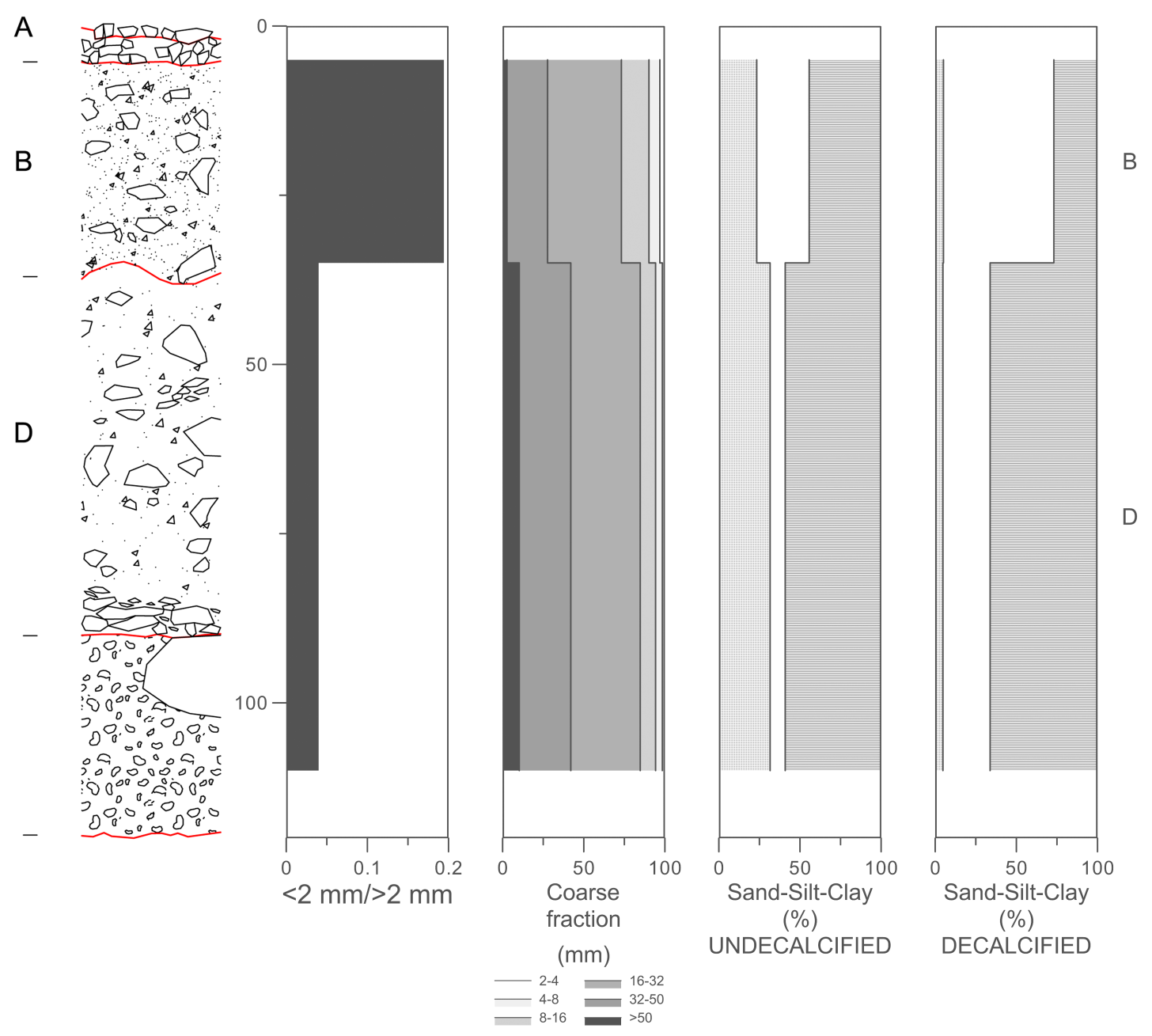
A
B
D
0
50
100
0
0.1
0.2
<2 mm/>2 mm
0
50
100
Coarse fraction (mm)
2-4
4-8
8-16
16-32
32-50
>50
0
50
100
Sand-Silt-Clay (%) UNDECALCIFIED
0
50
100
Sand-Silt-Clay (%) DECALCIFIED
B
D

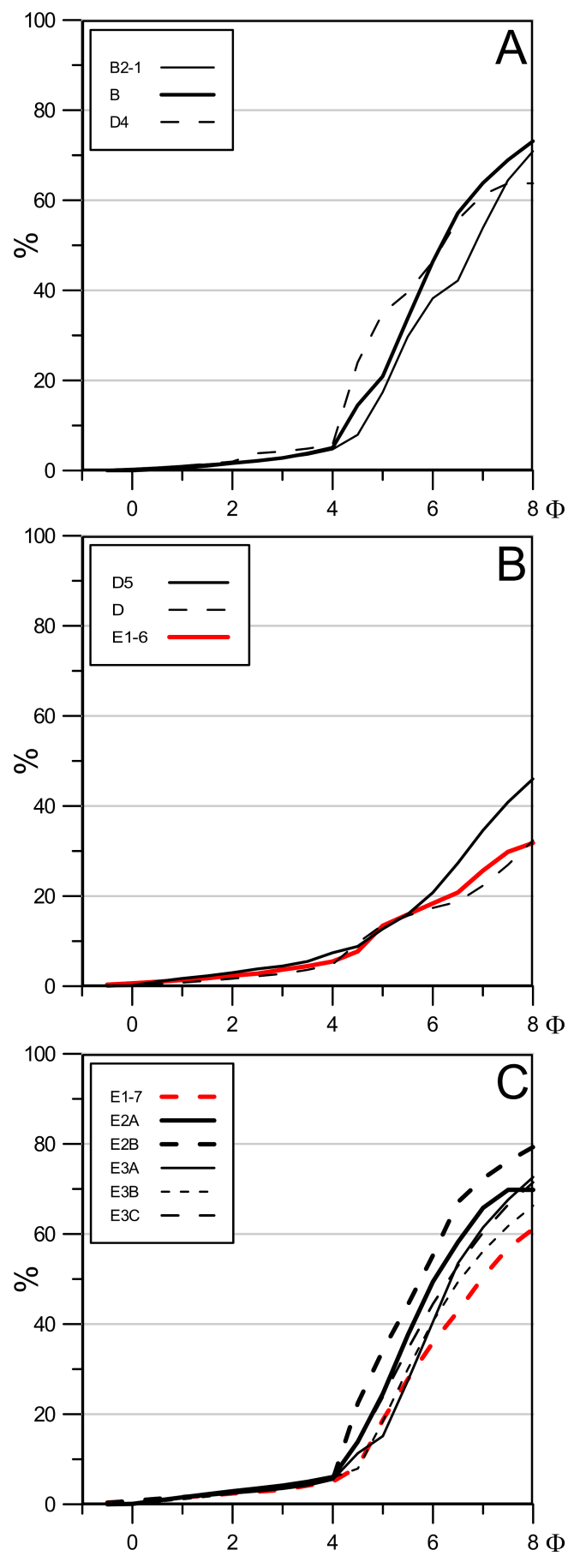
A
B2-1
B
D4
%
100
80
60
40
20
0
0
2
4
6
8 Φ
B
D5
D
E1-6
%
100
80
60
40
20
0
0
2
4
6
8 Φ
C
E1-7
E2A
E2B
E3A
E3B
E3C
%
100
80
60
40
20
0
0
2
4
6
8 Φ

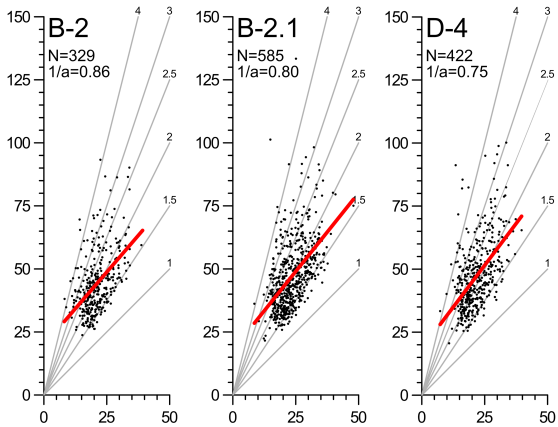
B-2
N=329
1/a=0.86

B-2.1
N=585
1/a=0.80

D-4
N=422
1/a=0.75

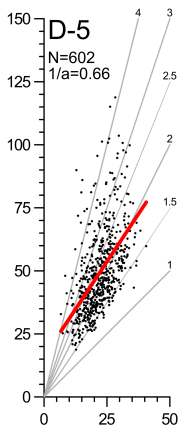
D-5
N=602
1/a=0.66

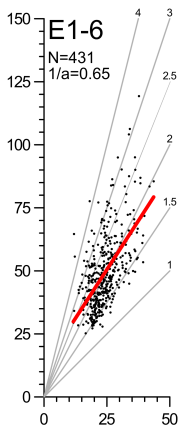
E1-6
N=431
1/a=0.65

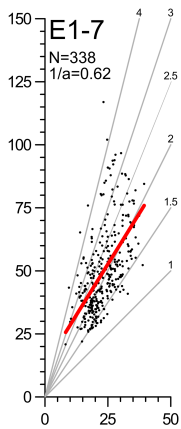
E1-7
N=338
1/a=0.62

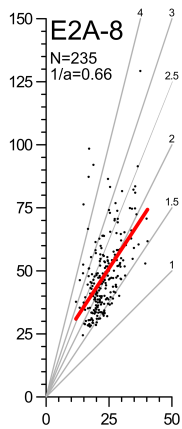
E2A-8
N=235
1/a=0.66

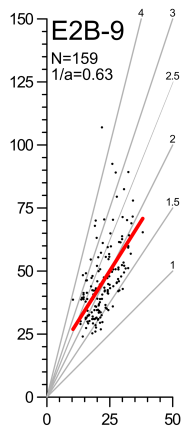
E2B-9
N=159
1/a=0.63

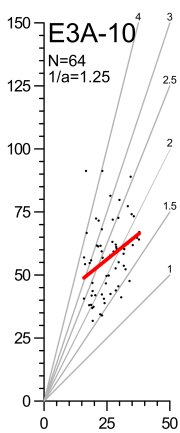
E3A-10
N=64
1/a=1.25

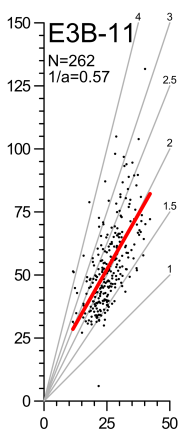
E3B-11
N=262
1/a=0.57

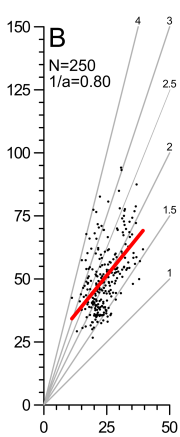
B
N=250
1/a=0.80

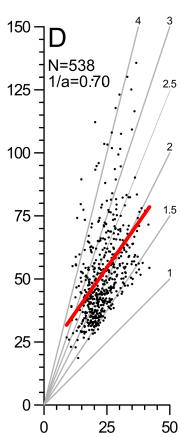
D
N=538
1/a=0.70

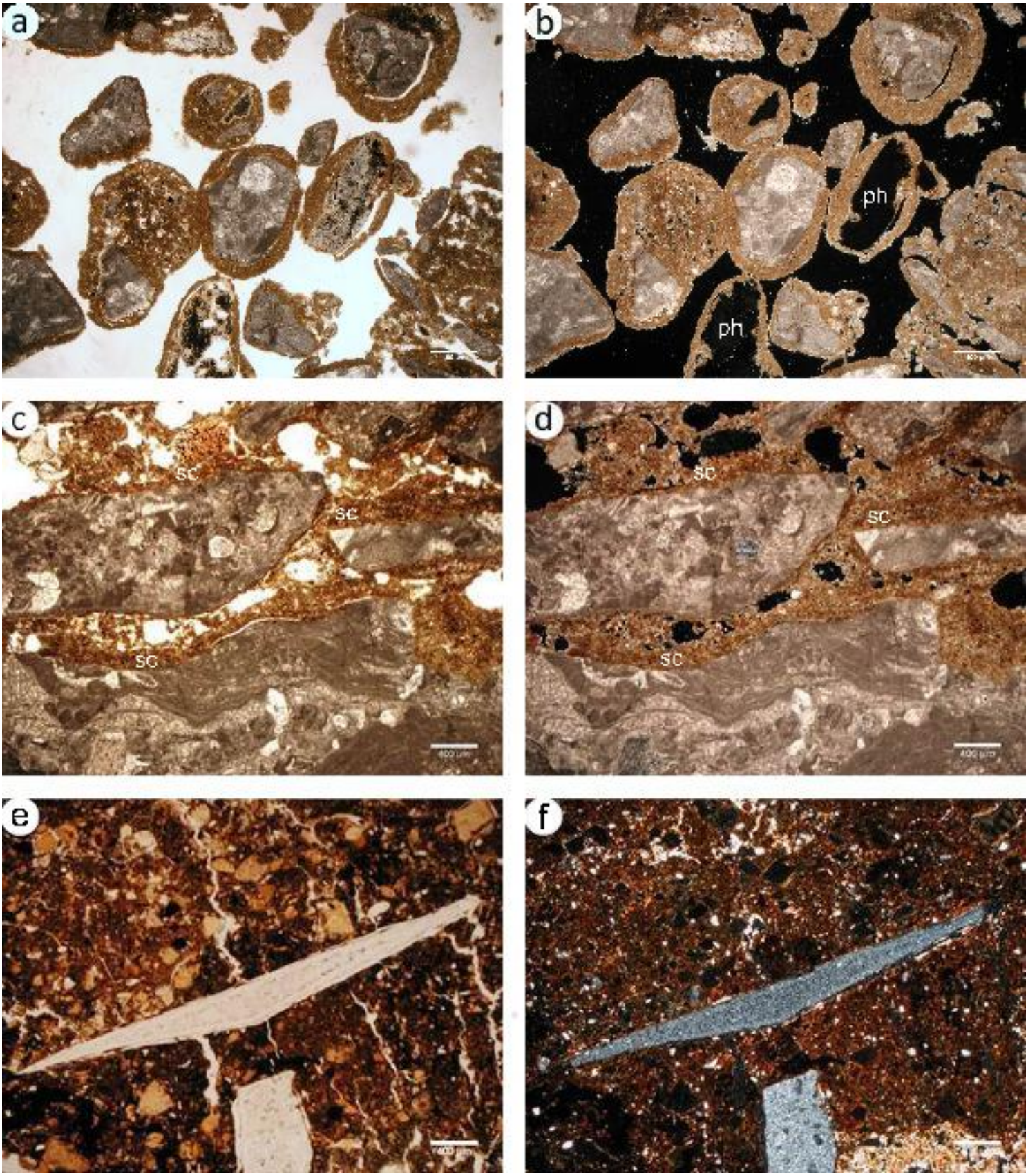
a
b
ph
ph
c
sc
sc
sc
d
sc
sc
sc
e
f

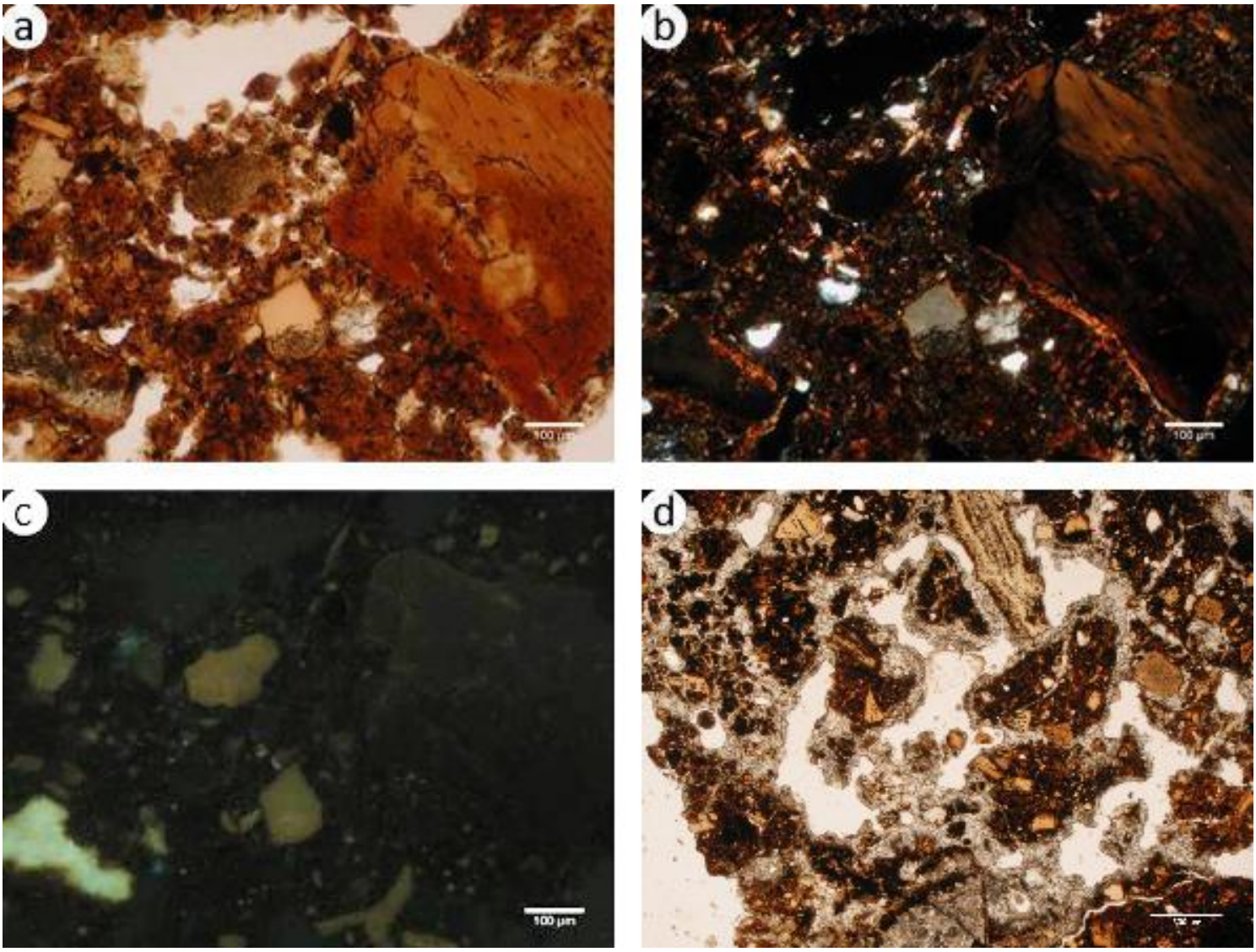
a
b
c
d
100 µm
100 µm
100 µm

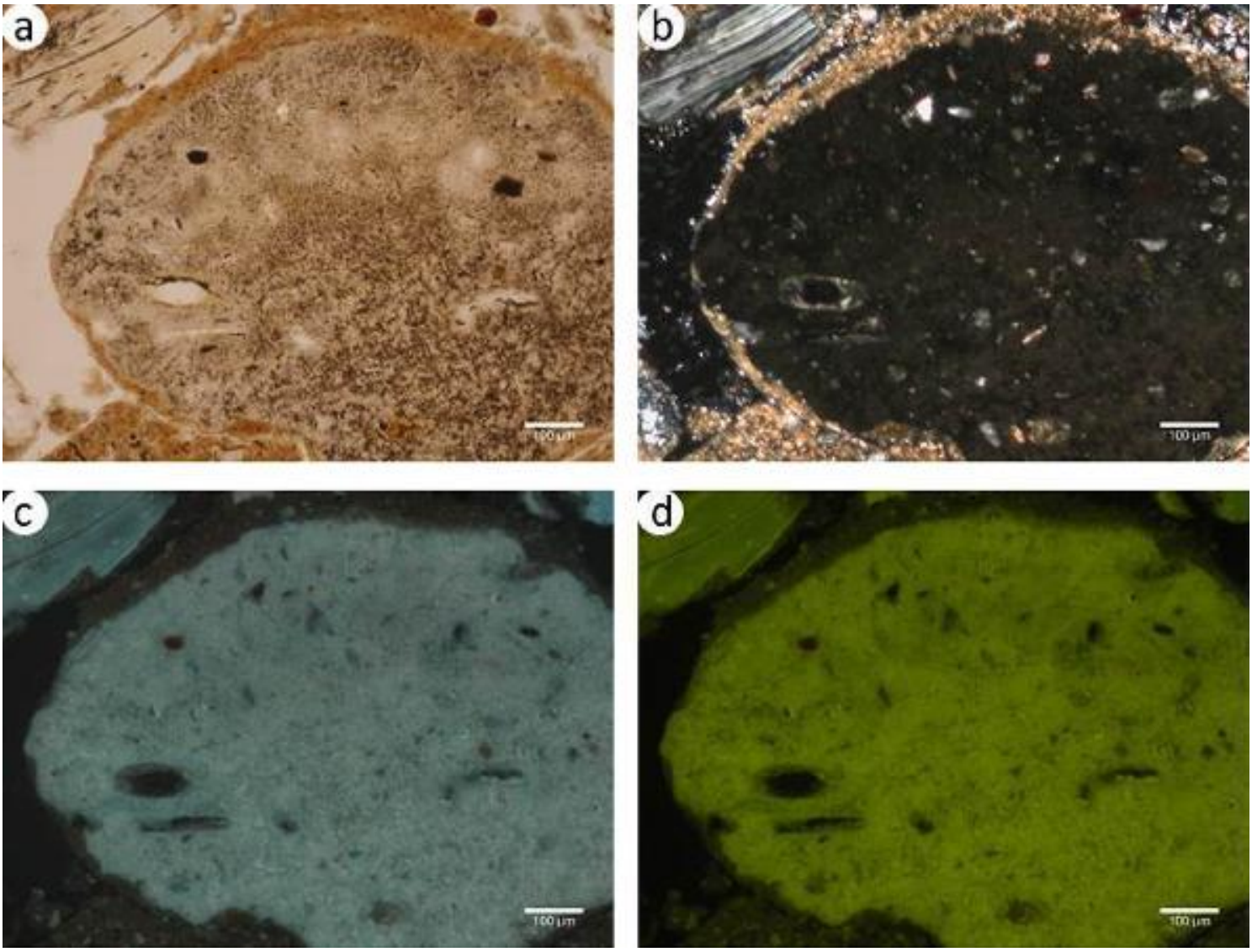
a
100 µm
b
100 µm
c
100 µm
d
100 µm

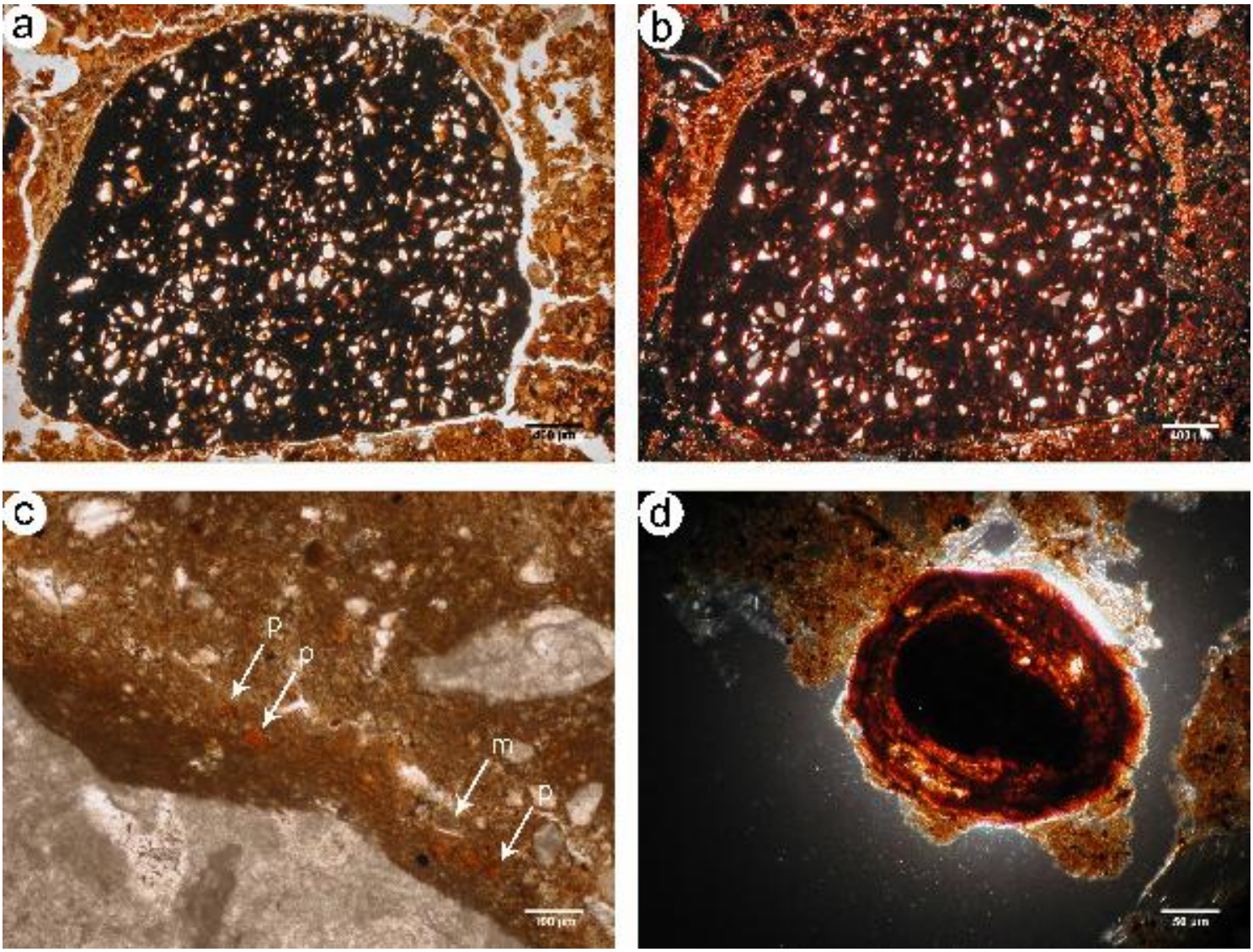
a
b
c
d
P
P
m
P

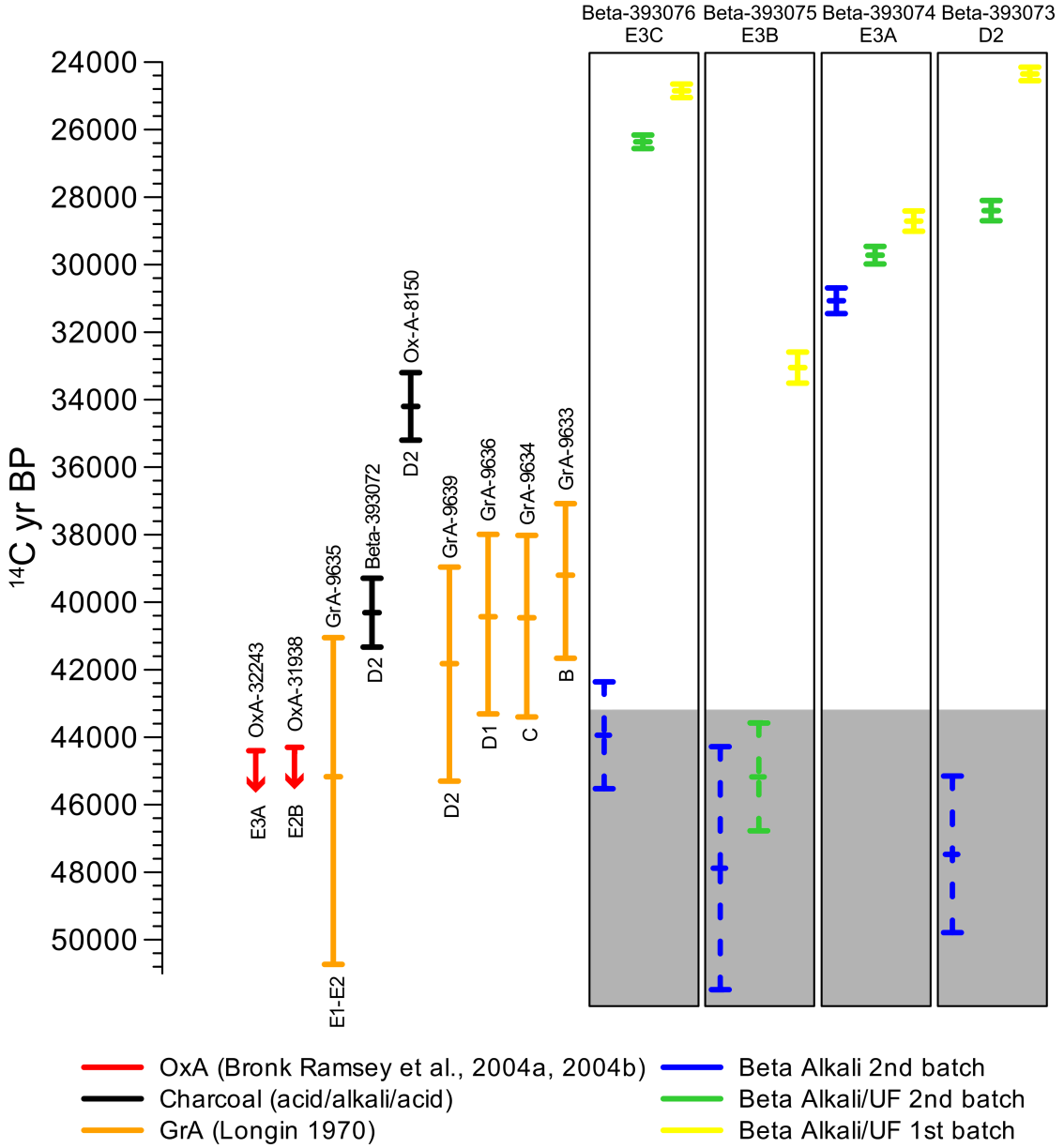
Beta-393076
E3C
Beta-393075
E3B
Beta-393074
E3A
Beta-393073
D2
24000
26000
28000
30000
32000
34000
36000
38000
40000
42000
44000
46000
48000
50000
14C yr BP
OxA-32243
E3A
OxA-31938
E2B
GrA-9635
E1-E2
Beta-393072
D2
Ox-A-8150
D2
GrA-9639
D2
GrA-9636
D1
GrA-9634
C
GrA-9633
B
OxA (Bronk Ramsey et al., 2004a, 2004b)
Charcoal (acid/alkali/acid)
GrA (Longin 1970)
Beta Alkali 2nd batch
Beta Alkali/UF 2nd batch
Beta Alkali/UF 1st batch

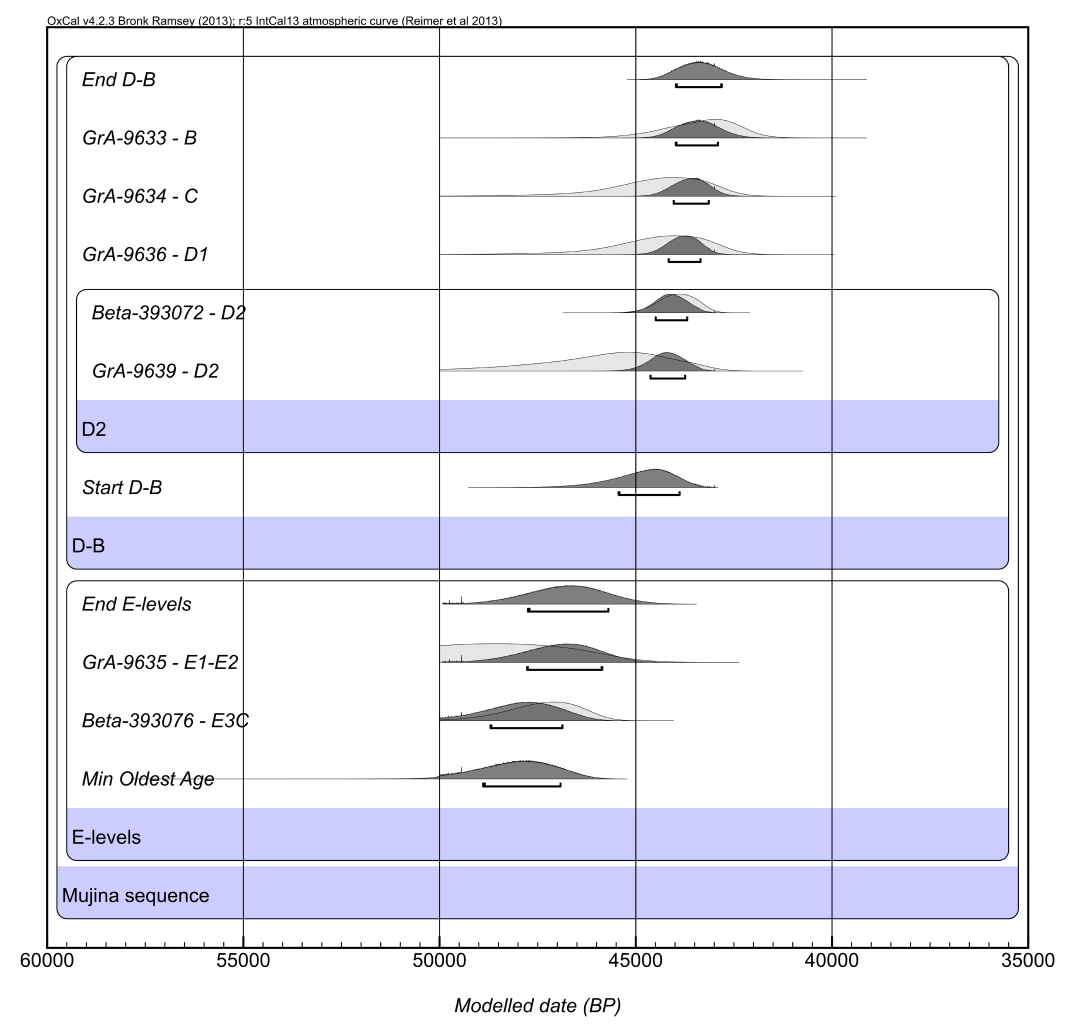
OxCal v4.2.3 Bronk Ramsey (2013); r:5 IntCal13 atmospheric curve (Reimer et al 2013)
End D-B
GrA-9633 - B
GrA-9634 - C
GrA-9636 - D1
Beta-393072 - D2
GrA-9639 - D2
D2
Start D-B
D-B
End E-levels
GrA-9635 - E1-E2
Beta-393076 - E3C
Min Oldest Age
E-levels
Mujina sequence
60000
55000
50000
45000
40000
35000
Modelled date (BP)

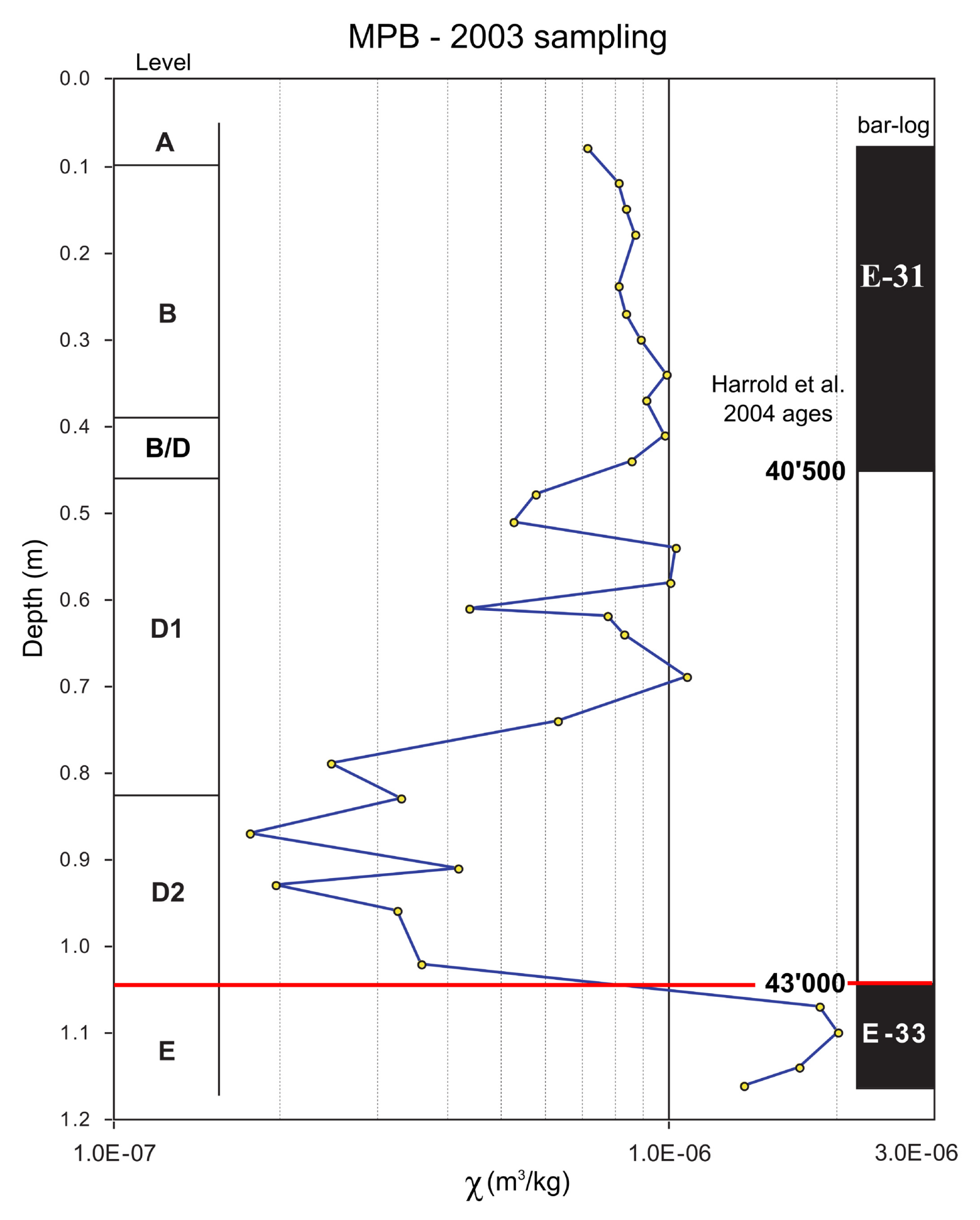
MPB - 2003 sampling
Level
0.0
0.1
0.2
0.3
0.4
0.5
0.6
0.7
0.8
0.9
1.0
1.1
1.2
A
B
B/D
D1
D2
E
Depth (m)
bar-log
E-31
Harrold et al.
2004 ages
40'500
43'000
E-33
1.0E-07
1.0E-06
3.0E-06
χ (m³/kg)

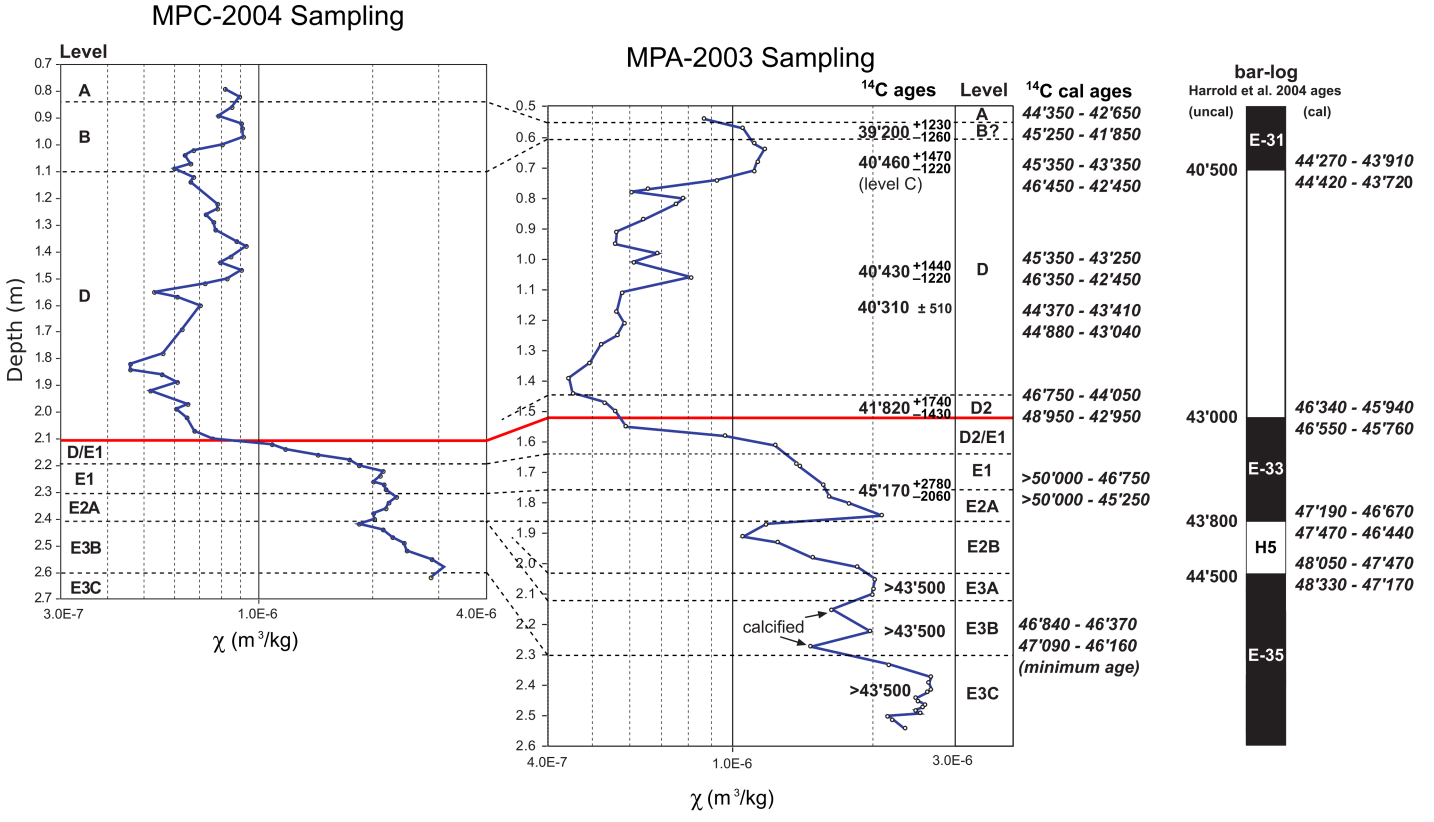
MPC-2004 Sampling
Level
A
B
D
D/E1
E1
E2A
E3B
E3C
Depth (m)
0.7
0.8
0.9
1.0
1.1
1.2
1.3
1.4
1.5
1.6
1.7
1.8
1.9
2.0
2.1
2.2
2.3
2.4
2.5
2.6
2.7
3.0E-7
1.0E-6
4.0E-6
χ (m³/kg)
MPA-2003 Sampling
14C ages
Level
14C cal ages
39'200 +1230 −1260
A
B?
44'350 - 42'650
45'250 - 41'850
40'460 +1470 −1220
(level C)
45'350 - 43'350
46'450 - 42'450
40'430 +1440 −1220
D
45'350 - 43'250
46'350 - 42'450
40'310 ± 510
44'370 - 43'410
44'880 - 43'040
41'820 +1740 −1430
D2
46'750 - 44'050
48'950 - 42'950
D2/E1
E1
45'170 +2780 −2060
>50'000 - 46'750
>50'000 - 45'250
E2A
E2B
>43'500
E3A
calcified
>43'500
E3B
46'840 - 46'370
47'090 - 46'160
(minimum age)
>43'500
E3C
0.5
0.6
0.7
0.8
0.9
1.0
1.1
1.2
1.3
1.4
1.5
1.6
1.7
1.8
1.9
2.0
2.1
2.2
2.3
2.4
2.5
2.6
4.0E-7
1.0E-6
3.0E-6
χ (m³/kg)
bar-log
Harrold et al. 2004 ages
(uncal)
(cal)
E-31
40'500
44'270 - 43'910
44'420 - 43'720
43'000
46'340 - 45'940
46'550 - 45'760
E-33
43'800
47'190 - 46'670
47'470 - 46'440
H5
44'500
48'050 - 47'470
48'330 - 47'170
E-35

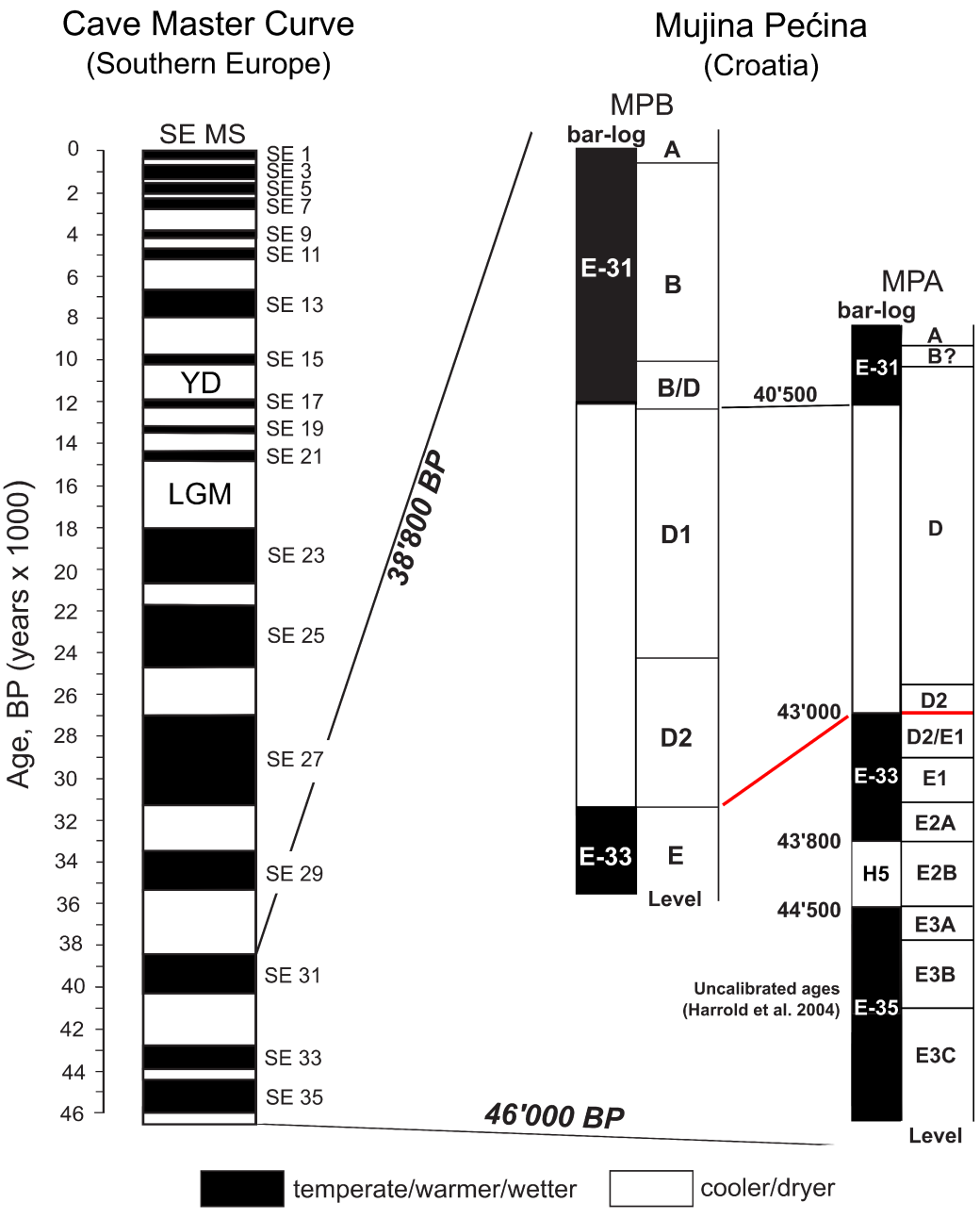
Cave Master Curve
(Southern Europe)
Mujina Pećina
(Croatia)
SE MS
MPB
bar-log
MPA
bar-log
Age, BP (years x 1000)
0
2
4
6
8
10
12
14
16
18
20
22
24
26
28
30
32
34
36
38
40
42
44
46
SE 1
SE 3
SE 5
SE 7
SE 9
SE 11
SE 13
SE 15
YD
SE 17
SE 19
SE 21
LGM
SE 23
SE 25
SE 27
SE 29
SE 31
SE 33
SE 35
38'800 BP
46'000 BP
A
B
B/D
D1
D2
E
E-31
E-33
Level
40'500
43'000
43'800
44'500
A
B?
D
D2
D2/E1
E1
E2A
E2B
E3A
E3B
E3C
E-31
E-33
H5
E-35
Level
Uncalibrated ages
(Harrold et al. 2004)
temperate/warmer/wetter
cooler/dryer

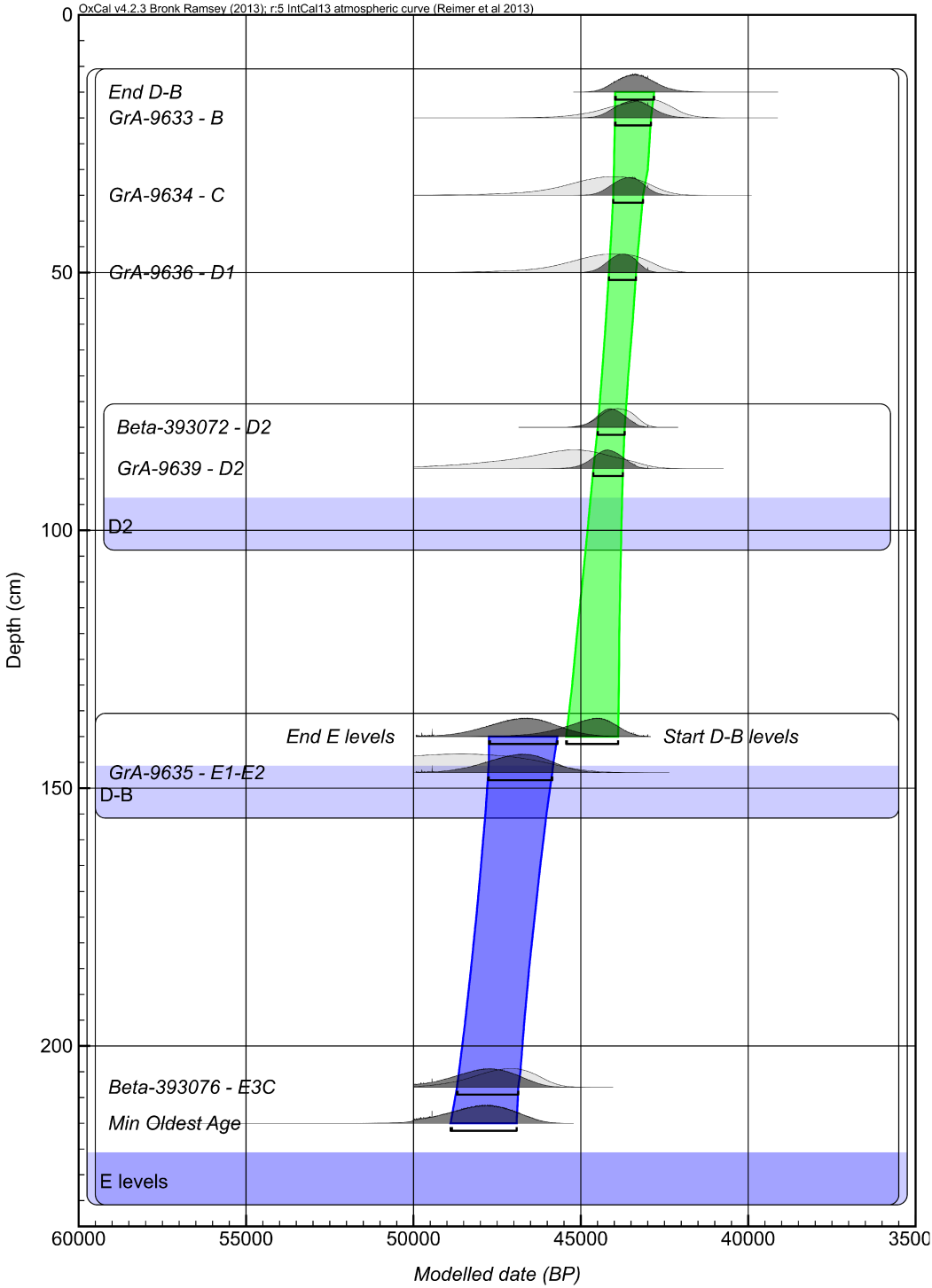
OxCal v4.2.3 Bronk Ramsey (2013); r:5 IntCal13 atmospheric curve (Reimer et al 2013)
End D-B
GrA-9633 - B
GrA-9634 - C
GrA-9636 - D1
Beta-393072 - D2
GrA-9639 - D2
D2
End E levels
Start D-B levels
GrA-9635 - E1-E2
D-B
Beta-393076 - E3C
Min Oldest Age
E levels
0
50
100
150
200
Depth (cm)
60000
55000
50000
45000
40000
3500
Modelled date (BP)

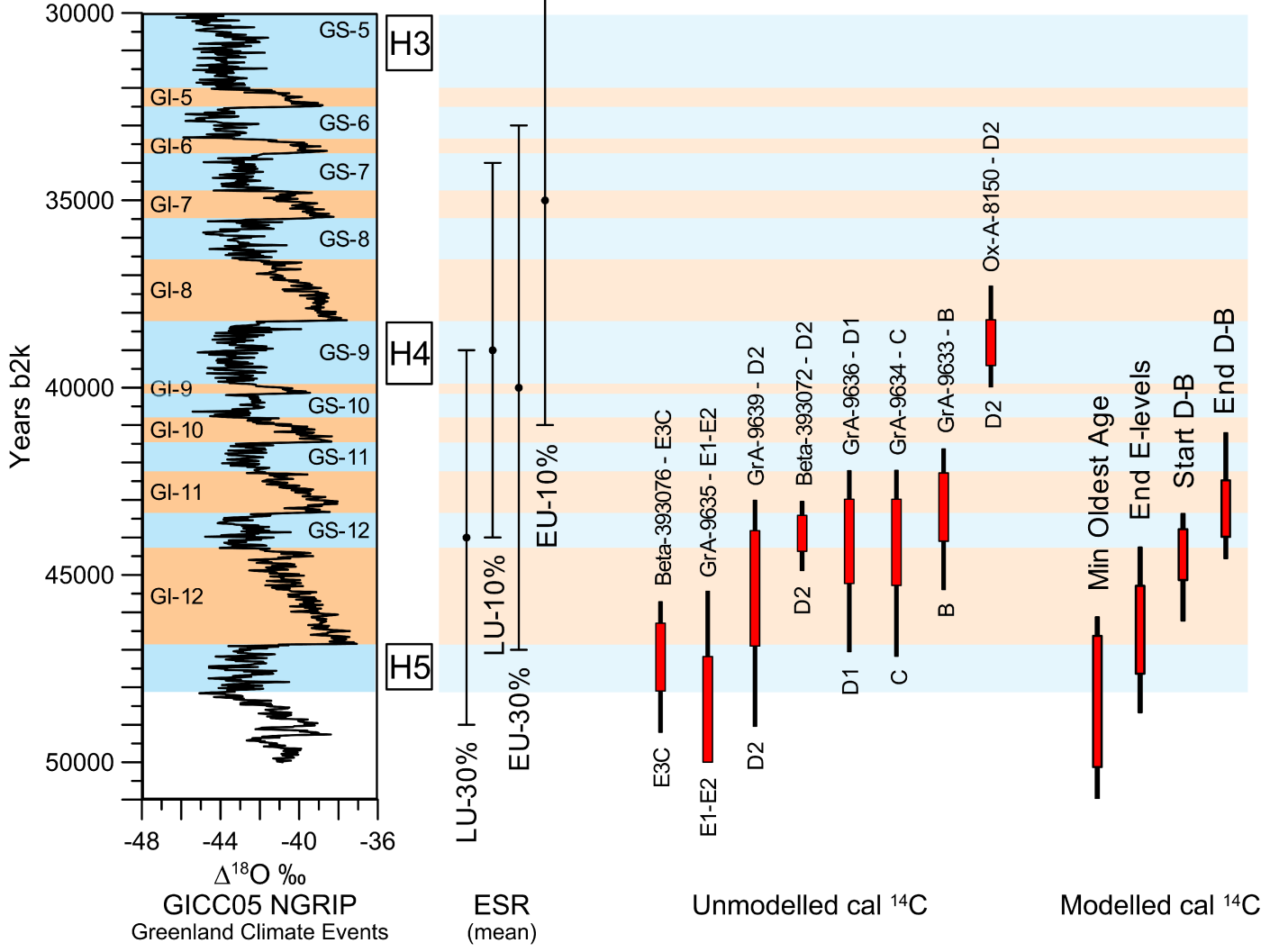
30000
35000
40000
45000
50000
Years b2k
GS-5
GI-5
GS-6
GI-6
GS-7
GI-7
GS-8
GI-8
GS-9
GI-9
GS-10
GI-10
GS-11
GI-11
GS-12
GI-12
H3
H4
H5
-48
-44
-40
-36
Δ18O ‰
GICC05 NGRIP
Greenland Climate Events
LU-30%
LU-10%
EU-30%
EU-10%
ESR
(mean)
Beta-393076 - E3C
GrA-9635 - E1-E2
GrA-9639 - D2
Beta-393072 - D2
GrA-9636 - D1
GrA-9634 - C
GrA-9633 - B
Ox-A-8150 - D2
E3C
E1-E2
D2
D2
D1
C
B
D2
Unmodelled cal 14C
Min Oldest Age
End E-levels
Start D-B
End D-B
Modelled cal 14C


43° 40' 0.0000" N
10 km
Hungary
Slovenia
CROATIA
Serbia and Herzegovina
ADRIATIC SEA
Montenegro
Italy
Mujina Pećina
Kaštela Bay
TROGIR
SPLIT
43° 30' 0.0000" N
16° 10' 0.0000" E
16° 30' 0.0000" E
ADRIATIC SEA

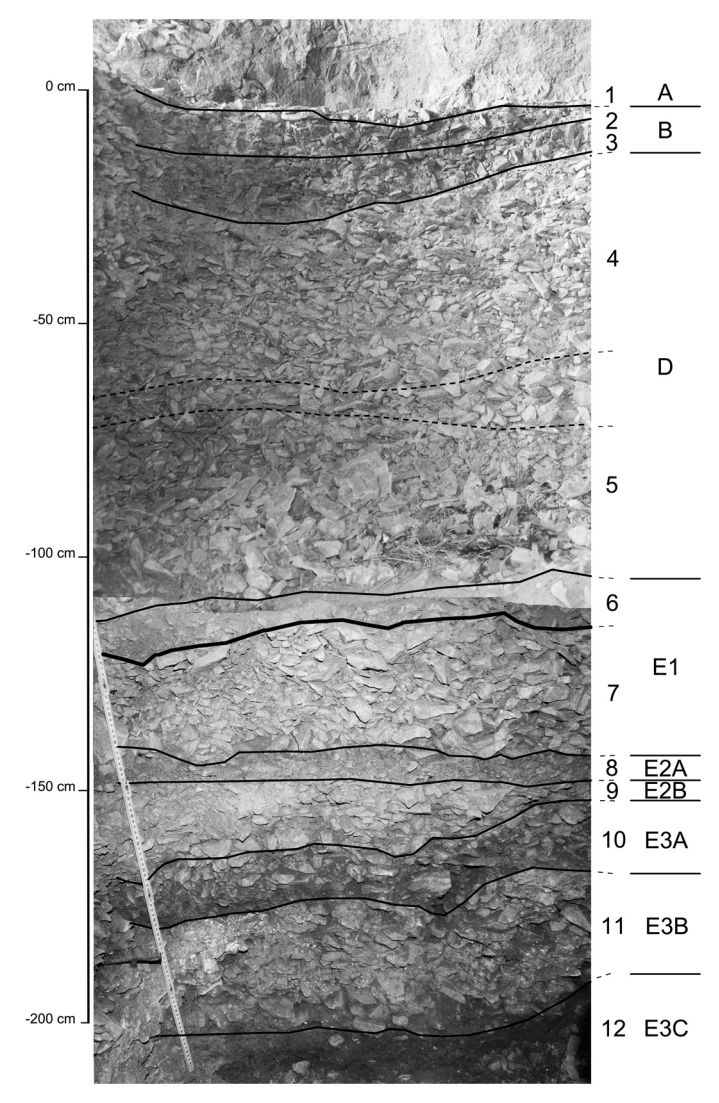
0 cm
-50 cm
-100 cm
-150 cm
-200 cm
1
2
3
4
5
6
7
8
9
10
11
12
A
B
D
E1
E2A
E2B
E3A
E3B
E3C

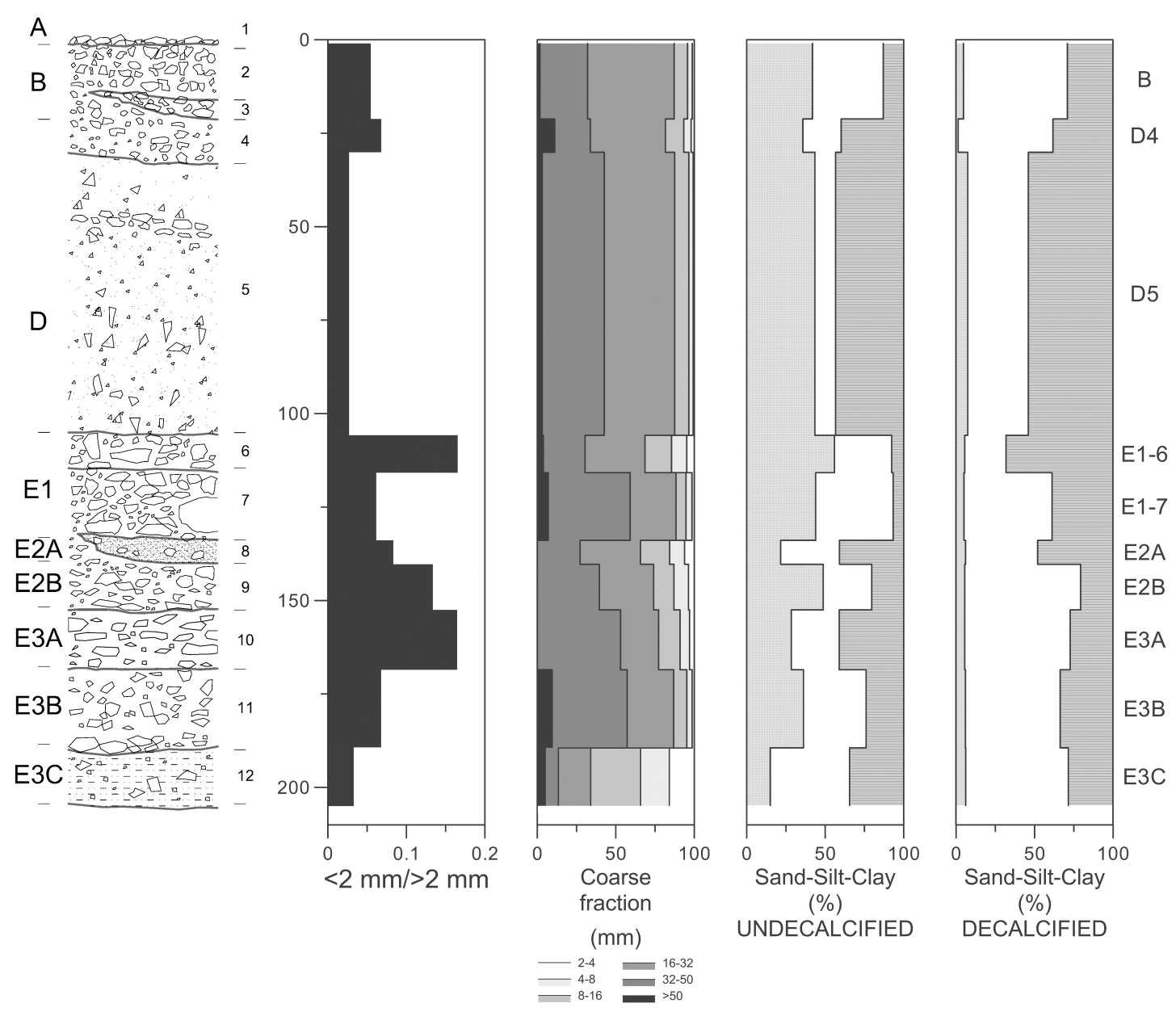
A
B
D
E1
E2A
E2B
E3A
E3B
E3C
1
2
3
4
5
6
7
8
9
10
11
12
0
50
100
150
200
0
0.1
0.2
<2 mm/>2 mm
0
50
100
Coarse fraction (mm)
2-4
4-8
8-16
16-32
32-50
>50
0
50
100
Sand-Silt-Clay (%) UNDECALCIFIED
0
50
100
Sand-Silt-Clay (%) DECALCIFIED
B
D4
D5
E1-6
E1-7
E2A
E2B
E3A
E3B
E3C

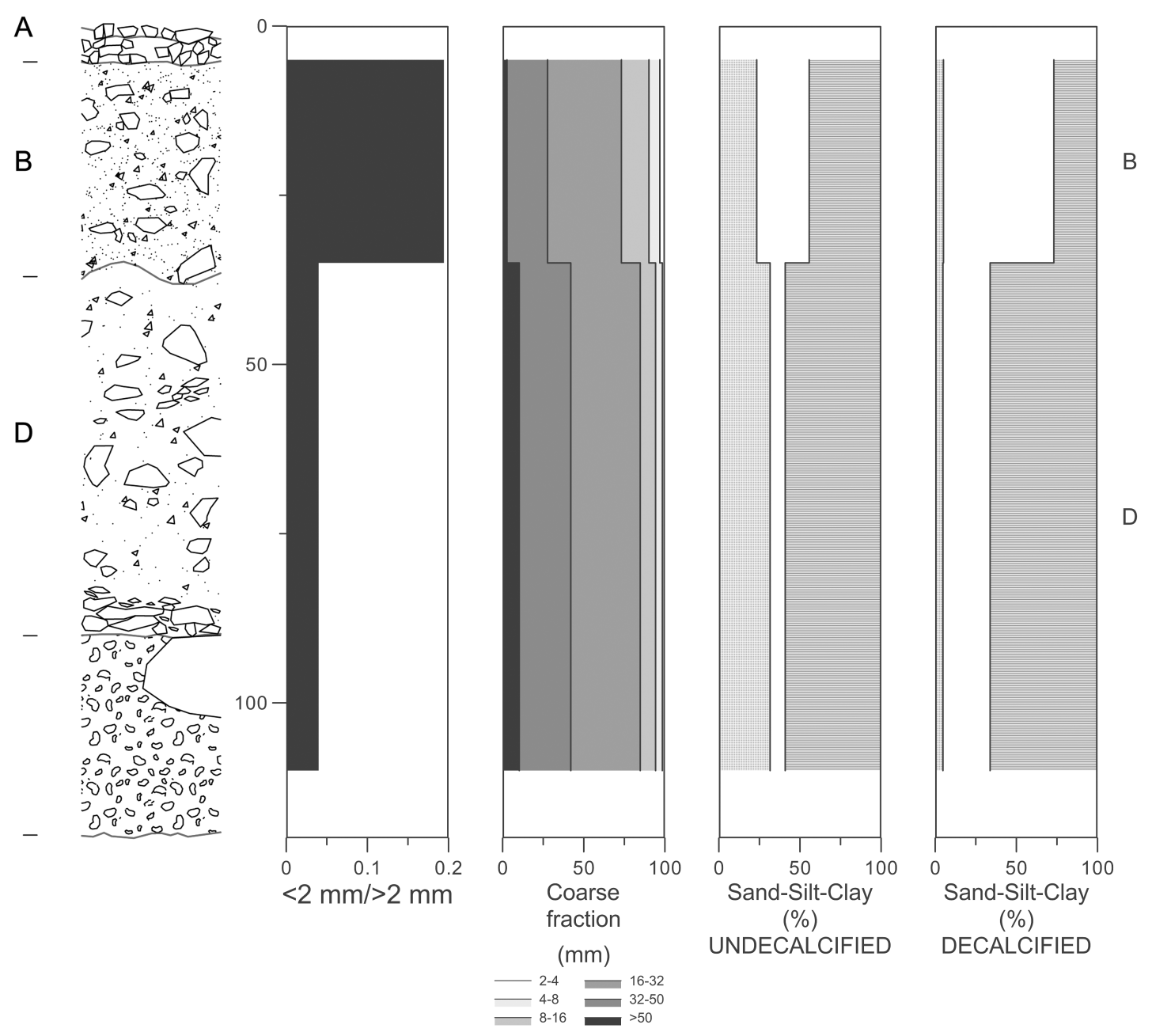
A
B
D
0
50
100
0
0.1
0.2
<2 mm/>2 mm
0
50
100
Coarse fraction (mm)
2-4
4-8
8-16
16-32
32-50
>50
0
50
100
Sand-Silt-Clay (%) UNDECALCIFIED
0
50
100
Sand-Silt-Clay (%) DECALCIFIED
B
D

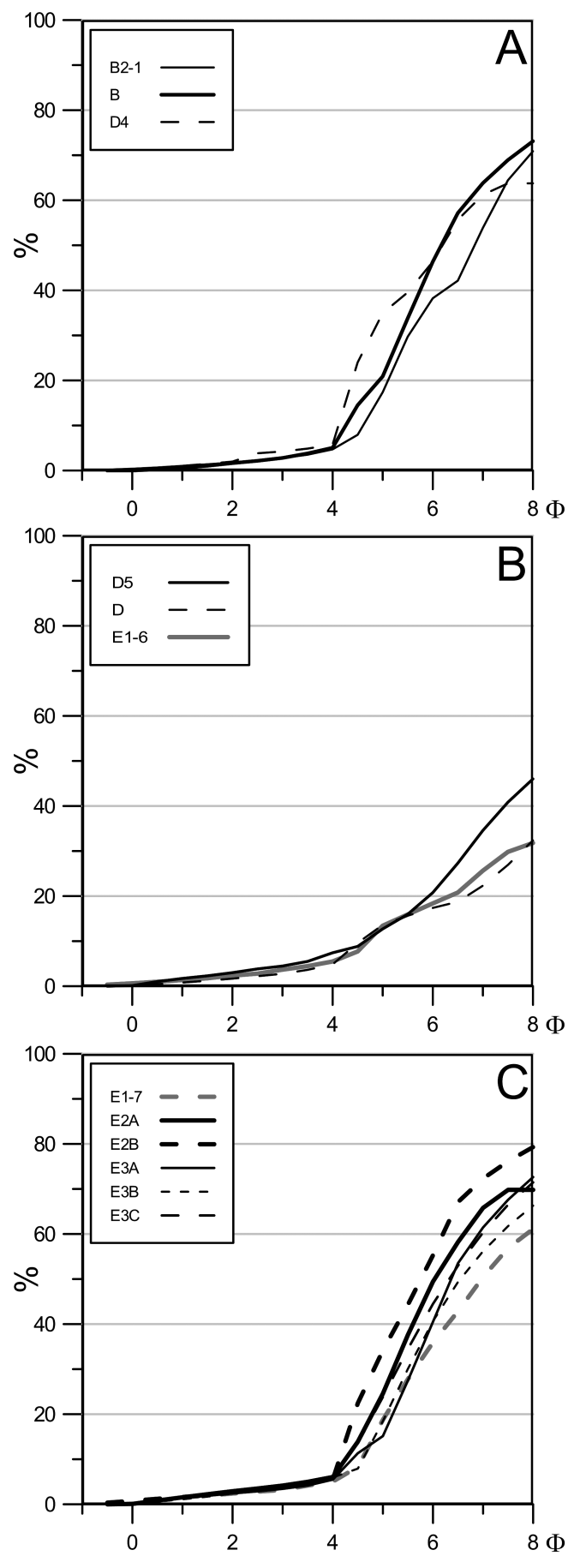
A
B2-1
B
D4
%
100
80
60
40
20
0
0
2
4
6
8 Φ
B
D5
D
E1-6
%
100
80
60
40
20
0
0
2
4
6
8 Φ
C
E1-7
E2A
E2B
E3A
E3B
E3C
%
100
80
60
40
20
0
0
2
4
6
8 Φ

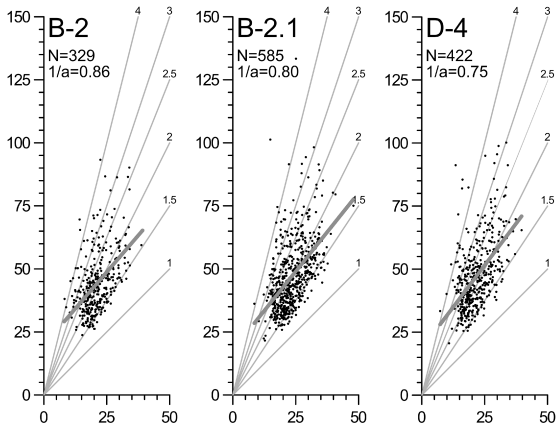
B-2
N=329
1/a=0.86

B-2.1
N=585
1/a=0.80

D-4
N=422
1/a=0.75

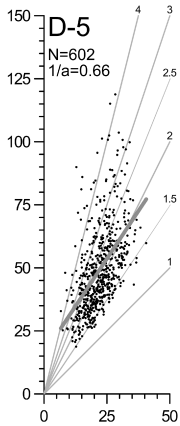
D-5
N=602
1/a=0.66

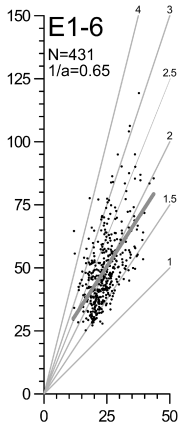
E1-6
N=431
1/a=0.65

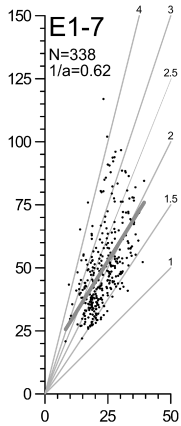
E1-7
N=338
1/a=0.62

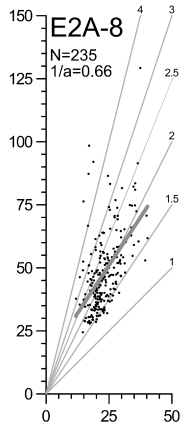
E2A-8
N=235
1/a=0.66

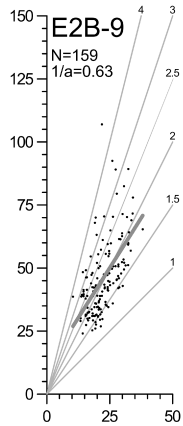
E2B-9
N=159
1/a=0.63

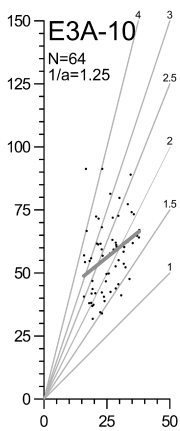
E3A-10
N=64
1/a=1.25

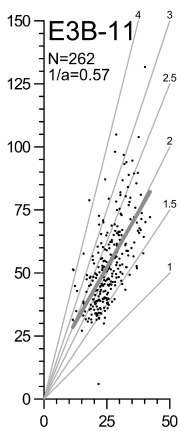
E3B-11
N=262
1/a=0.57

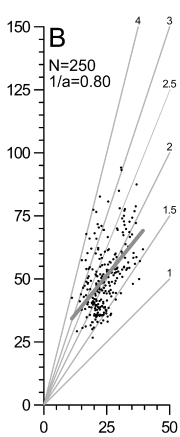
B
N=250
1/a=0.80

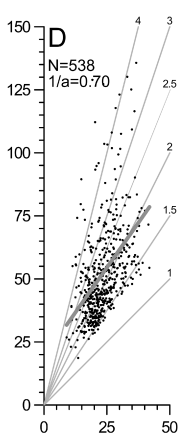
D
N=538
1/a=0.70

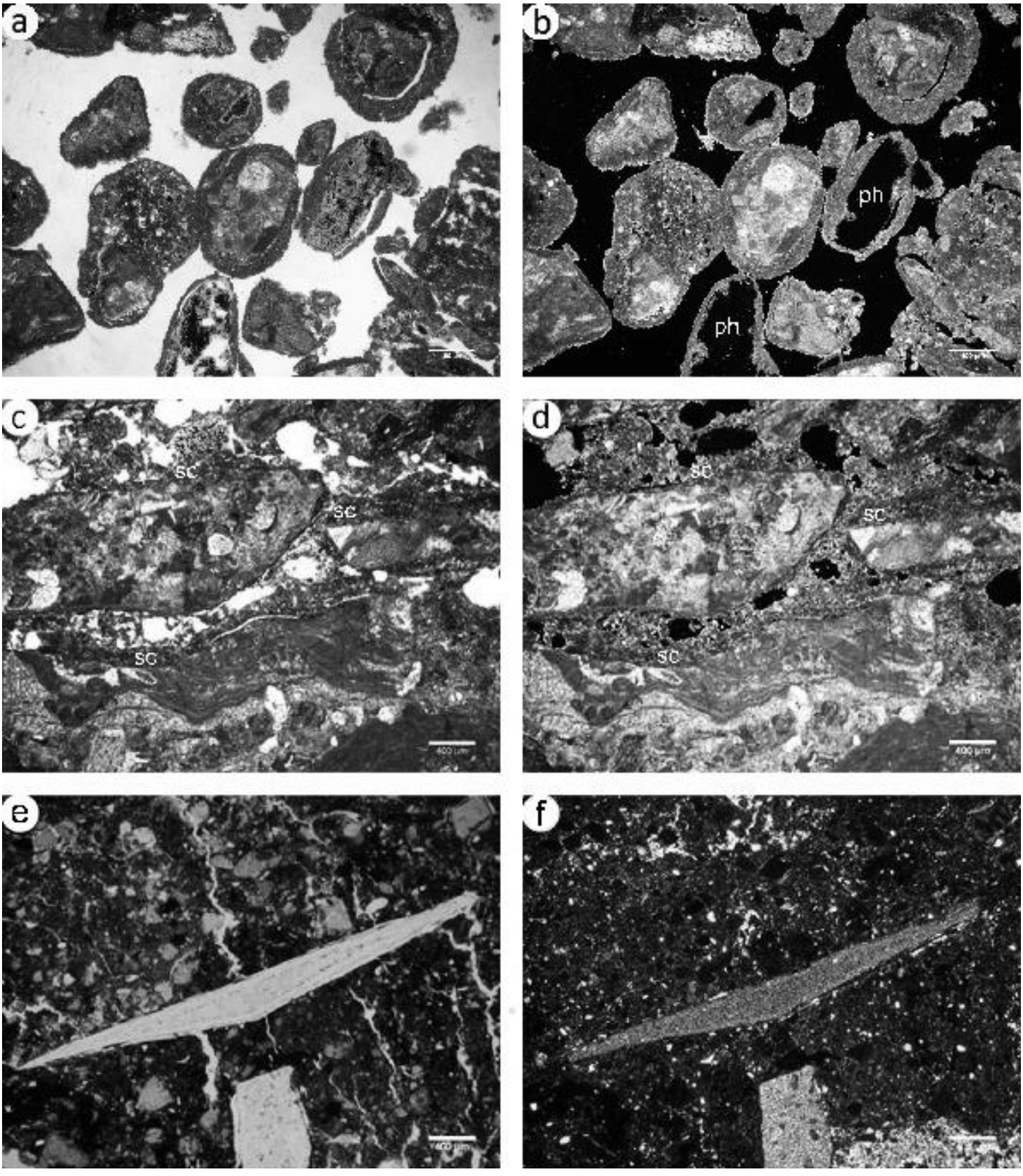
a
b
ph
ph
c
sc
sc
sc
d
sc
sc
sc
e
f

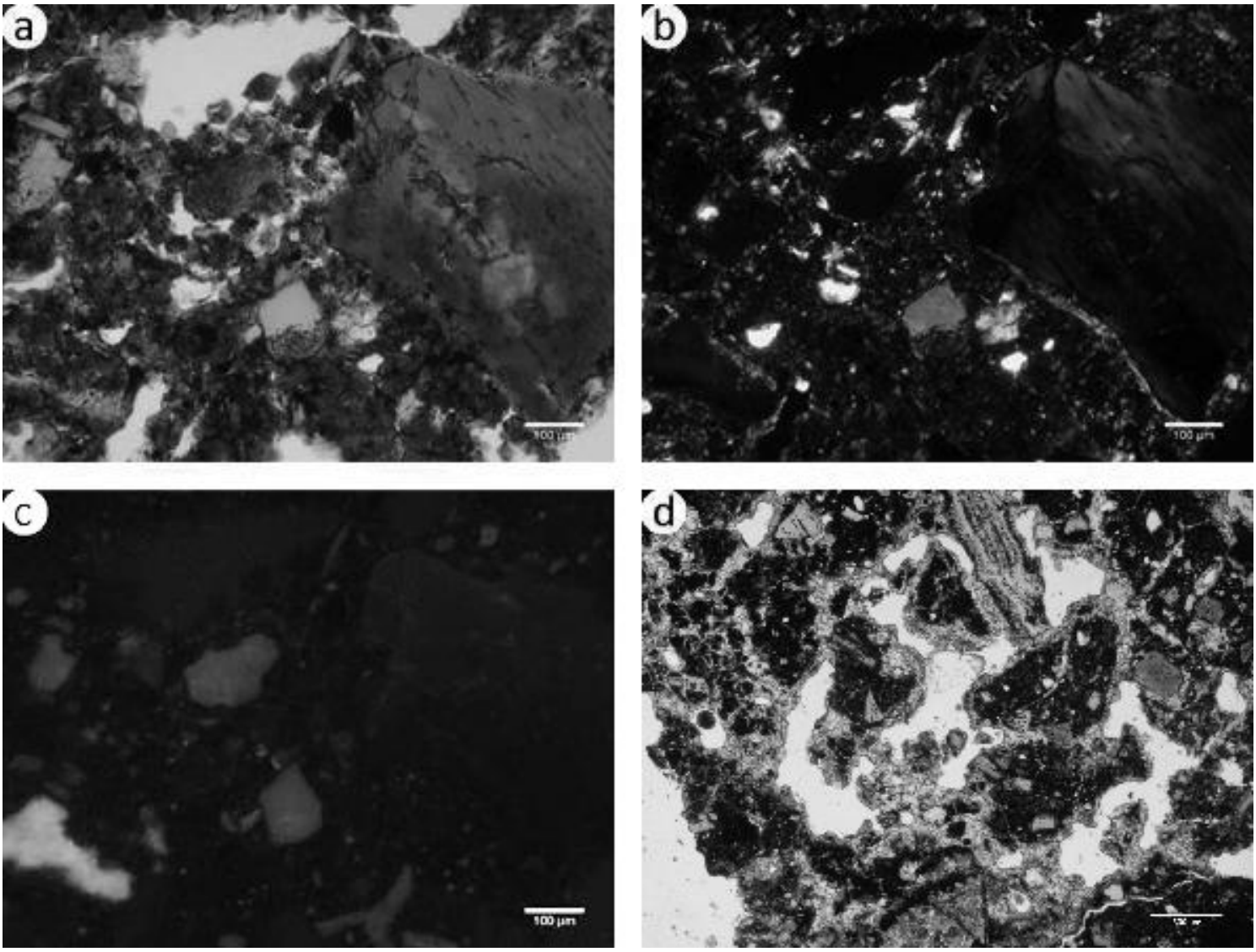
a
100 µm
b
100 µm
c
100 µm
d

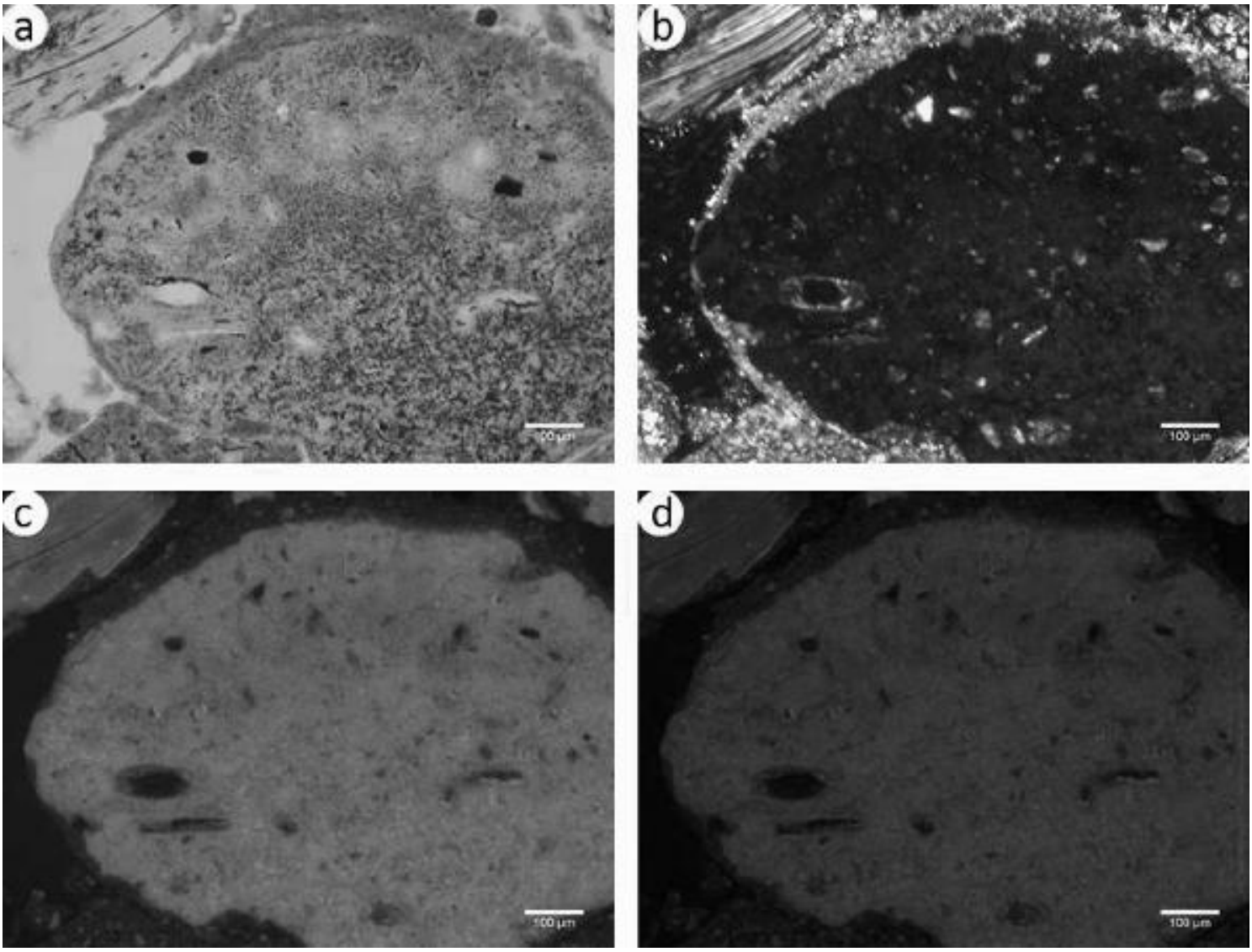
a
100 µm
b
100 µm
c
100 µm
d
100 µm

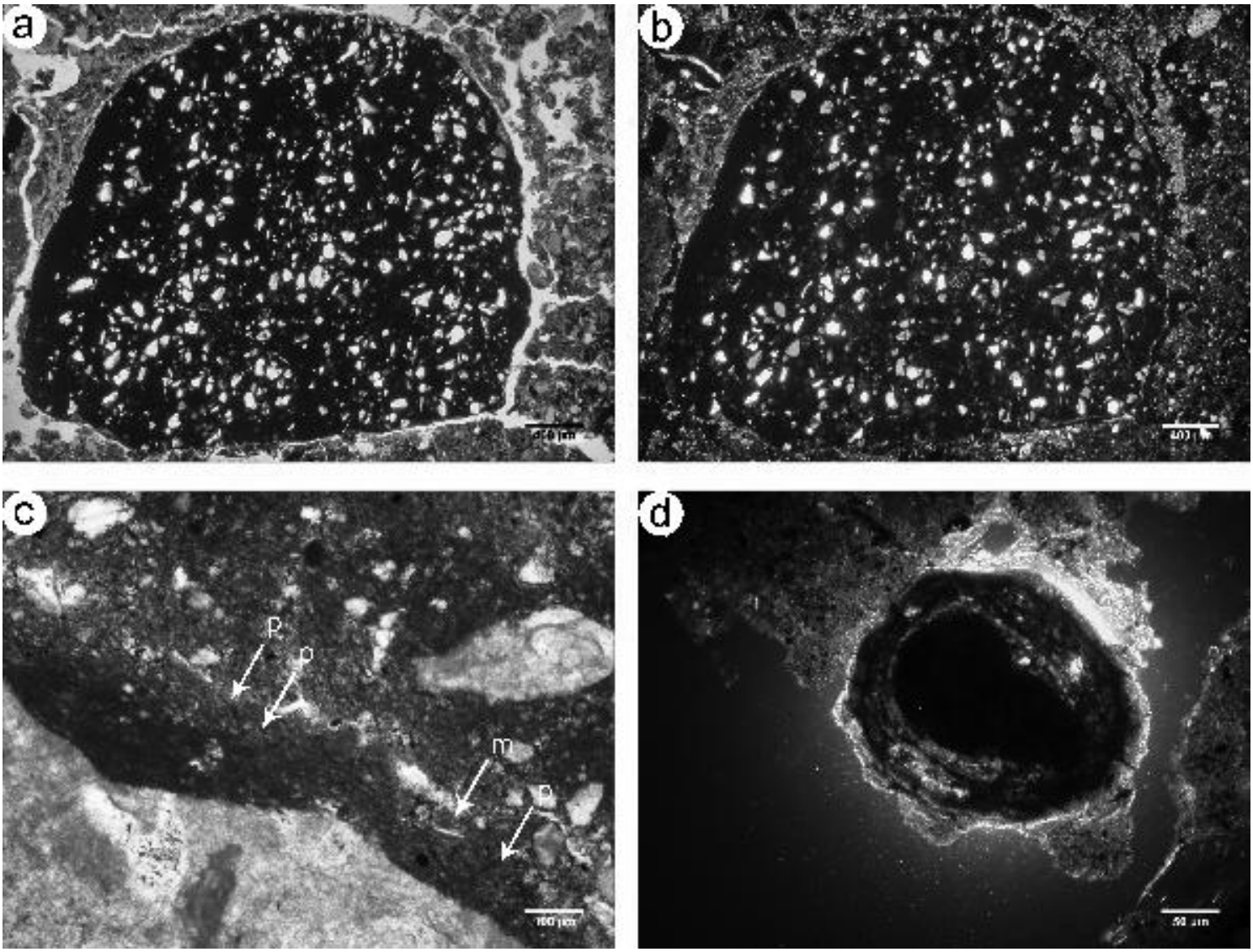
a
b
c
d
P
P
m
P

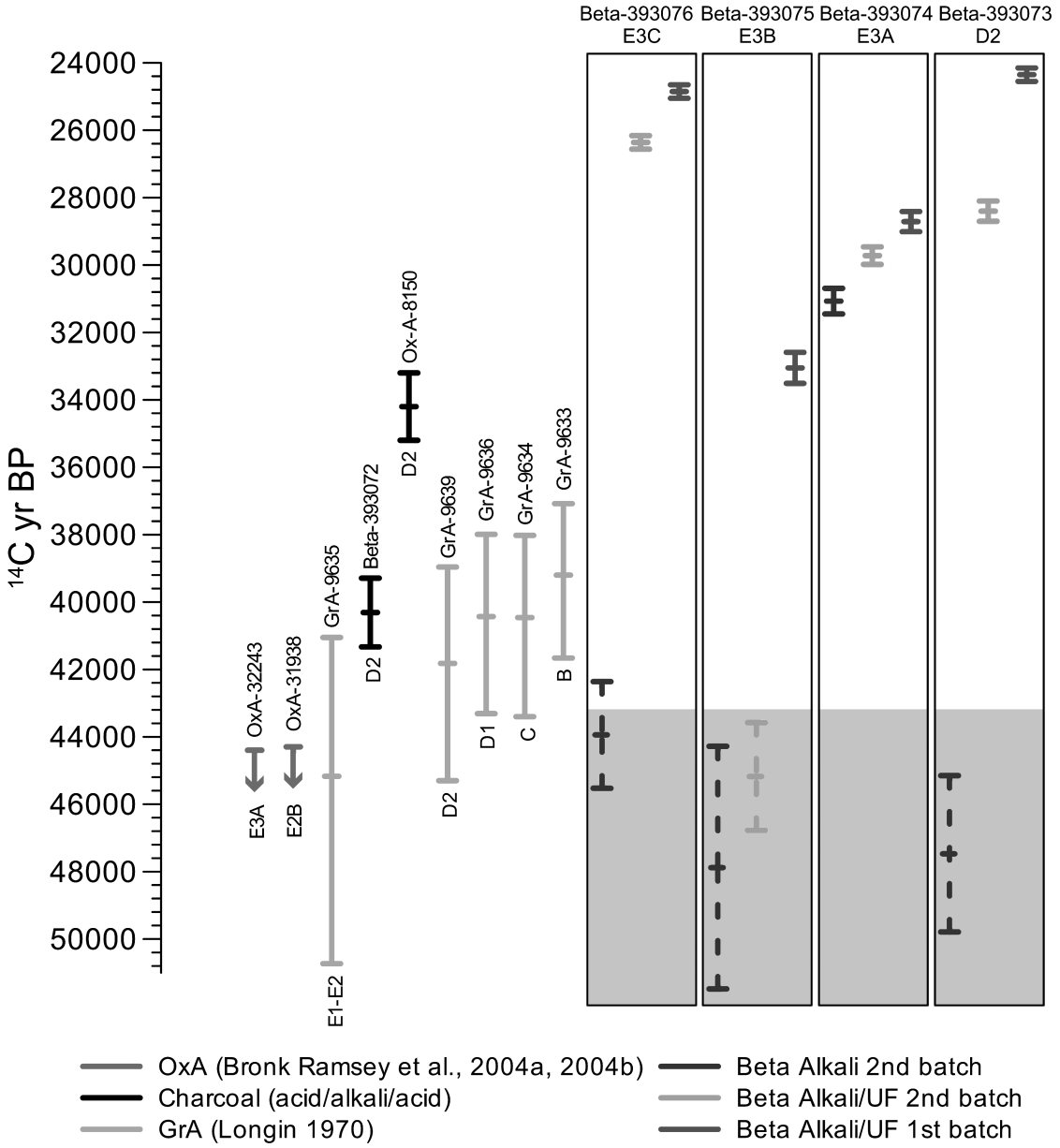
Beta-393076
E3C
Beta-393075
E3B
Beta-393074
E3A
Beta-393073
D2
24000
26000
28000
30000
32000
34000
36000
38000
40000
42000
44000
46000
48000
50000
14C yr BP
OxA-32243
E3A
OxA-31938
E2B
GrA-9635
E1-E2
D2
Beta-393072
D2
Ox-A-8150
D2
GrA-9639
D1
GrA-9636
C
GrA-9634
B
GrA-9633
OxA (Bronk Ramsey et al., 2004a, 2004b)
Charcoal (acid/alkali/acid)
GrA (Longin 1970)
Beta Alkali 2nd batch
Beta Alkali/UF 2nd batch
Beta Alkali/UF 1st batch

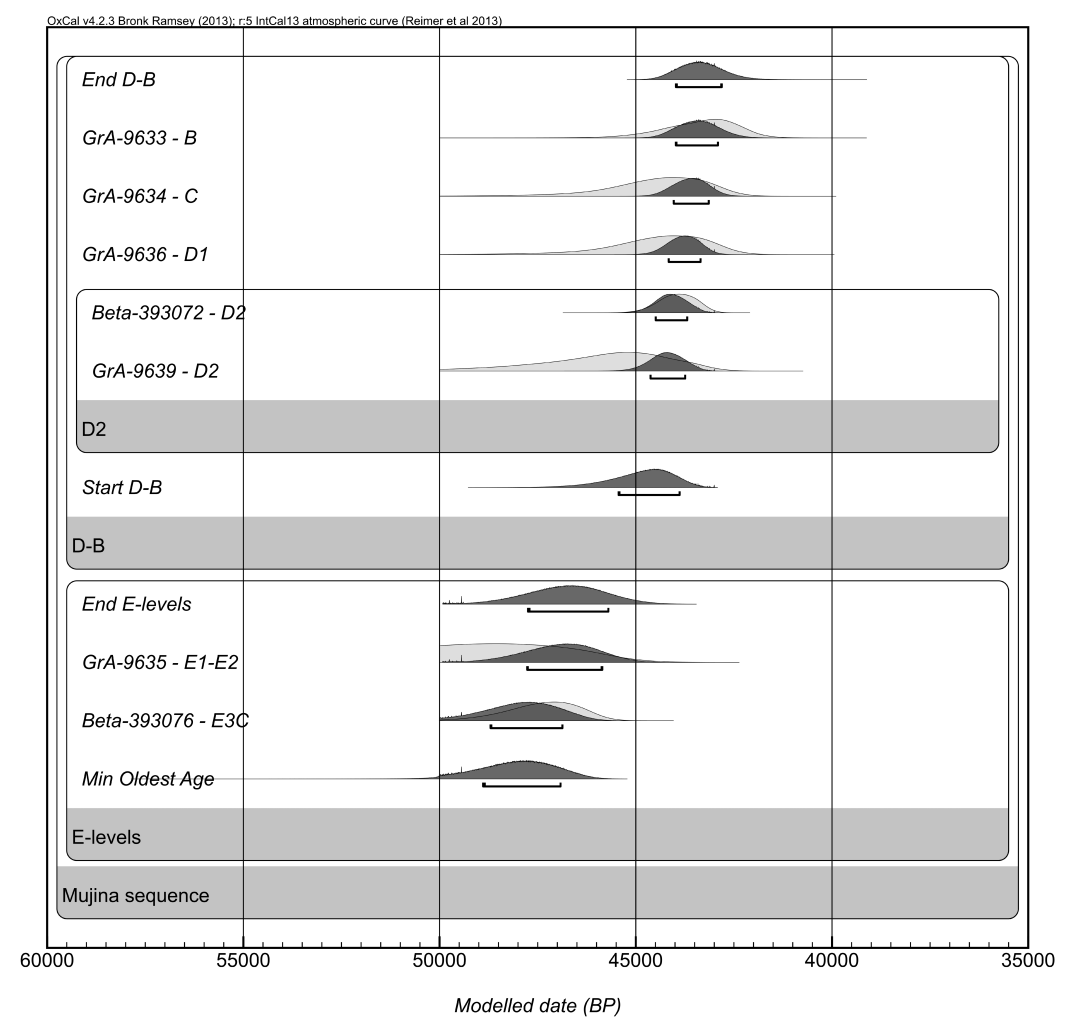
OxCal v4.2.3 Bronk Ramsey (2013); r:5 IntCal13 atmospheric curve (Reimer et al 2013)
End D-B
GrA-9633 - B
GrA-9634 - C
GrA-9636 - D1
Beta-393072 - D2
GrA-9639 - D2
D2
Start D-B
D-B
End E-levels
GrA-9635 - E1-E2
Beta-393076 - E3C
Min Oldest Age
E-levels
Mujina sequence
60000
55000
50000
45000
40000
35000
Modelled date (BP)

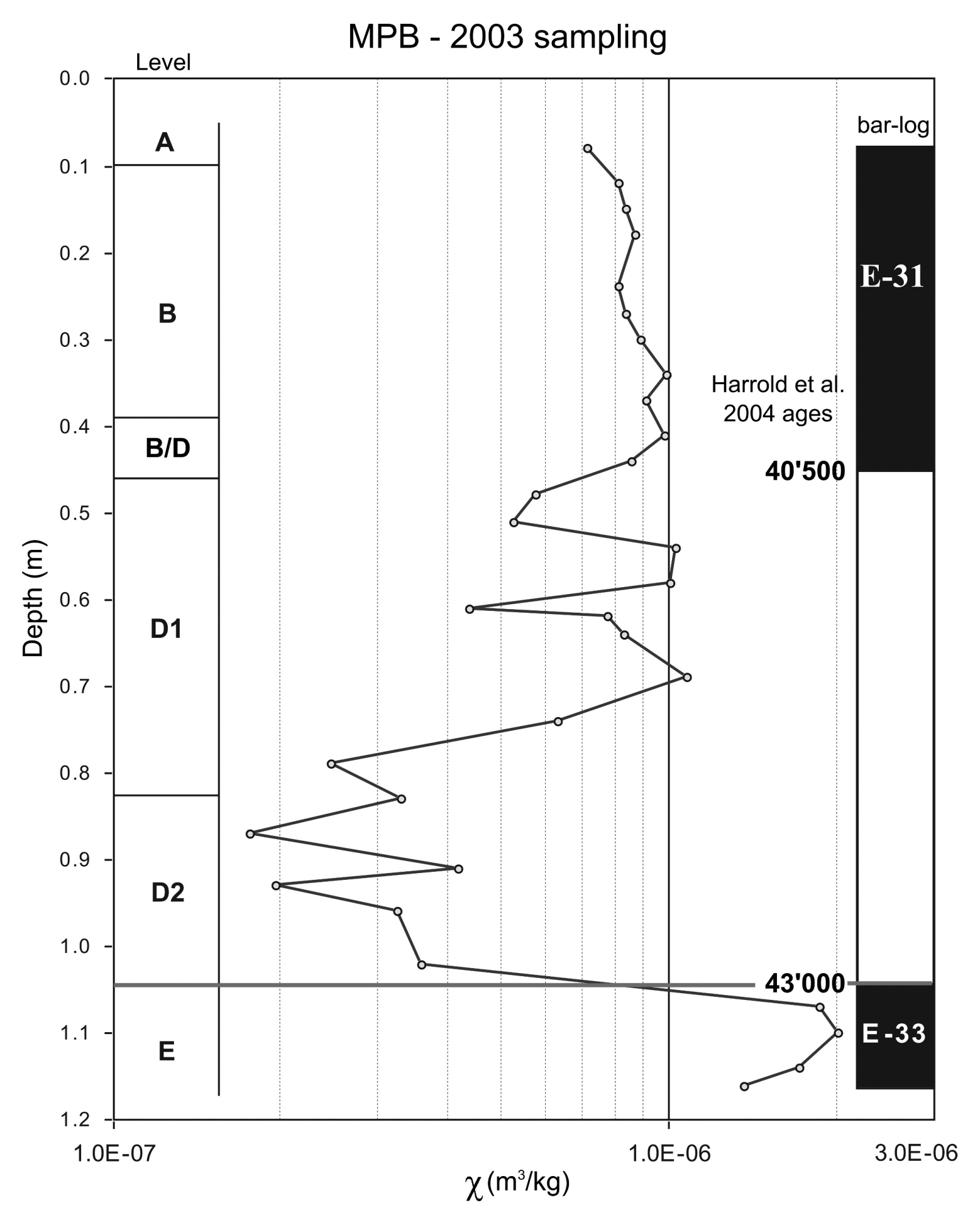
MPB - 2003 sampling
Level
0.0
0.1
0.2
0.3
0.4
0.5
0.6
0.7
0.8
0.9
1.0
1.1
1.2
A
B
B/D
D1
D2
E
Depth (m)
bar-log
E-31
Harrold et al.
2004 ages
40'500
43'000
E-33
1.0E-07
1.0E-06
3.0E-06
χ (m³/kg)

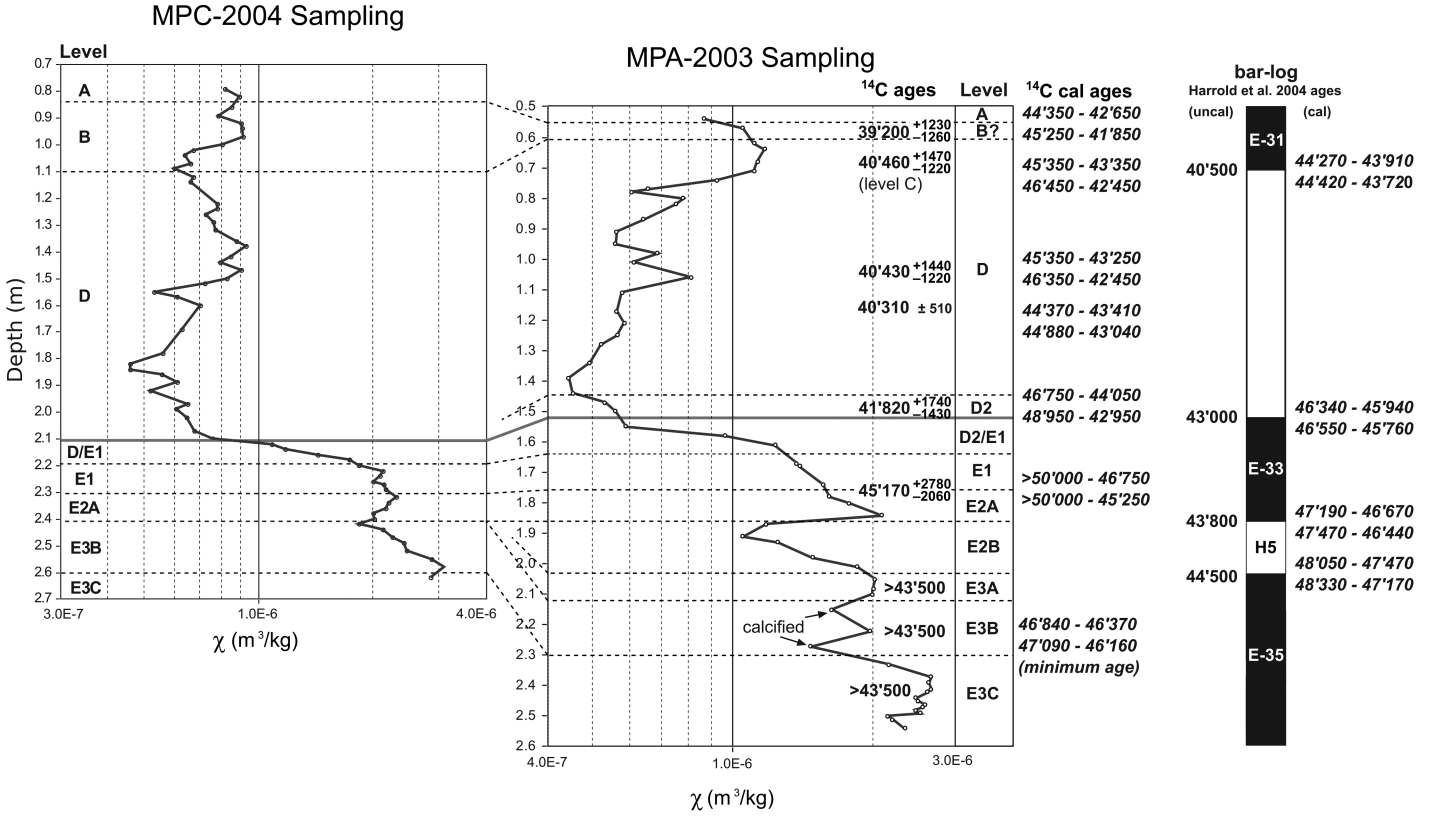
MPC-2004 Sampling
Level
A
B
D
D/E1
E1
E2A
E3B
E3C
Depth (m)
0.7
0.8
0.9
1.0
1.1
1.2
1.3
1.4
1.5
1.6
1.7
1.8
1.9
2.0
2.1
2.2
2.3
2.4
2.5
2.6
2.7
3.0E-7
1.0E-6
4.0E-6
χ (m³/kg)
MPA-2003 Sampling
14C ages
Level
14C cal ages
39'200 +1230 −1260
A
B?
44'350 - 42'650
45'250 - 41'850
40'460 +1470 −1220
(level C)
45'350 - 43'350
46'450 - 42'450
40'430 +1440 −1220
D
45'350 - 43'250
46'350 - 42'450
40'310 ± 510
44'370 - 43'410
44'880 - 43'040
46'750 - 44'050
41'820 +1740 −1430
D2
48'950 - 42'950
D2/E1
E1
45'170 +2780 −2060
>50'000 - 46'750
>50'000 - 45'250
E2A
E2B
>43'500
E3A
calcified
>43'500
E3B
46'840 - 46'370
47'090 - 46'160
(minimum age)
>43'500
E3C
0.5
0.6
0.7
0.8
0.9
1.0
1.1
1.2
1.3
1.4
1.5
1.6
1.7
1.8
1.9
2.0
2.1
2.2
2.3
2.4
2.5
2.6
4.0E-7
1.0E-6
3.0E-6
χ (m³/kg)
bar-log
Harrold et al. 2004 ages
(uncal)
(cal)
E-31
40'500
44'270 - 43'910
44'420 - 43'720
43'000
46'340 - 45'940
46'550 - 45'760
E-33
43'800
47'190 - 46'670
47'470 - 46'440
H5
48'050 - 47'470
44'500
48'330 - 47'170
E-35

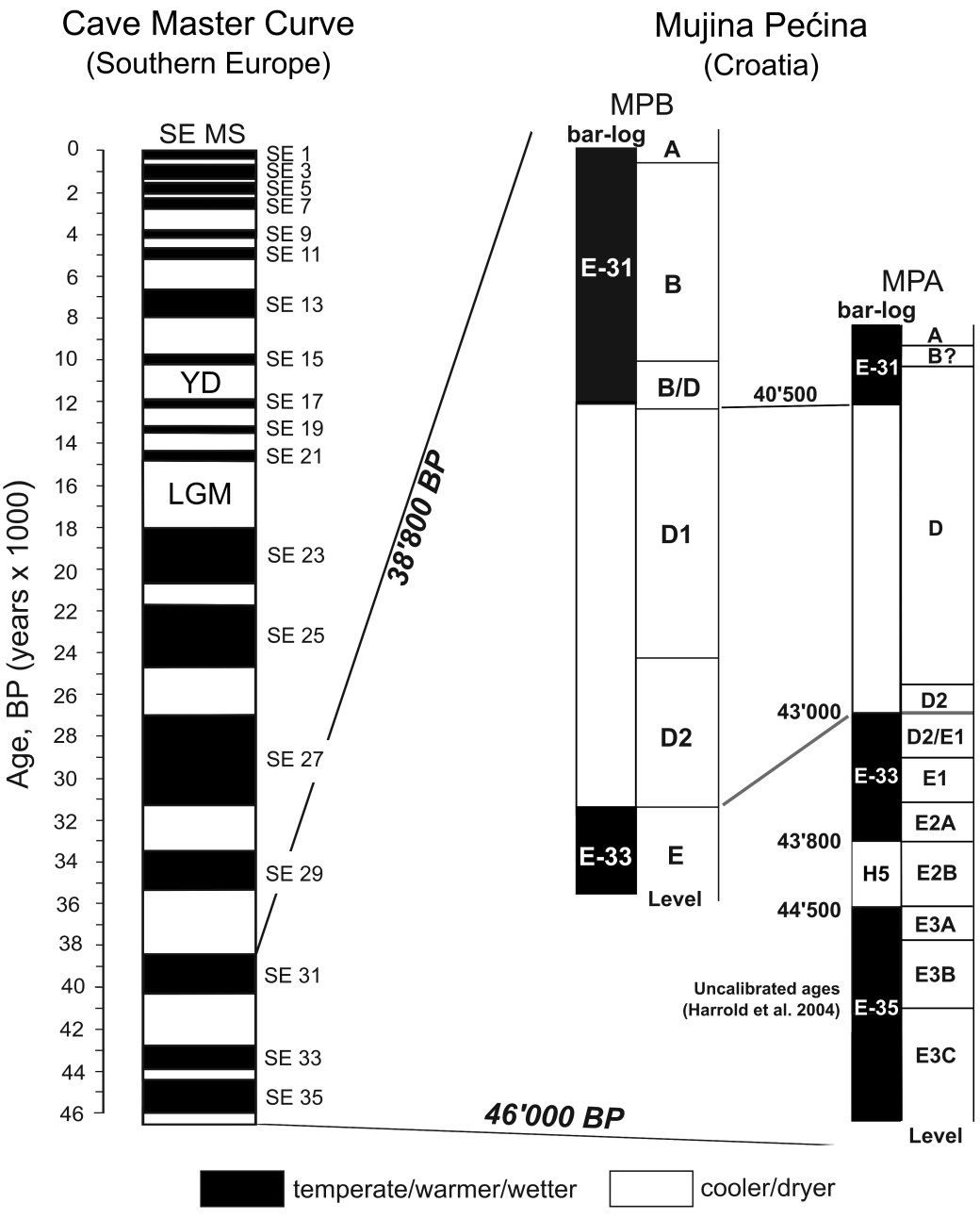
Cave Master Curve
(Southern Europe)
Mujina Pećina
(Croatia)
SE MS
MPB
bar-log
MPA
bar-log
Age, BP (years x 1000)
0
2
4
6
8
10
12
14
16
18
20
22
24
26
28
30
32
34
36
38
40
42
44
46
SE 1
SE 3
SE 5
SE 7
SE 9
SE 11
SE 13
SE 15
YD
SE 17
SE 19
SE 21
LGM
SE 23
SE 25
SE 27
SE 29
SE 31
SE 33
SE 35
38'800 BP
46'000 BP
A
B
B/D
D1
D2
E
E-31
E-33
Level
40'500
43'000
43'800
44'500
A
B?
D
D2
D2/E1
E1
E2A
E2B
E3A
E3B
E3C
H5
E-35
Uncalibrated ages
(Harrold et al. 2004)
temperate/warmer/wetter
cooler/dryer

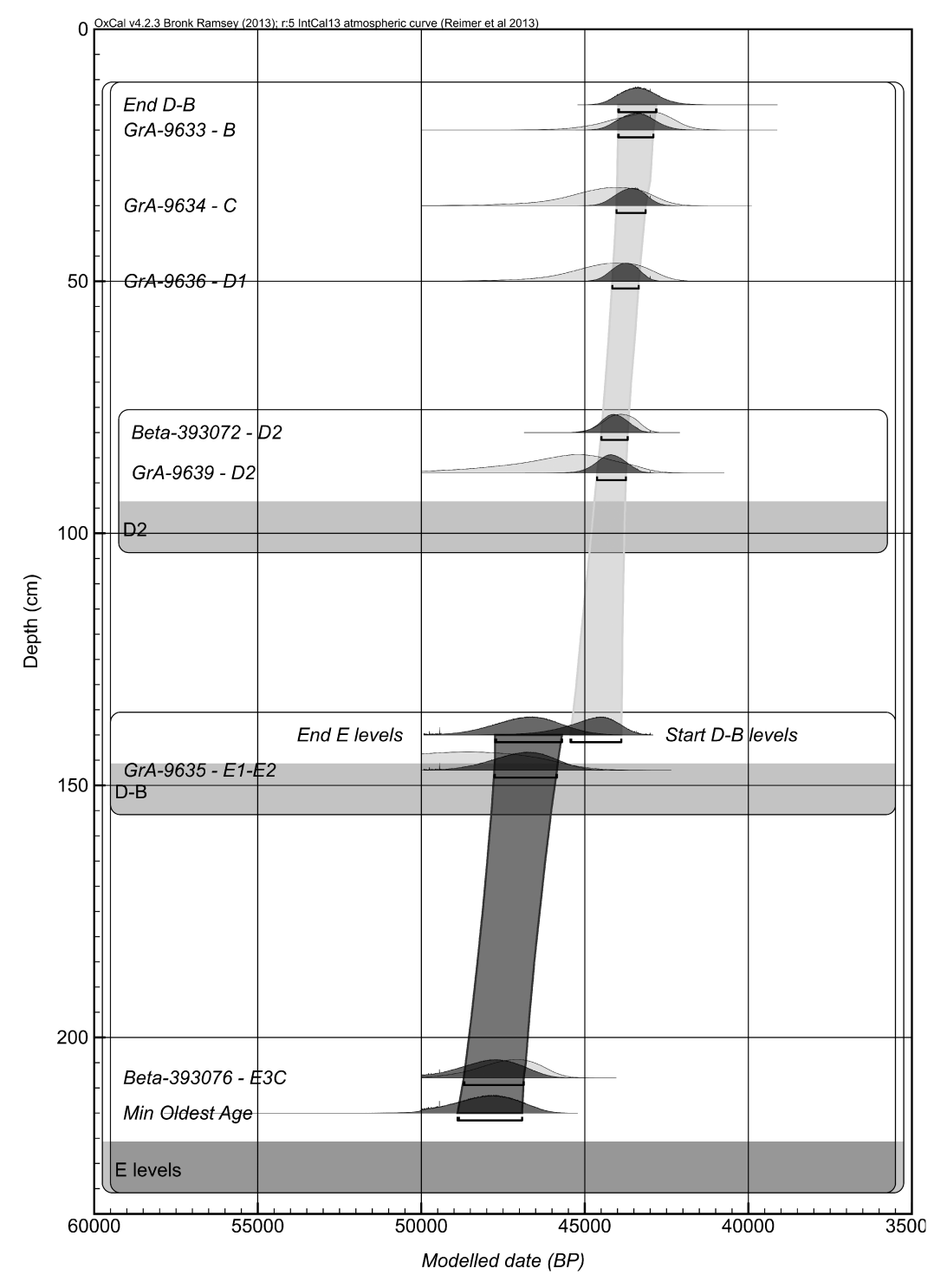
OxCal v4.2.3 Bronk Ramsey (2013); r:5 IntCal13 atmospheric curve (Reimer et al 2013)
End D-B
GrA-9633 - B
GrA-9634 - C
GrA-9636 - D1
Beta-393072 - D2
GrA-9639 - D2
D2
End E levels
Start D-B levels
GrA-9635 - E1-E2
D-B
Beta-393076 - E3C
Min Oldest Age
E levels
Depth (cm)
0
50
100
150
200
60000
55000
50000
45000
40000
3500
Modelled date (BP)

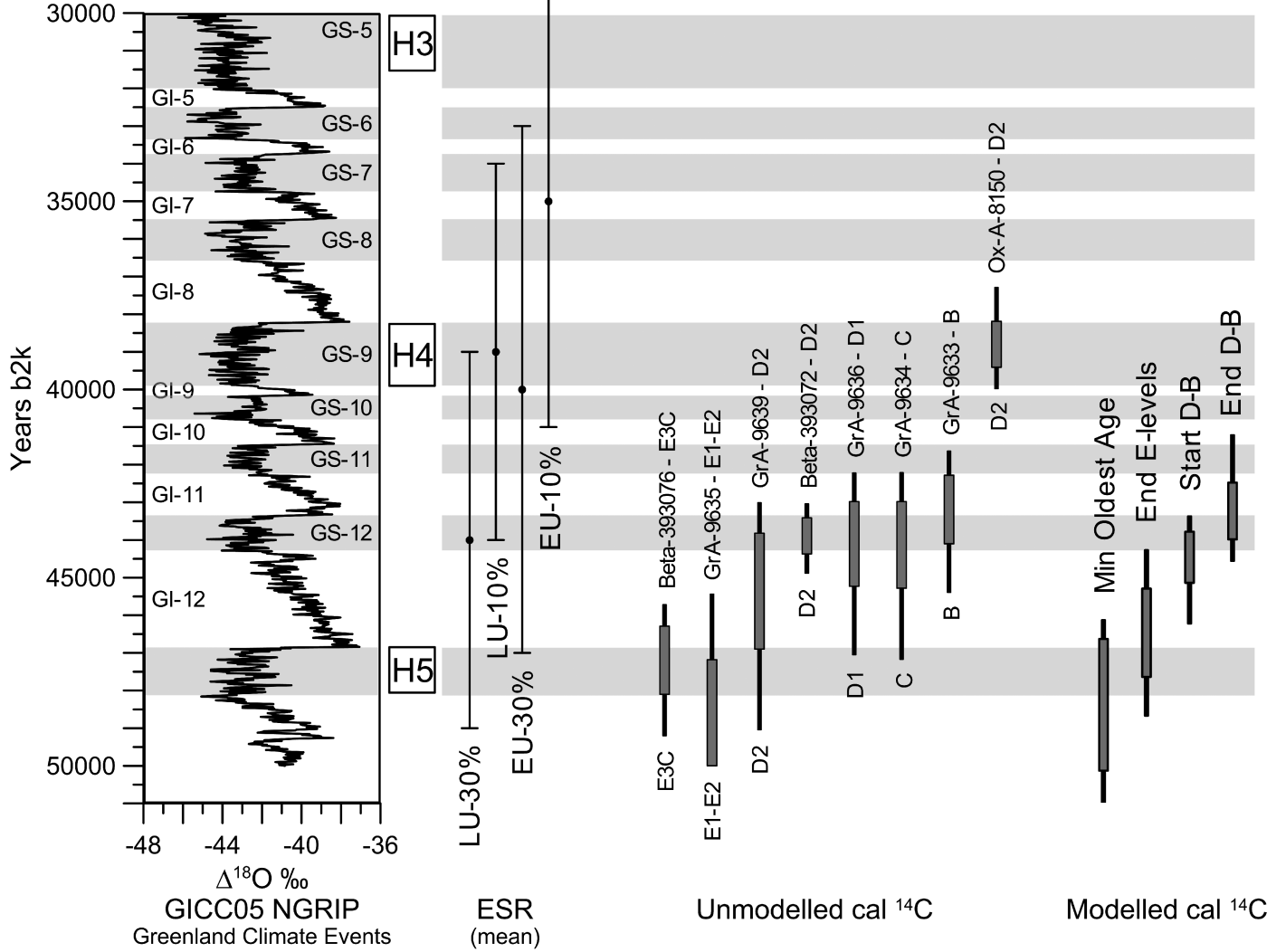
30000
35000
40000
45000
50000
Years b2k
GS-5
GI-5
GS-6
GI-6
GS-7
GI-7
GS-8
GI-8
GS-9
GI-9
GS-10
GI-10
GS-11
GI-11
GS-12
GI-12
H3
H4
H5
-48
-44
-40
-36
Δ18O ‰
GICC05 NGRIP
Greenland Climate Events
LU-30%
LU-10%
EU-30%
EU-10%
ESR
(mean)
Beta-393076 - E3C
GrA-9635 - E1-E2
GrA-9639 - D2
Beta-393072 - D2
GrA-9636 - D1
GrA-9634 - C
GrA-9633 - B
Ox-A-8150 - D2
E3C
E1-E2
D2
D2
D1
C
B
D2
Unmodelled cal 14C
Min Oldest Age
End E-levels
Start D-B
End D-B
Modelled cal 14C

Archaeological layers	Lithologic units	Relative depth (cm)	Munsell Colour (moist)	Field observations	Texture	Matrix	Aggregation	Boundary
A	1	0 - 5		Poorly sorted rubble, chaotically dispersed on the cave floor. Ow	A-SA	-	-	Sharp
B	2	5 - 10	strong brown 7.5YR 5/6	Poorly sorted rubble, Fw platy and chaotically dispersed clasts. SkS	A 16–32 mm up to 62 mm	SL	SD FGr	Abrupt
B	3	10 - 15	strong brown 7.5YR 5/6	Concave-upwards lens, including only the coarse fraction of the overlying level. Fr clasts parallel to depositional surfaces. SkS		-	-	Abrupt
D1	4	15 -33	yellowish red 5YR 5/6	Poorly sorted rubble. Moderately platy clasts chaotically arranged, Fw parallel to depositional surfaces. Partially cemented ($CaCO_3$). SkS	A (SA) up to 32 mm few larger	Fr-C SL	SD FGr	Diffuse
D2	5	33 - 105	yellowish red 5YR 4/6	Poorly sorted rubble. C platy clasts and flakes, usually parallel to depositional surfaces, Fw sloping, VFw vertical (mostly in the lower part of the bed); one layer of well-oriented platy clasts at about -45 cm. SkS-Ow. Moderately cemented	A 32–64 mm up to 128 mm	Fw-Fr SL	SD FGr	Abrupt
E1	6	105 - 117	reddish brown 5YR 4/3	Poorly sorted rubble,. Clasts more or less parallel to depositional surfaces, VFw verticalised (mostly the larger ones). SkS	A D <32 mm VFw 128 mm	Fr SL	MD FGr-MGr	Abrupt
E1	7	117 - 131	reddish brown 5YR 4/3	Poorly sorted rubble. Fr platy clasts, mostly parallel to depositional surfaces, Fw sloping. SkS-Ow	A 32-64 mm Fw >128 mm	VFw SL	SD FGr	Sharp
E2A	8	131 - 139	dark reddish brown 5YR 3/3	Matrix-rich rubble, poorly sorted. Matrix supported. Colour lightens downwards	A-SA 16–32 mm	SL	M MGr	Clear, slightly

					Fw 32–64 mm			undulating
E2B	9	139 - 151	dark reddish brown 5YR3/3	Poorly sorted rubble. Fw platy clasts, concentrated at the bottom. Matrix more Fr and lighter at top. SkS	A-SA C 32–64 mm Fw 64–128 mm	VFw SL	MD crumb	Sharp
E3A	10	151 - 168	dark reddish brown 5YR 2.5/2	Poorly sorted rubble. C platy clasts parallel to depositional surfaces. SkS	A C 32–64 mm Fr 64-128 mm	SL	MD coarse crumb	Sharp
E3B	11	168 - 188	dark reddish brown 5YR 2.5/2	Poorly sorted chaotical rubble. Fw platy clasts. SkS-Ow. White $CaCO_3$ specks. Moderately cemented.	A-SA C 64–128 mm Fr 64-128 mm	Fw SL	FG	Abrupt
E3C	12	188 - 215	very dark brown 7.5YR 2.5/2	Dark matrix with unsorted clasts. SkS	A-SA Fw 16-32 mm VFw 32-64 mm	SL	FG	Bedrock

Table 1. Field description of the Mujina Cave southern profile sedimentary sequence.
A: angular; SA: subangular. VFw: very few; Fw: Few; Fr: frequent; C: common; D: dominant. MD: medium developed; SD: strongly developed; FGr: fine granular; MGr: medium granular; SL: silty loam; SkS: skeleton supported; Ow: openwork.

Archaeological layers	Lithologic units	Relative depth (cm)	Munsell Color (moist)	Field observations	Texture	Matrix	Aggregation	Limit
A	1	0		Poorly sorted rubble, chaotically dispersed on the cave floor. Ow	A-SA	-	-	Sharp
A	2	0 - 5	dark brown 7.5YR 3/3	Poorly sorted rubble. Chaotically dispersed clasts. SkS	A	Fw SL	SD FG	Sharp subhorizontal
B	3	5 - 35	strong brown 7.5YR 5/6	Poorly sorted rubble, Fr-C chaotically dispersed platy clasts, VFw verticalised. To the South, the layer thins down and becomes stonier	A D 16-32 mm Vfw 32.64 mm Fw 64-128 mm	C SL	SD crumb	Clear undulating
D	4	35 - 110	yellowish red 5YR 4/6	Poorly sorted, rather loose rubble, with D platy elements; elements usually horizontal, Vfw vertical. Horizon of large platy, horizontal stones at -90 cm.,. Ow-SkS	A (size > 256 mm rare, 128 – 256 mm common, very small clasts are rare)	VFw SL	crumb	Abrupt
E1	5	110 -	reddish brown 5YR 4/3	See layer E1 of the southern profile.				

Table 2. Field description of the Mujina Cave eastern profile sedimentary sequence.
A: angular; SA: subangular. VFw: very few; Fw: Few; Fr: frequent; C: common; D: dominant. MD: medium developed; SD: strongly developed; FGr: fine granular; MGr: medium granular; SL: silty loam; SkS: skeleton supported; Ow: openwork.

Level	Grain-size composition		
	Sand	Silt	Clay
B-2.1	4.70	66.18	29.12
B	5.05	68.06	26.88
D-4	1.32	60.37	37.95
D-5	7.42	38.60	53.98
D	4.74	29.06	66.20
E1-6	5.49	26.31	68.20
E1-7	5.04	56.08	38.88
E2A	6.05	45.88	63.75
E2B	5.49	73.83	20.69
E3A	5.47	67.17	27.36
E3B	5.96	60.34	33.70
E3C	6.12	65.35	28.54

Table 3. Grain-size (Wentworth, 1922) of the <2 mm fraction of decalcified samples.

LU	Microstructure/porosity	c/f related distribution pattern	Coarse material Rock fragments	Mineral grains	Organic and biomineral components	Micromass colour and b-fabric	Pedofeatures
B-3	Poorly sorted-unsorted complex: SA blocky and well-dev granular Compound packing voids; planes; chambers; channels	Open porphyric	Limestone Fr SA-SR Chert C A-SR	Quartz C SA Feldspars Vf A Muscovite C Biotite Vf Glauconite Vf R Calcite Fr SA-SR	Bone C A-SR AOM Fw Phosphates Fr SA-R Coprolites C SA-R	Yellowish brown dusty (PPL) Pale yellow (OIL) A, Cr, Gs	Infillings of excrements Fe Co Fw Fe No Fr; typic, strongly impregnated dendritic, weakly impregnated orthic
D-4	Granular, medium-poorly dev Chambers and channels	Open porphyric	Limestone Fr-C A-SR Chert Vf A	Quartz C A Feldspar Fw A Muscovite C Calcite Fr A-SR	Bone Vf Shell Phosphates Fr Coprolites Fr	Greyish brown (PPL) Pale yellow (OIL) Cr	Fe Co/HCo on phosphates Dusty clay and silt Co Fe No Fr: typic, strongly impregnated dendritic, weakly impregnated orthic, aggregate, dendritic Compound layered clay and silt HCo Clay papules Earthworm calcite grains Fw Dusty clay pendants Fw Silt cappings and pendants
D-5	Poorly sorted granular, mod-strongly dev pellicular grain Chambers	Chitonic; gefuric	Limestone Fr A-SA (SR-R) Chert Vf SA	Muscovite C Calcite Fr A	Bone Vf Phosphates C SR-R	Greyish brown, dusty (PPL) Pale yellow (OIL) Cr	Coarse clay+silt cappings Fe HCo Fe No R
E2A-8 (1)	Poorly-medium dev fine granular	Porphyric	Limestone Fr A-SR Chert C A to SR	Quartz C SA Chalcedony Vf A Feldspar Fw Muscovite Fw Calcite Fr A-SA	Bone Fr (bone sand) Shell Vf Phosphates C A-SR	Yellowish brown speckled clay Gs	Fe/Mn No Fr (as in D.5) Calcite Co/HCo C

E2A-8 (2)	Poorly-medium dev fine granular	Porphyric	Limestone Fr A-SR Chert C A-R	Quartz C A-SR Muscovite C Calcite C SA	Bone Fr (bone sand) Phosphates Fr A-SA	Yellowish brown speckled clay Gs-St	Fe/Mn No (matrix) Fr Clay Co Vf Fe HCo Fw
E3C-12	Massive-well dev granular Planes, cracks	Porphyric	Limestone Fr A-SR Chert Fr A-R	Quartz C A-SA Muscovite C Glauconite Vf Opaques Fw	Bone Fr (bone sand) Charcoal C Fine AOM C Mineralised vegetal tissue residues C Punctuations Fr Phosphates Fr A-R	Yellowish brown, speckled clay Gs, Ps, Ss, parallel Sr	Calcite dense (in)complete infillings, Co/HCo Fr Clay coating frgs Vf Loose excrements Infillings Intrusive and matrix typic Fe-No Fw Rolling pedofeatures Vf

Table 4. Main micromorphological characteristics of the Mujina Pećina sediments. Numbers (1) and (2) under E2A-8 indicate that two thin sections were prepared from distinct monoliths.
Table abbreviations.
LU: Lithologic unit; mod: moderately; dev: developed; Fe – iron; Mn – manganese; frg(s) – fragment(s).
Shape. A: angular; SA: subangular; R: rounded; SR: subrounded.
Quantity. Vf: very few; Fw: few; C: common; Fr: frequent.
Pedofeatures. Co: coatings; HCo: hypocoatings; No: nodules.
B-fabric. A: amorphous; Cr: crystallitic; Gs: granostriated; Ps: porostriated; Stipple-speckled; St: strial; Sr: striated.
AOM: amorphous organic matter.

Lab #	Pretreatment	Age	Sigma	Level	Material	Source	$\delta^{13}C$
GrA-9633	(1)	39200	+1230-1060	B	bone	Rink et al., 2002	-18.69
GrA-9634	(1)	40460	+1470-1220	C	bone	Rink et al., 2002	-18.68
GrA-9636	(1)	40430	+1440-1220	D1	bone	Rink et al., 2002	-19.91
Beta-393073	(2) – I	24350	±100	D2	bone	this paper	-19.00
Beta-393073	(2) – II	28400	±150	D2	bone	this paper	-19.00
Beta-393073	(3) – II	47470	±1160	D2	bone	this paper	-19.00
OxA-8150	(4)	34200	±500	D2	charcoal	Rink et al., 2002	-22.30
Beta-393072	(4)	40310	±510	D2	charcoal	this paper	-22.40
GrA-9639	(1)	41820	+1740-1430	D2	bone	Rink et al., 2002	-19.70
GrA-9635	(1)	45170	+2780-2060	E1-E2	bone	Rink et al., 2002	-19-43
(P-37960)	(5)	failed	--	E2A	bone	this paper	--
OxA-31938	(5)	>44300		E2B	bone	this paper	-19.10
OxA-32243	(5)	>44400		E3A	bone	this paper	-19.84
Beta-393074	(2) – I	28710	±150	E3A	bone	this paper	-20.10
Beta-393074	(2) – II	29720	±130	E3A	bone	this paper	-20.10
Beta-393074	(3) – II	31070	±190	E3A	bone	this paper	-20.10
Beta-393075	(2) – I	33050	±230	E3B	bone	this paper	-19.40
Beta-393075	(2) – II	45180	±800	E3B	bone	this paper	-19.40
Beta-393075	(3) – II	47880	±1800	E3B	bone	this paper	-19.40
Beta-393076	(2) – I	24850	±100	E3C	bone	this paper	-20.3
Beta-393076	(2) – II	26360	±100	E3C	bone	this paper	-20.3
Beta-393076	(3) – II	43940	±790	E3C	bone	this paper	-20.3
(P-37961)	(5)	failed	--	E3C	bone	this paper	--
(P-38351)	(5)	failed	--	E3C	bone	this paper	--

Table 5. AMS ^{14}C age determinations for Mujina Pećina. Pretreatment methods as from information provided by the laboratories: (1) collagen extraction following Longin 1970; (2) acid+ultra-filtration; (3) alkali; (4) acid/alkali/acid; (5) collagen extraction following Bronk Ramsey et Al. 2004a, 2004b. Beta-Analytic datings were carried out in two batches (I and II) on the same samples. Numbers in brackets in laboratory number field indicate internal numbering of Oxford datings failed because of low collagen content.

		Unmodelled (BP)				Modelled (BP)			
		1 sigma		2 sigma		1 sigma		2 sigma	
Levels	**Lab #**	**from**	**to**	**from**	**to**	**from**	**to**	**from**	**to**
D-B levels duration						0	1970	0	3790
End D-B						43980	42800	44460	42170
B	GrA-9633	44100	42280	45390	41640	43980	42900	44450	42360
C	GrA-9634	45280	42980	47170	42210	44040	43140	44490	42740
D1	GrA-9636	45230	42980	47050	42220	44170	43350	44570	42990
D2	Beta-393072	44370	43410	44880	43040	44500	43680	44890	43310
D2	GrA-9639	46900	43820	49040	43010	44630	43740	45100	43340
Start D-B						45440	43880	46630	43390
Gap duration						430	2750	0	3910
E levels duration						0	1540	0	3400
End E-levels						47750	45690	48850	44790
E1-E2	GrA-9635	---	47180	---	45440	47770	45850	48870	45070
E3C	Beta-393076	48100	46290	49200	45720	48700	46860	49790	46270
Base E-levels						48900	46910	50000	46290

Table 6. Age estimates for a Bayesian model including two sequences separated by a gap. Estimate dates for the beginning and end of the sequences and of the gap, as well as durations are provided by the model. ---: beyond calibration limit.

File(s) excluded from PDF

The following file(s) will not be converted:

þÿ M u j i n a P e c i n a l o c a t i o n m a p . k m z

Please click 'Download zip file' to download the most recent files related to this submission.